Cranfield University

Roger Molinder

Zirconium as a coagulant for enhanced natural organic matter removal

Centre for Water Science
Department of Sustainable Systems
School of Applied Science

MSc. by Research Thesis

Cranfield University

Centre for Water Science
Department of Sustainable Systems
School of applied Science

MSc. by Research Thesis

2009

Roger Molinder

Zirconium as a coagulant for enhanced natural organic matter removal

Supervisors: Dr. Peter Jarvis and Dr. Bruce Jefferson

Academic Year 2008 to 2009

This thesis is submitted in partial fulfilment of the requirements for the degree of MSc. by Research

ABSTRACT

Coagulation is the most common way to remove the bulk of natural organic matter (NOM) from moorland source waters during drinking water treatment. Deteriorating water quality and tightening regulations have created the need for more effective treatment options. A review of the literature identified a range of enhanced treatment options that are available for NOM removal. A novel highly charged Zr coagulant (referred to as Zr-OCl) has also been proposed to enhance NOM removal. The aim of this thesis was to evaluate the use of Zr-OCl as a coagulant in continuous operation at pilot scale by benchmarking the performance of Zr-OCl against a conventional ferric coagulant (referred to as Fe-Coag). The potential use of Zr-OCl in a blend with Fe-Coag was also investigated. The removal of NOM, turbidity and disinfection by-product (DBP) precursors as well as the zeta potential and the strength of flocs was measured. The characteristics of Zr were related to the mechanisms of the coagulation process. It was clear that Zr-OCl could remove more NOM than Fe-coag displaying 7-10 % increased removal of dissolved organic carbon (DOC), 6-10 % increased removal of absorption of ultraviolet light at 254 nm (UV_{254}), 31- 62 % increased turbidity removal and 23-38 % lower THM-FP. Zr-OCl also added more charge to the system and operated over a wider zeta potential range which explained the increased removal. The higher charge and wider operational range was explained by the characteristics of Zr found in the literature review. The Zr-OCl flocs were stronger than the Fe-Coag flocs resulting in less breakage during solid-liquid removal. When different blends of Zr-OCl and Fe-Coag were used there was an incremental increase in performance as a result of an increased amount of Zr in the blend for a given dose. The possible use of Zr-OCl a coagulant was put into context by comparing it to the other treatment options investigated in the literature review.

Keywords:
Charge, Zeta potential, coagulation, blending, pilot-scale

ACKNOWLEDGEMENTS

I would like to thank my supervisors Dr. Peter Jarvis and Dr. Bruce Jefferson for all their help and support. I would also like to thank Jenny Banks from Yorkshire Water. A special thanks to Dr. Peter Jarvis for proof reading my written work.

For my laboratory work I have had the help of a lot of students and staff. I would particularly like to thank Dr. Emma Goslan and Jane Hubble but also Paul Barton, Rukhsana Ormesher, Ben Martin and Dr. Ewan McAdam.

During the many hours I spent in the pilot hall I had a lot of help from Richard Harnett from Water Innovate.

I would also like to thank Yorkshire Water for providing the funding for this project.

Finally I would like to thank Diane Purcell for all her love and support which has helped my through this MSc. by research project.

TABLE OF CONTENTS

TABLE OF TABLES

TABLE OF FIGURES

TABLE OF EQUATIONS

Equation 3:1 Frequency of collision in perikinetic flocculation: $I_{ij} = 4\pi D_{ij} R_{ij} n_i n_j$

I_{ij} = number of contact per unit time between particles of radius Ri and Rj

D_{ij} = mutual diffusion coefficient of particles i and j

R_{ij} = radius of interaction of the two particles

n_i, n_j = respective number concentration of i and j particles

Equation 3:2 Rate of collision in orthokinetic flocculation: $Hij = \frac{4}{3} n_i n_j R^3_{ij} \frac{dv}{dz}$

H_{ij} = the number of contacts between i and j particles per unit time.

n_i, n_j = respective number concentration of i and j particles.

R_{ij} = radius of interaction of the two particles

dv / dz = velocity gradient in laminar flow.

Equation 3:3 Rate of floc growth: $R_{floc} = \alpha R_{col} - R_{br}$

R_{floc} = the rate of floc growth

R_{col} = the rate of particle collision

R_{br} = the rate of floc breakage

α = the collision factor

Equation 5:1 Floc strength factor: Strength factor = $\frac{d(2)}{d(1)} \times 100$

$d(1)$ is the floc size before breakage

$d(2)$ is the floc size after breakage

Equation 5:2 Floc recovery factor: Recovery factor = $\frac{d(3) - d(2)}{d(1) - d(2)} \times 100$

$d(1)$ average floc size before breakage

$d(2)$ is floc size after breakage

$d(3)$ is the floc size after re-growth

ABBREVIATIONS

AOP	:	Advanced oxidation process
CD	:	Charge density
COD	:	Chemical oxygen demand
D_{50}	:	Median equivalent diameter
Da	:	Daltons
DAF	:	Dissolved air flotation
DOC	:	Dissolved organic carbon
DBP	:	Disinfection by product
DWI	:	Drinking Water Inspectorate
FAF	:	Fulvic acid fraction
FR	:	Fenton's reagent
PDADMAC	:	Polydiallyldimethyl-ammonium chloride
PFR	:	Photo Fenton's reagent
G	:	Velocity gradient
GAC	:	Granular activated carbon
GC-ECD	:	Gas chromatography - electron capture detector
HAA	:	Haloacetic acid
HAA-FP	:	Haloacetic acid formation potential
HAF	:	Humic acid fraction
HPSEC	:	High performance size exclusion chromatography
CPS	:	counts per second
MTBE	:	Methyl tert butyl ether
MIEX®	:	Magnetic ion exchange resin
MW	:	Molecular weight
NTU	:	Nephelometric turbidity unit
NOM	:	Natural organic matter
RPM	:	Rotations per minute
PAC	:	Powder activated carbon
PC	:	Personal computer
Q	:	Quartile
SUVA	:	Specific ultraviolet absorbance
THM	:	Trihalomethane
THM-FP	:	Trihalomethane formation potential
TOC	:	Total organic carbon
UV_{254}	:	Specific ultraviolet light with 254 nm wavelength absorption
WTW	:	Water treatment work
ε	:	Energy dissipation rate
IEP	:	Iso electric point
Fe-Coag	:	Ferripol XL (EA West, UK)
Zr-OCl	:	Zirconium oxychloride (Mel Chemicals, UK)

1. Introduction

Natural organic matter (NOM) is defined as a highly heterogeneous mixture of organic compounds which are known to vary both temporally and spatially with regards to solubility, hydrophobicity, functional group composition, charge density and molecular weight (MW) (Edzwald, 1993; Owen *et al.*, 1995).

NOM is the most common components of source waters throughout the world, and is especially abundant in water from moorland and mountain catchments (Sharp *et al.*, 2006a). Some of the negative attributes of NOM include that it can give the water a brown colour and also cause taste and odour problems. NOM can also react with chlorine during disinfection which results in the formation of disinfection by products (DBPs) (Goslan *et al.*, 2002). Among these DBPs, the trihalomethanes (THMs) and the haloacetic acids (HAAs) have been identified as possible human carcinogens making them a major concern to human health for the water industry (Regli *et al.*, 1992; Parsons and Byrne, 2005).

A common process to remove NOM is by coagulation with metal salts followed by sedimentation/ flotation and filtration. Elevated levels of NOM caused by heavy rainfall or snow melt have caused difficulties for many water treatment plants (WTPs) in the USA and the UK (Sharp *et al.*, 2005). The normal response to elevated NOM levels is to increase the coagulant dose which results both in increased chemical usage and a larger volume of sludge with associated increases in chemical and disposal costs (Edzwald and Tobiason, 1999). High concentrations of NOM have also shown to effect floc formation and can lead to the formation of fragile flocs which can easily break-up (Jarvis *et al.*, 2005a). This can cause carry over onto filters resulting in greater particle loads, turbidity breakthrough and reduced filter run times (Sharp *et al.*, 2006c) high particle load on to filters leading to reduced filter run times and increased particle breakthrough. Apart from conventional coagulation, there are several additional treatments which can be used in order to increase NOM removal efficiency and/or improve floc properties. For example magnetic ion exchange resin (MIEX®) pre-treatment and activated carbon (Hooper *et al.*, 1996; Singer and Bilyk, 2002).

However, these treatment options often require significant capital investment and can take a long time to implement (Parsons and Jefferson, 2006a; Mergen *et al.*, 2008).

Charge neutralisation is a fundamental mechanism by which NOM is removed during coagulation. This has most recently been shown by Sharp and co-workers (2006a; 2006b) who reported that optimum NOM removal was achieved when the zeta potential of the system was reduced to around zero. This is because optimum NOM removal occurs between the iso-electric point (i.e.p.) of the coagulant and the NOM (Sharp *et al.*, 2006a). The removal of NOM by means of coagulation is dependent on factors such as NOM concentration and composition, coagulant dose and pH (Edzwald and Tobiason, 1999; Sharp *et al.*, 2006b). Hence, there is a pH and a coagulant dose which constitutes optimum conditions at which NOM removal is maximised for a given coagulant and a given water (Duan and Gregory, 2003).

In this research, a novel coagulant for enhanced NOM removal is proposed which is based on the tetravalent Zr ion (Zr^{4+}), which carries a higher charge per mole then conventionally used coagulants based on Fe^{3+} and Al^{3+} ions. The novel coagulant proposed is Zr oxychloride (henceforth referred to as Zr-OCl). The hypothesis for using this chemical was that it could improve charge neutralisation and subsequent NOM removal by adding more charge to the system. This would in turn result in a higher NOM removal under optimum conditions compared to other coagulants for a given water. The use for Zr-OCl as an alternative to other treatment options for enhanced NOM removal, Zr-OCl offers the advantage that there is no need for capital investment in order to implement the use of it. This is because the same dosing equipment can be used for the addition of Zr-OCl as for the traditionally used coagulant. A further possible application for the use of Zr-OCl is in a blend together with a conventional coagulant during periods of high levels of DOC to enhance the coagulation process when the effectiveness of the conventional coagulant is not high enough to meet water quality standards.

This study will evaluate the potential use of the novel Zr-OCl coagulant for enhanced NOM removal. The use of Zr-OCl in a blend with a conventional Fe^{3+} based coagulant will also be evaluated.

2. Objectives

This study aims to evaluate the use of Zr-OCl as a coagulant in continuous operation at pilot scale. Zr-OCl will be tested as a primary coagulant where the performance will be benchmarked against a conventionally used Fe coagulant. Zr-OCl will also be dosed in combination with the Fe based coagulant. The NOM removal efficiency will be tested on a moorland water source with high DOC and low turbidity.

Objectives

- Compare the NOM removal of Zr-OCl with the NOM removal of a conventional Fe^{3+} based coagulant under optimum conditions at bench scale and in continuous operation at pilot scale.

- Understand the impacts on NOM removal of using Zr-OCl and a conventional Fe^{3+} coagulant in a blend. This will be undertaken at both bench scale and pilot scale.

- Compare the properties of flocs formed during treatment Zr-OCl with the flocs formed during treatment with a conventional Fe^{3+} based coagulant under optimum conditions at bench scale.

- Understand the impact on floc properties of using Zr-OCl and a conventional Fe^{3+} coagulant in a blend at bench scale.

3. Literature review

3.1 Introduction

Coagulation is the most common way to remove the bulk of NOM from moorland water sources during water treatment (Sharp, 2005). The process normally involves destabilisation of the NOM by the addition of a metal salt during rapid mixing (Faust and Aly, 1998a). The aggregates formed in this process are then removed using a solid-liquid separation process followed by a subsequent filtration stage to remove very small particles (Amirtharajah and O'Melia, 1990; Edzwald, 1995). NOM is a heterogeneous mixture of organic compounds which needs to be removed primarily since many of the compounds can serve as precursors for trihalomethanes (THMs) which been identified as possible human carcinogens are and therefore represent a significant threat to human health (Regli *et al.*, 1992; Owen *et al.*, 1995; Goslan *et al.*, 2002)

The maximum allowed levels of THMs are 100 μgL^{-1} in the UK and 80 μgL^{-1} in the US (Drinking Water Inspectorate in the UK, 1998; US Environmental Protection Agency (EPA), 1998). Also, levels of NOM in moorland water sources have increased during recent years (Worrall and Burt, 2004). The conventional way to increase NOM removal is by increasing the coagulant dose (Najm *et al.*, 1998). This leads to more chemical use, increased sludge production and increased costs (Edzwald and Tobiason, 1999). This has created a need for more efficient NOM removal treatment options. Several such treatment options already exist which enhance the treatment process in different ways (Bolto *et al.*, 2001; Murray and Parsons, 2004a; Tomaszewska *et al.*, 2004; Boyer and Singer, 2005).

This review will outline the characteristics needed for a chemical to remove NOM by coagulation. This will be done by a review of the mechanisms involved in the destabilisation process induced by the coagulant and the process which leads to the formation of aggregates during conventional treatment. A series of treatment options which can be used to enhance the NOM removal efficiency of the coagulation process will then be reviewed with regards to their characteristics and their performance

compared to conventional coagulation. The characteristics of the novel Zr coagulant will then be used to asses its use as a treatment option for removal of NOM.

3.2 Coagulation mechanisms

3.2.1 Introduction

Coagulation is a process for combining particles, colloids and dissolved material into larger aggregates (Amirtharajah and O'Melia, 1990). This involves chemically changing a suspension to overcome the forces maintaining the stabile system (Sharp, 2005). It is used in water treatment in combination with solid-liquid separation, such as sedimentation or flotation and filtration, for the removal of NOM and suspended particles. A number of mechanisms are involved in coagulation including double layer compression, adsorption, charge neutralisation, complexation, sweep flocculation and inter-particle bridging (Crozes *et al.*, 1995; Faust and Aly, 1998; Duan and Gregory, 2003). The operation of coagulation at a water treatment plant involves the addition of a coagulant used to destabilize the organic material. The destabilized organic material is then mixed causing the individual compounds to aggregate (Jarvis *et al.*, 2005a). These aggregates are referred to as flocs which can be removed by solid liquid separation using sedimentation/ flotation and subsequent filtration.

3.2.2 Surface charge and solubility

All particles in solution carry a surface charge, which is almost invariably negative (Dentel, 1991). This surface charge interacts with the surrounding water molecules and controls the particles solubility (Sharp, 2005). An understanding of surface charge is therefore important to understand how particles are destabilised during coagulation. Organic material in water can be characterised by its size and solubility, which controls the mechanism by which it is stabilised in the water. Hydrophilic organic material is stabilised by a layer of water molecules which adhere to the particle while hydrophobic organic material is stabilised by an electrostatic repulsion between particles. This repulsion originates from ions which are either attached to the surface from the solution or dissolve out from the solid's surface (Faust and Aly, 1998a). Like all dissolved particles, the organic material carries a surface charge (Dentel, 1991). The negative surface charge attracts ions of opposite charge which form a layer

around the colloid called the Stern Layer. At the edge of the Stern layer is the plane of shear at which the electrostatic attractions between the oppositely charged ions are, in part, overcome by Brownian motion. This causes diffusion of ions into what is called the diffuse region and causes electro neutrality to be established at some distance from the surface (Faust and Aly, 1998a). The boundary between the Stern layer and the plane of shear is named the diffuse double layer or the Gouy – Chapman layer. The potential gradient over this region is the zeta potential (Faust and Aly, 1998). The zeta potential can be measured by the application of a voltage which causes the particle to move. The ions in the Stern layer will move with the colloid and the ions in the diffuse layer will remain stationary. Measurement of the velocity of motion can then be used to determine the zeta potential (Sharp, 2005).

3.2.3 Destabilisation mechanisms

Destabilisation of particles, colloids and dissolved material occurs through compression of the double layer, adsorption, charge neutralisation, complexation, sweep flocculation and inter-particle bridging (Tamamuski and Tamaki, 1959; Black and Willems, 1961; Black *et al.*, 1963; LaMer and Healy, 1963; Packham, 1965; Faust and Aly, 1998; Bratby, 2006). Several of these mechanisms occur simultaneously but the dominating mechanisms depend on several parameters such as the concentration and character of the NOM, pH and type of coagulant. The destabilising mechanisms are described below.

3.2.3.1 Double layer compression

Double layer compression is an electrostatic interaction which occurs when positively charged counter ions of the coagulant enter the double layer of the NOM. If enough counter ions enter the double layer, they will overcome the stabilising effect of the potential-determining ions and the zeta potential will decrease. This causes the thickness of the double layer to decrease while the particle's charge remains constant. With a high enough concentration of counterions, coagulation can occur (Faust and Aly, 1998). However, if the concentration of counterions becomes too high the charge will be reversed and the NOM will re-stabilize. This destabilising effect increases with increased valence of the counter ion according to the Schulze – Hardy rule such as a lower concentration of ions of a higher valence will induce the same destabilising

effect as a higher concentration of an ion with a lower valence. Therefore coagulants based on highly charged ions are expected to have a greater effect on NOM stability (Gregory, 1993).

3.2.3.2 Adsorption

Adsorption is defined as the increase in concentration of a particular component at the surface or interface between two phases (Faust and Aly, 1987). All atoms in solids and liquids are subject to attraction forces. A molecule in the centre of, for example, a liquid drop is attracted equally from all sides. At the surface of the drop, the attractive forces between molecules result in a net attraction into the bulk phase normal to the surface plane (Faust and Aly, 1998). The molecules at the surface are therefore pulled towards the centre, causing the surface to shrink to the smallest area that can enclose the liquid. These forces are characterised as the surface tension and is defined as the work required to expand the surface by 1 cm^2. The unbalanced attractive field at the surface of a particle results in surface tension, or free energy. Adsorption partially balances these forces resulting in a reduction of free energy and a net release of energy into the solvent (Faust and Aly, 1998).

For adsorption between two particles to occur in a solvent with subsequent net release of energy, the attraction between the solid surface and the solvent must be greater then the energy of repulsion caused by electrostatic effects. Also, the energy needed to remove the solvent molecules from the solid surface must be less then the energy released by adsorption (Bratby, 2006). Adsorption between particles can therefore follow another destabilization process which has reduced the particle's affinity for the water, such as the energy needed to remove the solvent molecules for the solid surface has been reduced. Adsorption can occur through ionic, covalent, hydrogen or dipolar bonding. This is called chemical bonding and is always enhanced by van der Waals forces (Bratby, 2006). Adsorption through van der Waals forces only is named physical adsorption.

3.2.3.3 Charge neutralisation

Charge neutralisation is believed to be the prevailing destabilisation mechanism for colloidal NOM (Duan and Gregory, 2003). Adsorption of excess counter ions onto the surface of a particle can induce charge neutralisation and subsequent coagulation. This was shown by Tamamuski and Tamaki (1959) who compared the destabilization of AgI sols with dodecylammonium ($C_{12}H_{25}NH_3^+$) and Na^+. According to electrostatic models, both counterions should induce coagulation in the same manner. The organic amine proved effective at concentrations of 6×10^{-5} M while Na^+ was effective at 10^{-1} M suggesting a coagulation mechanism other than electrostatic interaction. At concentrations above the one needed for coagulation, a charge reversal was seen and the particles were re-stabilized. This was explained by an adsorption of excess counterions.

3.2.3.4 Complexation

Complexation is thought to be the prevailing destabilisation mechanism for more hydrophilic, soluble organic compounds such as fulvic acids and involves chemical bonding between an organic compound and a metal ion (Gregor *et al.*, 1997; Jefferson *et al.*, 2006). Hydroxy metal cations are known to form stable complexes with the hydroxyl and carboxyl functional groups of humic and fulvic acids (Baohua *et al.*, 1994). Complexation between metal coagulant and NOM has been confirmed by the existence of Fe-O-C bonds (Rose *et al.*, 1998; Vilge'-Ritter *et al.*, 1999). These bonds are also formed during chemical adsorption and as a result it can be difficult to distinguish between complexation and adsorption in many practical cases (Baohua *et al.*, 1994; Duan and Gregory, 2003) The resulting metal-NOM complex will stay in solution until either the binding capacity of the organic compounds has been satisfied, or the solubility of the complex is exceeded. This will cause the complex to precipitate (Gregor *et al.*, 1997).

The formation of metal-NOM precipitates was first proposed by Black and Willems (1961) and Black *et al.* (1963) who focused on water with high levels of DOC above 25 mgL^{-1}. A stoichiometric relationship between the colour of the water and the amount of coagulant needed for colour removal was observed. The same relationship was also found later by Hall and Packham (1965) who described the coagulation of organic compounds with alum and ferric chloride in the presence of dilute clay suspensions. It was also found that the pH value for optimum removal (pH 3.8) was closely related to the pH of zero electromobility. The best colour removal was recorded at a pH just below the iso electric point, where mobility of the flocs was positive and just above the pH of maximum positive charge.

3.2.3.5 Sweep flocculation

Entrapment of NOM within hydrolysed forms of metal salts also induces destabilisation and subsequent coagulation. This effect was seen by Matijivic *et al.* (1963) when they used aluminiun nitrate to destabilise AgI and AgBr at pH 5. Coagulation was seen at a relatively low dose, attributed to adsorption- charge neultralisation mechanisms. With increased alumninium nitrate concentration, restabilisation of colloids was first observed followed by coagulation at high doses where $Al(OH)_{3(s)}$ was precipitated. This was the result of entrapment of the colloids in which they are physically destabilised by $Al(OH)_{3(s)}$. The same process was observed for the coagulation of dispersed clays by Packham (1965) and this was termed sweep flocculation. Later work on the removal of humic substances using Al based coagulants identified pH and Al dose as key factors determining which removal mechanism would prevail (Semmens and Field, 1980; Dempsey *et al.*, 1984; Dempsey *et al.*, 1985). Semmens and Field (1980) found that the removal of organic substances from a water with a DOC of 10-16 mgL^{-1} using alum at pH 6 and above was due to adsorption of the organic substances on precipitated $Al(OH)_{3(s)}$. At pH 5 and below, precipitation of organic compounds by soluble Al species was observed. The results were in agreement with Dempsey *et al.* (1984) and Dempsey *et al.* (1985) who reported that the removal of humic substances occurred by adsorption onto precipitated $Al(OH)_{3(s)}$ at a pH above 7. At a pH less then 5, removal of humic substances occurred by precipitation with small polymers and monomers of Al. At pH between 5 and 7 both processes could occur depending on the type of coagulant used

(alum or PACl) and on the concentration of DOC. The formation of hydroxide species of Al is favoured by a high Al concentration. Following the stoichiometric relationship between DOC and coagulant, adsorption onto precipitated $Al(OH)_3$ was favoured at high DOC concentrations. At low DOC concentrations, the precipitation of humic substances by soluble Al species was favoured. Consequently, the prevailing removal mechanism is dependent on pH and coagulant dose such as a high pH and/or high dose favours sweep flocculation while low pH and/or low dose favours complexation.

3.2.3.6 Particle bridging

Polymers are used in water treatment both as primary coagulants and as coagulant aids. High MW polymers have the ability to destabilize particle dispersions through inter particle bridging. A model for the bridging process has been proposed by LaMer and Healy (1963). Some of the reactive groups of a polymer can adsorb on to a particle leaving other parts of the polymer extended into the solution. Attachment to another particle by an extended part of the polymer, bridges them together (Faust and Aly, 1987).

3.2.4 Aggregation

3.2.4.1 Introduction

Following destabilisation by mechanisms described previously, particles that collide with each other can connect and form larger particles in a process called aggregation. For aggregation to occur, destabilized particles must come into contact with one another. This process is induced at a WTP by mixing (Jarvis *et al.*, 2005a). The transportation of particles leading to collisions between them is controlled by three major physical processes (Thomas *et al.*, 1999). These are perikinetic flocculation (or Brownian diffusion), orthokinetic flocculation (or fluid shear) and differential settling.

3.2.4.2 Physical processes involved in aggregation

Perikinetic flocculation is caused by the thermal energy of the fluid causing water molecules surrounding a particle to move at random, which is termed Brownian motion. Collisions with the water molecules cause a random movement of the particle which is dependent on the force of kT, the product of the Boltzmann's constant k and the absolute temperature T.

Orthokinetic flocculation is an aggregation process induced by velocity gradients. This is achieved in water treatment by inducing a shear motion in the liquid by mixing. This enables particles to make contact by movement with the surrounding liquid (Bratby, 2006).

Differential settling is the result of particle collision following differences in their settling velocity.

3.2.4.3 Models describing aggregation

The work of Von Smoluchowski (1917) on particle transport in coagulation processes is the basis for current understanding of the process. Von Smoluchowski (1917) developed a model for perikinetic flocculation describing how the diffusional flux of particles towards a single stationary particle determines the frequency of collision (Bratby, 2006). The particles were assumed to diffuse towards the stationary particle in a radial direction. The number of particles diffusing radially through the surface of a sphere centred on the stationary particle is proportional to the particle concentration gradient, the particles Brownian diffusion and the surface area of the sphere. By assuming that diffusion is experienced by the central particle, Von Smoluchowski's presented the following equation:

$$I_{ij} = 4\pi D_{ij} R_{ij} n_i n_j$$

(Equation 3:1)

Where

I_{ij} = number of contact per unit time between particles of radius Ri and Rj

D_{ij} = mutual diffusion coefficient of particles i and j

R_{ij} = radius of interaction of the two particles

n_i, n_j = respective number concentration of i and j particles

Floc size limits the effect of Brownian motion. The potential energy barrier between particles increases approximately proportionally to the area of the floc. This is expressed in Von Smoluchowski's equation such as if particle size is increased to >1µm, the effect of perikinesis becomes negligible and orthokinetic flocculation is needed for further aggregation.

For two particles to come close enough for aggregation between them to occur they must travel in the liquid. This is achieved in orthokinetic flocculation by particle movement in the liquid as a result of applied velocity gradient. Von Smoluchowski's model for orthokinesis assumes spherical particles moving in laminar flow:

$$Hij = \frac{4}{3} n_i n_j R^3{}_{ij} \frac{dv}{dz}$$

(Equation 3:2)

Where

H_{ij} = the number of contacts between i and j particles per unit time.

n_i, n_j = respective number concentration of i and j particles.

R_{ij} = radius of interaction of the two particles

dv / dz = velocity gradient in laminar flow.

The greater the velocity gradient in the liquid the more particle contacts there will be. This increases aggregation but also floc breakage. Flocs will therefore, for any given shear rate, not continue to grow but reach a steady state. Floc growth is a balance between aggregation and floc breakage (Ducoste and Clark, 1998; Biggs and Lant, 2000). Initially, the rate of aggregation is higher then the rate of breakage but with increasing floc size the rate of breakage will increase. The rate of floc growth can be summarised as the difference between the rate of aggregation and the rate of floc breakage according to the following equation (Gregory, 1989):

$$R_{floc} = \alpha R_{col} - R_{br}$$

(Equation 3:3)

Where

R_{floc} = the rate of floc growth

R_{col} = the rate of particle collision

R_{br} = the rate of floc breakage

α = the collision factor

The collision factor is the fraction of collisions which result in attachment. The collision factor and the rate of particle collision describe aggregation. The collision factor depends on shear rate and particle size such that for a given shear rate, the collision factor decreases with increased particle size (Jarvis *et al.*, 2005a). Steady state is reached when the rate of aggregation equals the rate of breakage (equation 3:3).

When the destabilised particles connect, they must attach to each other to be able to aggregate and form flocs. Attachment is made more favourable by the destabilisation process because it reduces the repulsive forces between particles and also reduces their affinity for the water.

3.2.5 Floc strength

3.2.5.1 Introduction

The strength of the flocs formed depends on the interparticle bonds between its components including the strength and number of individual bonds (Bache *et al.*, 1997). A floc will break if the stress applied at the surface is larger than the strength of the bonds within it (Boller and Blaser, 1998). Jarvis *et al.* (2005a) list two modes of floc breakage: surface erosion and large-scale fragmentation. Surface erosion is defined as the removal of small particles from the floc surface. This results in an increase in the small particle size range. The cleavage of flocs into similar sized pieces is termed large-scale fragmentation which occurs without an increase in primary particle concentration. Surface erosion is believed to be the result of shearing stress acting tangentially to the floc surface while fragmentation is thought to occur from tensile stress acting normally across the floc (Jarvis *et al.*, 2005a).

3.2.5.2 Measuring floc strength

There are several ways of determining the strength of flocs. The most basic one is to determine the floc strength factor which was introduced by Francois (1987). The strength factor is defined as the ratio of floc size before and after breakage at a particular shear level. A higher strength factor means that the flocs are less sensitive to breakage as a result of increased shear rate and are therefore considered stronger. Since the strength factor is not a constant it changes depending as a result of the applied shear force during breakage. Therefore, strength factors can only be compared for similar breakage conditions. Another consideration of floc strength is the steady state floc size for a given shear condition. Applying a shear force will induce floc growth due to particle collision. With increased floc size, floc breakage will increase until the rate of growth and breakage is equal and steady state floc size is reached. A stronger floc will reach steady state later and grow larger for a given shear condition.

3.3 Characteristics needed of a coagulant for NOM removal

The removal efficiency of NOM by coagulation depends on the type of coagulant used and the character of the NOM (Edzwald and Tobiason, 1999; Sharp *et al.*, 2006b). For a given coagulant, optimum removal depends on pH and coagulant dose (Black and Willems, 1961; Black *et al.*, 1963; Duan and Gregory, 2003). Optimum coagulation conditions have been found to coincide with charge neutralisation and optimum NOM removal has been reported to occur between the iso-electric point (i.e.p.) of the coagulant and the NOM (Kvinnesland and Odengaard, 2004; Sharp *et al.*, 2006a). NOM is predominately negatively charged at pH levels of natural waters so a coagulant will need to add positive charge in order to achieve charge neutralisation. Coagulants that can add more charge have been reported to remove more NOM than coagulants that add less charge (Bolto *et al.*, 1999; Bell-Ajy *et al.*, 2000). Other removal mechanisms identified for NOM removal with coagulation are complexation and adsorption (Baohua *et al.*, 1994; Vilge'-Ritter *et al.*, 1999). Both these mechanisms involve interactions between the coagulant and the NOM in the form of chemical bonds and leads to the formation of insoluble precipitates (Baohua *et al.*, 1994; Rose *et al.*, 1998; Duan and Gregory, 2003). This implies that the efficiency of a coagulant is also dependent on its affinity for the NOM.

For optimum solid-liquid separation, the characteristics of the flocs formed following aggregation needs to fit the chosen separation mechanism. Dense and fast settling flocs are required in the case of sedimentation and low density flocs in the case of flotation. Flotation is becoming more widespread due to advantages such as rapid start up and high loading rates (Gregory, 1993; Parsons and Jefferson, 2006a). However, regardless of the chosen separation mechanism, floc strength is a key characteristic (Jarvis *et al.*, 2005a). A strong floc will increase removal efficiency by resisting breakage under shear conditions which are prevalent in water treatment plants (Boller and Blaser, 1998; McCurdy *et al.*, 2004; Jarvis *et al.*, 2005a).

NOM removal by coagulation is conventionally carried out using metal salts of aluminium and iron (Amirtharajah and O'Melia, 1990). If the NOM removal needs to be increased from what can be achieved by optimising pH and dose conditions, other treatment options can be considered, like MIEX® pretreatment, polymers, activated carbon and oxidation (Hooper *et al.*, 1996; Kam and Gregory, 2001; Bose and Reckow, 2007; Kitis *et al.*, 2007). These can aid in the coagulation process by adding additional charge, increase floc size, break down small MW NOM or adsorb uncharged NOM (Nowack *et al.*, 1999; Bolto *et al.*, 2001; Shon *et al.*, 2005; Mergen *et al.*, 2008). Many of these treatment options require significant capital investment and take a long time to implement (Murray and Parsons 2004a; Murray and Parsons, 2004b; Parsons and Jefferson, 2006a; Mergen *et al.*, 2008). However, despite increased capital costs, savings can be made by using lower coagulant doses and by reduced sludge production (Najm *et al.*, 1998; Edzwald and Tobiasson, 1999; Singer and Bylik, 2002).

3.4 Characteristics of a commonly used coagulant

Commonly used coagulants are salts based on aluminium or iron, like aluminium sulphate (also known as alum), ferric sulphate and ferric chloride (Amirtharajah and O'Melia, 1990; Duan and Gregory, 2003). When these salts are added to water, the Fe^{3+} and Al^{3+} ions undergo a hydrolysation mechanism (Snoeyink and Jenkins, 1980a). Water molecules are attracted to the metal ions and form a primary hydration shell as well as a secondary hydration shell (ref 2 in Duan and Gregory). Water molecules in the primary hydration shell are polarised by the metal ion, which can lead to a loss of protons and the formation of OH^- ions according to the following sequence (Duan and Gregory, 2003):

$$Me^{3+} \rightarrow Me(OH)^{2+} \rightarrow Me(OH)_2^{+} \rightarrow Me(OH)_3 \rightarrow Me(OH)_4^{-}$$

This mechanism is dependent on pH such as the above sequence proceeds from left to right with increased pH (Snoeyink and Jenkins, 1980a). The formation of hydrolysed species can be described graphically by plotting the mole fraction of the different species against pH (Figure 3.1).

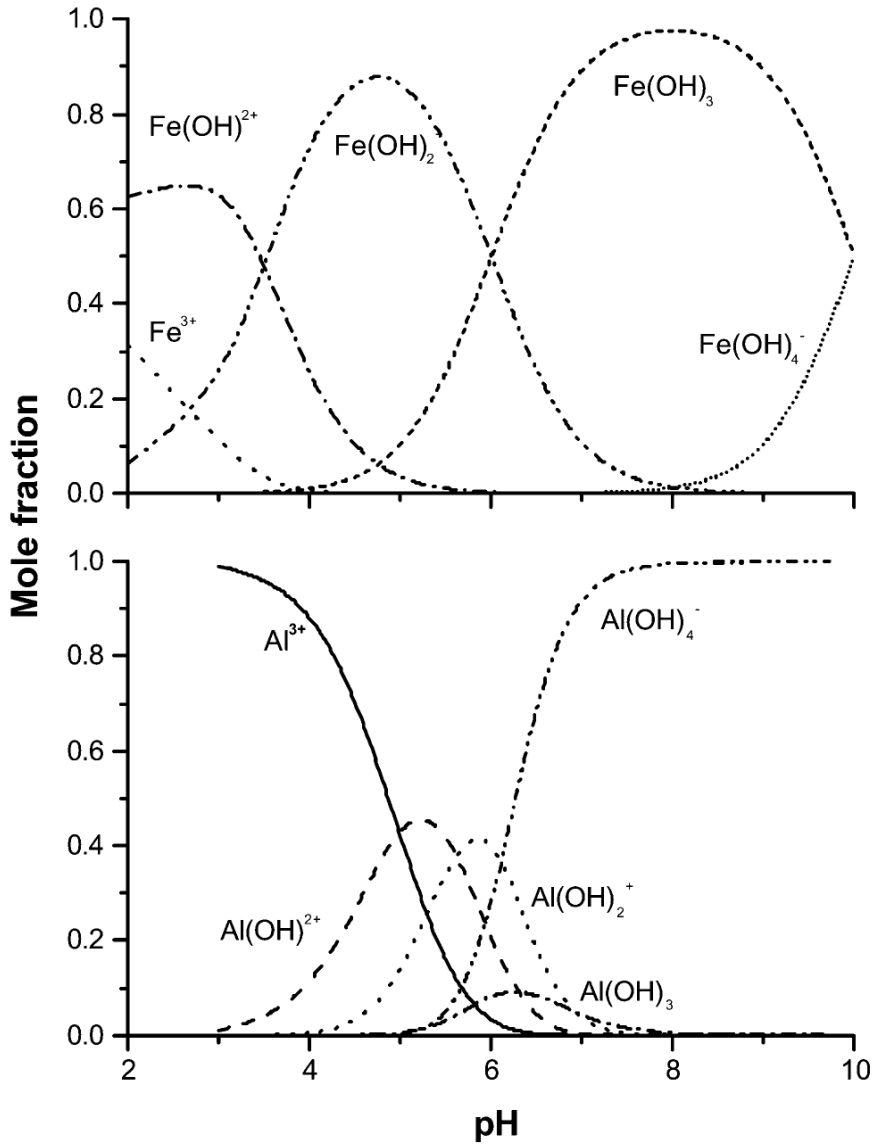

Figure 3.1: Mole fractions of species of Fe and Al in water under pH conditions between 2 and 10 (Figure from Duan and Gregory, 2003).

Due to the aim of this review, the focus of the rest of this section will be on the characteristics of Fe based salts. The need for enchanced NOM removal comes from high levels of NOM causing insufficient NOM removal and poor floc formation (Jarvis *et al.*, 2005a; Sharp *et al.*, 2006c). Fe salts have been reported to outperform Al salts with regards to both NOM removal and floc formation (Edwald and Tobiasson, 1999; Ratnaweera *et al.*, 1999; Bell-Aji *et al.*, 2000). The higher NOM removal capacity of Fe salts compared to Al salts have been particularly evident at high NOM concentrations (Budd *et al.*, 2004; Kastl *et al.*, 2004). Due to the context of enhanced NOM removal, the focus will therefore be on the characteristics of Fe salts.

The commonly used Fe salts in coagulation are based on the Fe^{3+} ion, which together with the Fe^{2+} ion are the only Fe ions of importance in aqueous chemistry (Cotton *et al.*, 1999b; Duan and Gregory, 2003).

At pH < 1 the only species on solution is the Fe^{3+} ion (Cotton et al., 1999a). In the pH range of 1-2 the $Fe(OH)^{2+}$ species will form (Figure 3.1). Apart from the $Fe(OH)^{2+}$ species a dimer is also formed ($Fe_2(OH)_2^{4+}$) (Johnson and Amirtharajah, 1983). A trimeric species ($Fe_3(OH)_4^{5+}$) has also been postulated (Hong-Xiao and Stumm, 1987). However, the optimum pH for coagulation with Fe based metal salts are normally between 4.5 and 5.5 (Amirtharajah amd O'Melia, 1990). In this region, the $Fe(OH)_2^+$ is the predominant soluble species and remains so up to a pH of around 8 (Snoeyink and Jenkins, 1980b)(Figure 3.1). At pH values above 9 the most common ion in solution is the negatively charged $Fe(OH)_4^-$ while most of the Fe will have precipitated in its solid $Fe(OH)_3$ form (Snoeyink and Jenkins, 1980b). Precipitated Fe hydroxides can be formed. Both hydrolytic and redox reactions needs to be considered and there is little agreement in the literature on the exact formation and structure of these precipitates (Deng, 1997; Duan and Gregory, 2003). A discussion on Fe precipitates where therefore considered to be outside the scope of this review.

3.5 Treatment options for enhanced NOM removal with coagulation

3.5.1 Introduction

In addition to coagulation using metal salts, several treatments can be added to enhance the efficiency of the coagulation process for removal of NOM. These processes include magnetic ion exchange (MIEX®) resin pre-treatment, oxidation processes, polymers and activated carbon. In this chapter, these additional treatment options will be reviewed with regards to their ability to improve NOM removal by looking at the additional removal of UV_{254}, DOC, THM-FP and turbidity compared with standard coagulation (Table 3.1). The main advantages, as well as disadvantages, of the treatment options will also be presented and summarised.

3.5.2 Magnetic ion exchange (MIEX®) resin pre-treatment

3.5.2.1 Introduction

MIEX® is a type 1 strong base anion (SBA) resin consisting of beads with a particle size of 150-180 µm. The resin is used in the chloride form and has ammonia functional groups (Mergen *et al.,* 2008). The beads have a macro porous polyacrylic structure with a dispersed magnetic component. The resin beads remove anions by ion exchange with Cl^- and can therefore be used in water treatment for removal of organics such as humic substances which are essentially anionic polyelectrolytes (Bolto and Gregory, 2007). The ion exchange process can be divided into three stages: 1) ion exchange; 2) separation from the treated water; 3) regeneration. At full scale, the ion exchange reaction is carried out in a mixed reactor. The resin is separated from the water in a settler in which the resin clarifies rapidly due to its high density and magnetic properties (Mergen *et al.,* 2008). Between 80-95 % of the resin is recirculated into the reactor and the rest is regenerated using a concentrated brine solution (Sani *et al*., 2008). Since MIEX® can only remove dissolved anions and not particulate matter, a downstream solid-liquid separation is required. Depending on the effectiveness of the separation process, MIEX® treatment can also result in carry over of resin fines (Boyer and Singer, 2006). MIEX® treatment is therefore suitable as a pre-treatment to coagulation.

3.5.2.2 Combination of MIEX® resin and coagulation for enhanced NOM removal

Several researchers have reported more effective removal of DOC, UV_{254} and THM-FP for MIEX® compared with regular coagulation and adding MIEX® as a pretreatment together with coagulation has resulted in better removal than with coagulation alone and the coagulant dose could be reduced by 30 - 75 % (Singer and Bilyk, 2002; Drikas *et al.*, 2003; Fearing *et al.*, 2004; Boyer and Singer, 2005; Boyer and Singer, 2006; Kitis *et al*., 2007; Mergen *et al.*, 2008).

Singer and Bilyk (2002) investigated the effect of MIEX® to enhance the coagulation DBP precursors in nine surface waters (Table 3.1). The effect of MIEX® pretreatment on the requitisite alum dose needed for subsequent coagulation of turbidity was also evaluated. Enhanced coagulation with MIEX® was very effective for removing THMs

and haloacetic acid (HAA) precursors from all waters tested. The best results were seen in the waters with high SUVA. Residual DOC, UV_{254}, THM-FP and HAA-FP were all lower as a result of combined MIEX® and alum treatment compared to alum coagulation alone. The coagulant demand was also substantially lowered. Boyer and Singer (2006) evaluated the NOM and bromide removal capacity of MIEX® on a continuous–flow pilot scale basis. The raw water used had moderate UV_{254} absorbance and DOC concentration, low turbidity and alkalinity. MIEX® treated water was coagulated at bench scale using alum and measured for turbidity. The coagulant demand was reduced by 67 % following MIEX® treatment. This was attributed to the removal of organic material with a high coagulant demand by MIEX®.

Fearing *et al.* (2004) tested MIEX® as pretreatment on a high SUVA humic rich water at bench scale. They observed removals of above 80 % DOC and around 85 % UV_{254} absorbance when MIEX® was used alone. When combined with significantly reduced doses of coagulant, a slight improvement in DOC and UV_{254} removal was observed. The THM-FP potential of the treated water was however significantly reduced compared to treatment with coagulation only. Kitis *et al.* (2007) treated raw water samples from five drinking water treatment plants around the city of Istanbul (Table 3.1). Jar tests were applied to test the impacts of MIEX® pretreatment prior to coagulation on coagulant demand. Depending on the raw water, the use of MIEX® as a pre-treatment to coagulation with alum reduced the coagulant demand by 25 – 50 %. Increasing MIEX® dose generally decreased the SUVA values indicating that the MIEX® resin preferably removed UV_{254} absorbing fractions of NOM. This is in agreement with Boyer and Singer (2005) who tested MIEX® as a pretreatment at bench scale on four different waters with low turbidity and low to moderate DOC concentrations. They found that the removal of UV_{254} absorbing substances for MIEX® was more effective on waters with a SUVA > 3.0 mg $m^{-1}L^{-1}$and less effective on water with a SUVA < 3.0 mg $m^{-1}L^{-1}$. This suggested that removal of UV_{254} absorbing material increased as the raw water SUVA increased. Jonhson and Singer (2004) treated highly coloured, high NOM water with different doses of MIEX®. The DOC concentration and UV_{254} absorbance decreased at about the same rate with increasing MIEX® dose. This meant that the SUVA of the treated water was relatively constant for each dose suggesting that both hydrophobic and hydrophilic substances

were removed to the same degree. Drikas et al. (2003) reported increased removal of DOC and UV_{254} on a low SUVA water. However, no reduction in coagulant dose was achieved (Table 3.1).

Singer *et al.*, (2007) operated a pilot plant for four to five weeks at each of four US water treatment plants to evaluate the effectiveness of MIEX®. Raw and treated water was fractionated into its hydrophobic, transphilic and hydrophilic fractions. The results showed a more effective removal of the hydrophobic and transphilic fractions than of the hydrophilic fraction, which also included hydrophilic bases and neutral species. The DOC of the raw water was fractionated according to molecular weight using membranes with MW cut offs of 1, 10 and 30 kDa. The MIEX® resin was least effective at removing the <1 kDa fraction and increased in effectiveness as the MW of the NOM increased, being most effective at removing the largest molecular weight fraction. Mergen *et al.* (2008) tested MIEX® as a pretreatment at bench scale on three waters with different hydrophobicity. In order to more appropriately mirror how the resin is used operationally, the MIEX® resin was contacted with raw water 15 consecutive times without regeneration resulting in bed volumes equivalent to those at full-scale. The results showed that for the most hydrophobic water, the removal capacity of the resin was reduced from 65 to 4 % between the first and the 15th use. This was explained by saturation of the resin or blocking of the resin pores by the high MW humic and fulvic acids that dominated the hydrophobic water**.** In summary, adding MIEX® as a pre-treatment can increase NOM removal and reduce coagulant dose, but the efficiency of the resin is reduced with time, especially when treating hydrophobic water.

3.5.3 Oxidation processes

3.5.3.1 Introduction

Oxidation processes in NOM removal involves the mineralisation or break down of organic material. In principle, oxidation reactions allow degradation of organic pollutants into small harmless species and ultimately into CO_2 (Shon *et al.*, 2005). This eliminates sludge production with subsequent cost reduction. A common oxidation treatment is ozonation which has been widely adopted as a pre oxidant prior to coagulation (Yan *et al.*, 2007). Other, more sophisticated oxidation techniques are the so called advanced oxidation processes (AOPs). These include Fenton's reagent (FR), photo Fenton's reagent and TiO_2 photocatalysis.

The aim of an AOP is to bring about the formation of hydroxyl radicals ($HO^{\cdot}$). The $HO^{\cdot}$ is the second strongest oxidizing agent after fluorine (Parsons and Williams, 2004). This can be achieved using UV photolysis through photo-induced processes such as in photo Fenton's reagent or photocatalysis on the surface of TiO_2. Illumination of the TiO_2 material with UV light induces the excitement of electrons in the material making it highly oxidative, which in turn causes oxidation of H_2O into $HO^{\cdot}$ radicals (Huang *et al.*, 2008; Liu *et al.*, 2008). NOM is degraded by oxidation both on the surface of the TiO_2 material as well as by the $OH^{\cdot}$ radicals. Details of the oxidation reactions are described elsewhere (Bertelli and Selly, 2006).

The hydroxyl radical can also be formed by the "dark" Fenton's process which involves the use of an oxidising agent (for example H_2O_2) and a catalyst (often a metal salt) (Wadley and Waite, 2004). AOPs can oxidize organic compounds significantly faster than ozone (Parsons and Jefferson, 2006b). For example, the rate constant for oxidation of benzene is 2 $M^{-1}s^{-1}$ for ozone and 7.8×10^9 $M^{-1}s^{-1}$ for $HO^{\cdot}$ (Parsons and Williams, 2004). However, a hydroxyl radical can also form following decomposition of ozone in water during treatment (William, 1999). A series of simple reactions will follow the formation of a hydroxyl radical. A very large number of reactions are possible which are very difficult to predict. The rate of oxidation depends on the concentrations of NOM, hydroxyl radical and oxygen (Parsons and Williams, 2004).

3.5.3.2 Combinations of oxidation processes and coagulation

Murray and Parsons (2004a) compared NOM removal using a range of AOPs and also performed an economic assessment of the processes (Table 3.1). The removal efficiency of DOC and UV_{254} from synthetic and real humic rich water were tested. Comparisons between Fenton's reagent (FR), photo Fenton's reagent (PFR) and TiO_2 photocatalysis were carried out at bench scale and compared with coagulation using ferric sulphate and alum. The PFR and TiO_2 processes removed DOC levels quickly and 90 % reduction in UV_{254} was achieved within 30 minutes. NOM removal was influenced by TiO_2 dose and the optimum dose identified was 5 gL^{-1}. All AOP processes tested outperformed the traditional metal salts for UV_{254} removal. All AOP processes removed an excess of 80 % DOC and the two Fenton's processes outperformed TiO_2 photocatalysis. This removal resulted in reduction of THM-FP from 140 to below 10 μgL^{-1} which was well below UK and US standards. However, economic assessment of the processes revealed that they were not economic at the present time compared with conventional coagulation.

TiO_2 photocatalysis in combination with coagulation was studied by Huang *et al.* (2008). The reaction kinetics increased with increasing TiO_2 dosage while increasing initial TOC concentration was found to decrease the reaction kinetics (Huang *et al.*, 2008). The TiO_2/UV process has been found to change NOM molecular characteristics in terms of MW and SUVA due to the preferential transformation and removal of hydrophobic high MW organic compounds. For this reason the TiO_2/UV process has been found to be effective in controlling fouling of low pressure membranes (Huang *et al.*, 2008).

Shon *et al.* (2005) tested the effect of $FeCl_3$ flocculation as a pretreatment to TiO_2 photocatalysis for DOC removal and found improved results compared to TiO_2 treatment alone. Photocatalysis caused degradation of large MW organic material into smaller molecules. After 2 hrs, degradation of the high MW fraction was complete and degradation of the small MW fraction started. Pretreatment with $FeCl_3$ removed the large MW material and the small MW hydrophilic NOM which was still in the water after coagulation could be degraded by TiO_2 photocatalysis.

An increase in the amount of small MW NOM by oxidation was also reported by Becker and O'Melia (2001) when ozone was used as a pretreatment to coagulation with alum. Breakdown of large MW organic material into smaller more oxygenated compounds increased the coagulant demand. A model water with a TOC of 10 mgL^{-1} was used, for which the optimum coagulant dose was 100 mgL^{-1} of alum. Filtered water DOC without preozonation was approximately 2 mgL^{-1}, but with preozonation using ozone doses between 0.1 and 2.0 mg O_3/mg DOC, filtered water DOC increased to 3.5 mgL^{-1}. The effect of preozonation was also tested on a water containing TOC concentration of 1 mgL^{-1} for which the optimum alum dose was 20 mgL^{-1}. Preozonation with a dose of 1-2 mg O_3/mg DOC, caused a 50 % reduction in optimum alum dose to 10 mgL^{-1}. For this water, the amount of dissolved organic matter was small and the optimum alum dose was set by the particles and adsorbed organic matter. When ozone reacts with the organic matter adsorbed to the particle surface, it can alter the stability of the particle resulting in a reduced coagulant demand (Becker and O'Melia, 2001).

Bose and Reckhow (2007) studied ozonation prior to adsorption onto preformed aluminium hydroxide flocs. They reported increased removal of organic material by direct adsorption to preformed aluminium hydroxide on water with a low concentration of DOC. They observed a reduced adsorption of the fulvic and the humic acid fraction and an increased adsorption of the hydrophilic neutral fraction as a result of preozonation. On raw, unfractionated water, an increase in ozone dose resulted in a reduction in DOC removal by alum coagulation. The ozone appeared to react preferably with the humic and fulvic fractions thereby magnifying the detrimental effects of ozone on coagulation seen on the fractionated water. When ozonation was applied to pre coagulated raw water, an increase in adsorption to preformed aluminium hydroxide flocs was observed (Bose and Reckhow, 2007). This followed the removal of humic and fulvic acid fractions by coagulation. The results showed an ability of ozone to improve removal of NOM fractions which are difficult to remove using coagulation. However, Yan *et al.* (2007) reported how ozone can reduce the removal of NOM by coagulation (Table 3.1). The impact of pre-ozonation on coagulation for particle and NOM removal was investigated at pilot scale on water sampled from north China source water. At doses of 1.0 mgL^{-1} O_3 pre-ozonation functioned as a coagulant aid in the removal of UV_{254} and turbidity. At doses of 2.0

mgL^{-1} pre-ozonation had a negative impact on UV_{254} removal but was still beneficial for turbidity removal. This was the result of a shift towards a more hydrophilic NOM composition with a larger fraction of low MW organic material with increased ozone dose. This shift consequently led to reduced coagulation performance.

Chen *et al*. (2007) conducted a two year long pilot study to investigate different treatment options (Table 3.1). Among them were coagulation followed by air flotation and filtration with and without preozonation. It was found that preozonation increased NOM removal and decreased THM-FP (Table 3.1). Ozonation was also found to reduce biodegradability by decomposing refractory organic matter and a combination of ozonation and biological activated carbon gave the best results in terms of biostability control. The same combination also successfully satisfied the COD_{Mn} national standard criteria in China with a concentration of 2.79 mgL^{-1}. The COD_{Mn} concentration after treatment with conventional coagulation air flotation filtration was 5 mgL^{-1} and preozonation did not enhance COD_{Mn} removal. This was attributed to the incomplete oxidation of organic matter with limited ozone dosage.

3.5.4 Polymers

3.5.4.1 Introduction

Polymers are compounds with repeated linked units of high MW that range from a few thousand up to tens of millions. They are widely used in water treatment as primary coagulants dosed in the coagulation stage and as coagulant aids where the polymer is added after destabilisation to aid in the aggregation process (Bolto and Gregory, 2007). All polymers used in water treatment are water soluble and most of them are synthetic while there are some natural polymers available as well. Polymers can be characterised as being cationic, anionic or non-ionic. The cationic and anionic polymers have a functional group in their linked units which ionise when they dissociate making positively or negatively charged sites available. The main mechanisms of action for polymers in water treatment are adsorption and polymer bridging. The more prevalent mechanism is dependent on which type of polymer is used. Polymers which remove NOM with adsorption mechanisms are more useful as primary coagulants while polymer bridging is a useful mechanism for producing stronger flocs. Therefore, polymers which are efficient at polymer bridging are useful as coagulant aids to improve aggregation. Dosed as a primary coagulant a polymer can improve the coagulation process by reducing the coagulant dose needed and enable more removal mechanisms for NOM (Bolto and Gregory, 2007). Polymer bridging leads to the formation of larger and stronger flocs (Bolto and Gregory, 2007).

Polymer adsorption into organic material can be the result of electrostatic interaction, hydrogen bonding, hydrophobic interaction and ion binding (Bolto and Gregory, 2007). Electrostatic interaction is caused by the attraction between oppositely charged ionic groups (for example a cationic polyelectrolyte on a negatively charged surface). Adsorption via hydrogen bonding can occur at suitable H-bonding sites on the particle surface with for example amide groups on the polymer. Ion binding occurs between anionic polyeletrolytes and negatively charged surfaces despite electrostatic repulsion. This type of adsorption is made possible by the presence of divalent metal ions which act as bridges between the polymer and the particle (Berg *et al.*, 1993).

Tails of adsorbed polymers have the ability of adsorbing to other particles and bridge them together. Flocs formed in this way grow larger for a given shear rate then those formed by metal salts (Bolto and Gregory, 2007) and are hence stronger (Yukselen and Gregory, 2004). For successful polymer bridging, there must be sufficient unoccupied surface area on the particles to allow adsorption to the polymer chains. Overdosing results in particles covered in polymer and no bridging takes place. If the polymer dose is too low, not enough bridging contacts can be formed making optimisation of polymer dose essential for successful particle bridging.

The most relevant modes of action for NOM removal using coagulants are charge neutralisation through electrostatic interactions and polymer bridging. Cationic polymers are the most suitable to use as primary coagulants for NOM removal because they reduce the negative surface charge of dissolved organics through electrostatic interaction, hence decreasing the repulsive charge between them. Kleimann *et al.* (2005) found that cationic polymer doses resulting in a zeta potential close to zero gave optimum flocculation of latex particles. The correlation between optimum dose and charge neutralisation has also been found for coagulation of humic substances (Kvinnesland and Odengaard, 2004). Further, higher charge density (CD) polyeletrolytes have been found to be more efficient in removing humic substances then low CD polyeletrolytes (Kam and Gregory, 2001).

3.5.4.2 Combinations of polymers and coagulation for enhanced NOM removal

Edzwald and Tobiason (1999) compared the removal efficiency of alum with and without the addition of a cationic polymer (Table 3.1). A dual coagulation strategy was developed for alum and cationic polymer for use in a full scale dissolved air flotation plant. When the polymer was added to the process, the removal of DOC was increased by 8 % (Table 3.1). More importantly, the alum dose was reduced and the need for NaOH dosing to correct the pH was eliminated. Sludge production was also decreased by 30 %, most likely as a result of the reduced alum dose. No difference in residual turbidity was observed as turbidity after filtration was below 0.1 NTU following both treatment strategies. Despite the cost of the polymer being 8 times more than that of alum, the overall chemical cost was reduced when polymer was

added to the process. This combined with the lower cost associated with a reduced sludge production, resulted in a total reduced cost of 22 %.

Dosing alum together with the cationic polymer polydiallyldimethyl-ammonium chloride (PDADMAC) increased NOM removal and reduced the coagulant demand on reconstituted water containing aquatic NOM at bench scale (Bolto *et al.*, 1999; Bolto *et al.*, 2001) (Table 3.1). Bolto *et al.* (1999) observed a synergistic effect from using alum and polymer together when comparing the performance of a set of different polymers and alum. When polymer and alum were used separately, alum was the more effective coagulant and the performance of polymer was dependent on the charge density such as an increase in charge increased removal. Polymers were also found to perform better in the presence of particles. Dosing alum together with polymer proved an accessible way of introducing suspended matter hence increasing the performance of polymer and resulting in a synergistic effect on removal. The solids served as both an adsorbent for NOM as well as a nucleating species for precipitating the NOM-polymer complex (Bolto *et al.*, 2001).

The addition of the cationic polymer PDADMAC to coagulation with ferric sulphate did not improve floc structure (Jarvis *et al.*, 2006) (Table 3.1). Floc size and compaction was reduced when polymer was added together with ferric sulphate. Kim *et al.* (2001) have reported that flocs formed with charge neutralization are smaller and less compact then flocs formed with sweep flocculation on a high DOC river water. This suggested that addition of polymer enhanced the charge neutralization process. It was suggested that the charge neutralization process was favoured over sweep flocculation due to rapid adsorption of polymer onto microflocs and colloid particles (Jarvis *et al.*, 2006).

3.5.5 Activated carbon

3.5.5.1 Introduction

Activated carbon is used for the removal of NOM by adsorption either as granular activated carbon (GAC) with a particle diameter of 1 – 2 mm diameter or as powder activated carbon (PAC) with a particle diameter of < 0.1 mm (Parsons and Jefferson, 2006a). In the granular form it is used in contacters or "columns". Water is fed into the top and NOM is adsorbed onto the activated carbon as the water is passed through the contactor. PAC is usually added to the water in the form of a slurry either in a mixing tank or in a flocculator tank (Faust and Aly, 1998).

Activated carbon can be produced from a variety of sources, for example wood, coconut shells, bone and coal. The adsorptive properties of activated carbon are due to its large surface area and highly porous nature (Faust and Aly, 1987). The activation process involves pyrolysis at high temperatures and oxidation of the carbon and can be varied to alter the surface properties for specific purposes. During activation, a large internal surface area is created consisting of pores. For example, the internal surface area of ground coal can be increased from 10 – 1000 m^2g^{-1} (Parsons and Jefferson, 2006a). Depending on commercial brand, the internal surface area can range between 400 and 1800 m^2g^{-1} (Faust and Aly, 1987) and approach 99 % of the total area of the activated carbon particle. The pores can be divided into macro and micropores, where macropores are defined as having a diameter greater than 500 Å. The micropores commonly branch off from the macropores and they have a diameter of 10 – 500 Å. The walls of the interior micropore system contribute to most of the internal surface of the activated carbon. It is in the micropores that most of the adsorption occurs while the macropores functions as conduits for transport of organics from the surface (Faust and Aly, 1998).

Four distinct steps are involved in the physical adsorption of organic compounds, namely bulk solution transport, film diffusion transport, pore transport and adsorption (Snoeyink, 1990). The organics must first be transported from the bulk solution to the boundary layer surrounding the activated carbon particle in a process called bulk solution transport. This can occur as a result of turbulent mixing in the case of flow

through a GAC contactor or during mixing with PAC. It can also occur by diffusion if the activated carbon is suspended in a sedimentation basin. When water flows past the activated carbon particle, a stationary layer called the hydrodynamic boundary layer is formed. Transport of organics through this layer is called film diffusion transport. Pore transport to available adsorption sites occurs by either pore diffusion through the solution in the pores or by surface diffusion along the surface after adsorption has taken place. The final step is adsorption to the surface of the pore.

Several properties of the activated carbon such as surface area, pore size distribution, and surface chemistry determine the adsorption efficiency of organic compounds. The surface area is related to adsorptive capacity such as increased surface area increases adsorption capacity (Faust and Aly, 1998b). This is restricted to the surface area available to the organics which in turn is determined by the pore size distribution. A large volume of macropores corresponds to a large adsorption capacity for high MW organics and a large volume of micropores is correlated with capacity for small MW organics (Snoeyink, 1990). Lee *et al.* (1981) compared the adsorption of fulvic acids derived from peat on a selection of activated carbons with different pore size distributions. It was found that activated carbons with a small volume of macropores had a relatively low adsorption capacity for the large fulvic acid molecule. The results showed correlation between pore volume within pores of a given size and the adsorption of humic substances of a given size. The surface chemistry of activated carbon also affects adsorption properties. For example, simple aromatic compounds have been found to absorb weakly to activated carbon surfaces oxygenated with ammonium persulfate (Coughlin and Ezra, 1968). Oxides consisting of acidic functional groups reduced the adsorption of oxalic and succinic acids on activated carbon (Puri, 1980). This was contributed to blockage of the surface due to preferential adsorption of water. The affinity of a particle to a surface is dependent on its affinity for the solution. Therefore, the adsorption of any organic molecule to activated carbon is a function of the organic molecule's solubility in water, such as the adsorption efficiency is increased with decreased solubility. This is because the solute – solvent bond needs to be broken before adsorption.

Molecular weight and size of an organic substance also affect its adsorption to activated carbon since these characteristics impact on the solubility of the substance. The adsorption on activated carbon of a series of alkylbenzenes increased with increased molecular weight as a result of sulfonation going from the unsubstituted to the sulfonated tetradecylbenzene (Weber and Morris, 1964). The increase in side chain length reduced the solubility in water and increased the adsorption capacity.

The more polar a substance is the more soluble it is in water and the less likely it is to adsorb on activated carbon. The introduction of a functional group on the molecule, for example a carboxyl group (-COOH), can increase solubility. Hydrogen bonds form between the partially negative atoms of the carboxyl group and the partially positive hydrogen atoms of water. Giusti *et al.* (1974) investigated the adsorption on activated carbon of straight chain aliphatic compounds of less than four carbon atoms with different functional groups. The results showed a substantial effect of functionality on adsorption. There was a correlation between the adsorption derived from any given functional group and its impact on polarity such as a stronger impact on polarity induced stronger adsorption.

Branching in the chain of an organic molecule reduces adsorbability. This was reported by Belfort (1979) who showed that adsorption of alcohols decreased accordingly; normal > iso > tertiary. The results were explained by changes in geometry of the molecules, which become more spherical with increased branching. This means a reduction in surface area available for interaction with the activated carbon surface.

3.5.5.2 Activated carbon and coagulation for enhanced NOM removal

Tomaszewska *et al.* (2004) investigated the removal of humic acids and phenol from model solution by coagulation and adsorption on PAC using PAX XL-69 polyaluminum chloride as the coagulant. The results showed that the addition of PAC was more effective then coagulation alone. This was in agreement with Uyak *et al.* (2007) who investigated the removal of DBP precursors from the Terkos Lake near the city of Istanbul by enhanced coagulation and powdered activated carbon (Table 3.1). The water was hydrophobic in nature containing a large amount of humic

material. The maximum DOC removal achieved using enhanced coagulation with ferric chloride alone was 45 %. The addition of PAC dosing increased the DOC removal by 31 % compared to with coagulation alone. Zhang *et al.* (2008) also reported increased DOC removal as well as increased removal of UV_{254} (Table 3.1). PAC was found to mostly remove uncharged low molecular weight organics but unable to remove organic material with MW < 1000 Dalton (Uyak *et al.*, 2007; Zhang *et al.*, 2008)

The effect of coagulation on GAC performance with regards to the removal of NOM and DBPs were investigated by Hooper *et al.* (1996). Coagulation effectively removed large MW compounds which are not well adsorbed by GAC. Organics with MW <500 Da was not removed by GAC. Using coagulation before GAC dosing increased the NOM removal by GAC. The coagulant reduced the NOM concentration making removal by GAC easier. Coagulation also removed the larger MW organic material which would otherwise out-compete smaller material for adsorption sites. Using coagulation before GAC meant that the smaller MW material could be adsorbed. Also, using enhanced coagulation before GAC treatment meant that the incoming water was of a lower pH. This, in turn, induced a decrease in the solubility of organics and neutralisation of the GAC surface by hydrogen ion adsorption. Coagulation prior to adsorption on GAC was also investigated by Nowack *et al.* (1999) who reported increased efficiency of GAC on coagulated water. This was attributed to a lower NOM concentration which made the remaining organics more adsorbable. This increased the service life for GAC.

Najm *et al.* (1998) investigated the removal of TOC and DBP precursors from Colorado River water using coagulation and PAC in different doses at bench scale (Table 3.1). Cost estimation for each dosing combination was performed. The results showed that the combination of coagulant and PAC can be more cost effective then using coagulation alone. PAC reduced coagulant demand which in turn resulted in less sludge.

Table 3.1: Treatment options for enhanced NOM removal.

Treatment option	Raw water characteristics	Increased removal compared with conventional coagulation	Advantage over conventional coagulation	Disadvantage compared with conventional coagulation	Reference
		Water with SUVA > 3.0 mg $m^{-1}L^{-1}$			
MIEX pretreatment + coagulation	SUVA: 5.1 mg $m^{-1}L^{-1}$ DOC: 4.3 mgL^{-1} UV_{254}: 22.0 m^{-1} Turbidity: 21.2 NTU	29% reduced coagulant dose to reach a turbidity of 0.1 NTU 29% reduced coagulant dose to reach a DOC of 1.5-1.8 mgL^{-1}	29% reduced coagulant dose		Kitis *et al.*, 2007
	SUVA: 4.5 mg $m^{-1}L^{-1}$ TOC: 10.6 mgL^{-1} UV_{254}: 47.7 m^{-1} THM-FP: 335 μgL^{-1} Turbidity: 3.0 NTU	37% increased TOC removal 16% increased UV_{254} removal 55% reduced THM-FP	83 % reduced coagulant dose		Singer and Bilyk, 2002
	SUVA: 4.0 mg $m^{-1}L^{-1}$ TOC: 26.4 mgL^{-1} UV_{254}: 109.6 m^{-1} THM-FP: 665 μgL^{-1} Turbidity: 3.4 NTU	21% increased TOC removal 16% increased UV_{254} removal 15% reduced THM-FP	70 % reduced coagulant dose		Singer and Bilyk, 2002
	SUVA: 3.9 mg $m^{-1}L^{-1}$ DOC: 2.6 mgL^{-1} UV_{254}: 10.2 m^{-1} Turbidity: 4.2 NTU	60% reduced coagulant dose to reach a turbidity of 0.1 NTU 50% reduced coagulant dose to reach a DOC of 1.5-1.8 mgL^{-1}	50-60% reduced coagulant dose		Kitis *et al.*, 2007
	SUVA: 3.9 mg $m^{-1}L^{-1}$ DOC: 2.8 mgL^{-1} UV_{254}: 10.8 m^{-1} Turbidity: 21.5 NTU	0% reduced coagulant dose to reach a turbidity of 0.1 NTU 25% reduced coagulant dose to reach a DOC of 1.5-1.8 mgL^{-1}	25% reduced coagulant dose for DOC removal	No reduction in coagulant dose for turbidity removal	Kitis *et al.*, 2007

Treatment option	Raw water characteristics	Increased removal compared with conventional coagulation	Advantage over conventional coagulation	Disadvantage compared with conventional coagulation	Reference
MIEX pretreatment + coagulation	SUVA 3.5 mg $m^{-1}L^{-1}$ TOC: 5.1 mgL^{-1} UV_{254}: 17.5 m^{-1} THM-FP: 190 μgL^{-1} Turbidity: 6.7 NTU	37% increased TOC removal 16% increased UV_{254} removal 25% reduced THM-FP	77 % reduced coagulant dose		Singer and Bilyk, 2002
	SUVA: 3.5 mg $m^{-1}L^{-1}$ DOC: 10.0 mgL^{-1} UV_{254}: 34.6 m^{-1}	23% increased DOC removal 18% increased UV_{254} removal	50% reduced coagulant dose		Drikas *et al.*, 2003
	SUVA: 3.5 mg $m^{-1}L^{-1}$ DOC: 3.1 mgL^{-1} UV_{254}: 10.7 m^{-1} Turbidity: 1.0 NTU	25% reduced coagulant dose to reach a turbidity of 0.1 NTU 50% reduced coagulant dose to reach a DOC of 1.5-1.8 mgL^{-1}	25-50% reduced coagulant dose		Kitis *et al.*, 2007

Treatment option	Raw water characteristics	Increased removal compared with conventional coagulation	Advantage over conventional coagulation	Disadvantage compared with conventional coagulation	Reference
		Water with a SUVA < 3.0 mg $m^{-1}L^{-1}$			
MIEX pretreatment + coagulation	SUVA: 3.0 mg $m^{-1}L^{-1}$ TOC: 2.8 mgL^{-1} UV_{254}: 8.1 m^{-1} THM-FP: 164 Turbidity: 7.7 NTU	42% increased TOC removal 48% increased UV_{254} removal 45% reduced THM-FP	66 % reduced coagulant dose		Singer and Bilyk, 2002
	SUVA: 2.0 mg $m^{-1}L^{-1}$ TOC: 2.8 mgL^{-1} UV_{254}: 5.6 m^{-1} THM-FP: 119 μgL^{-1} Turbidity: 4.1 NTU	47% increased TOC removal 52% increased UV_{254} removal 64% reduced THM-FP	50 % reduced coagulant dose		Singer and Bilyk, 2002
	SUVA: 2.7 mg $m^{-1}L^{-1}$ TOC: 4.3 mgL^{-1} UV_{254}: 10.6 m^{-1} THM-FP: 131 μgL^{-1} Turbidity: 7.1 NTU	TOC:- 36% increased UV_{254} removal 47% reduced THM-FP	70 % reduced coagulant dose		Singer and Bilyk, 2002
	SUVA: 2.7 mg $m^{-1}L^{-1}$ DOC: 3.1 mgL^{-1} UV_{254}: 8.4 m^{-1} Turbidity: 1.4 NTU	0% reduced coagulant dose to reach a turbidity of 0.1 NTU		No reduction in coagulant dose	Kitis *et al.*, 2007

Treatment option	Raw water characteristics	Increased removal compared with conventional coagulation	Advantage over conventional coagulation	Disadvantage compared with conventional coagulation	Reference
MIEX pretreatment + coagulation	SUVA: 2.7 mg $m^{-1}L^{-1}$ TOC: 8.7 mgL^{-1} UV_{254}: 13.5 m^{-1} THM-FP: 239 μgL^{-1} Turbidity: 55 NTU	28% increased TOC removal 50% increased UV_{254} removal 36% reduced THM-FP	56 % reduced coagulant dose		Singer and Bilyk, 2002
	SUVA: 1.4 mg $m^{-1}L^{-1}$ TOC: 2.6 mgL^{-1} UV_{254}: 3.0 m^{-1} THM-FP: 73 μgL^{-1} Turbidity: 1.9 NTU	23% increased TOC removal 50% increased UV_{254} removal 39% reduced THM-FP		No reduction in coagulant dose	Singer and Bilyk, 2002
	SUVA: 2.4 mg $m^{-1}L^{-1}$ DOC: 5.8 mgL^{-1} UV_{254}: 13.7 m^{-1}	36% increased DOC removal 36% increased UV_{254} removal		No reduction in coagulant dose	Drikas *et al.*, 2003
	SUVA[a]: 1.9 mg $m^{-1}L^{-1}$ TOC: 4.6 mgL^{-1} UV_{254}: 8.8 m^{-1} THM-FP: - Turbidity: 2.7 NTU	TOC:- 52% increased UV_{254} removal THM-FP:-	60 % reduced coagulant dose		Singer and Bilyk, 2002

[a] = SUVA based on TOC

Treatment option	Raw water characteristics	Increased removal compared with conventional coagulation	Advantage over conventional coagulation	Disadvantage compared with conventional coagulation	Reference
		Water with a SUVA > 3.0 mg $m^{-1}L^{-1}$			
Polymer and coagulation	SUVA: 7.4mg $m^{-1}L^{-1}$ DOC: 6.9mgL^{-1} UV_{254}: 50.8m^{-1} Turbidity: 5.0 NTU	DOC: 2% increase in removal Turbidity 30 % higher turbidity		Negligible increase in DOC removal and an increase in turbidity. No improvement on floc structure.	Jarvis *et al.* 2006
		Water with unknown SUVA			
Polymer and coagulation	-	Increased removal DOC: 8 %	40 % reduced coagulant dose 30 % less sludge production 22% lower cost		Edzwald and Tobiason 1999
	-	No increased UV_{254} removal	43% reduced coagulant dose		Bolto *et al.* 2001
	-	7 % increased UV_{254} removal		No reduction in coagulant dose	Bolto *et al.* 2001
	-	2 % increased UV_{254} removal	67% reduced coagulant dose		Bolto *et al.* 2001

Treatment option	Raw water characteristics	Increased removal compared with conventional coagulation	Advantage over conventional coagulation	Disadvantage compared with conventional coagulation	Reference
Polymer and coagulation	Reconstituted water DOC: 5mgL^{-1}	No increased UV_{254} removal	43% reduced coagulant dose		Bolto *et al.* 1999
	Reconstituted water DOC: 5mgL^{-1}	5% increased UV_{254} removal	67% reduced coagulant dose		Bolto *et al.* 1999
	Reconstituted water DOC: 5mgL^{-1}	No increased UV_{254} removal	67% reduced coagulant dose		Bolto *et al.* 1999
		Water with a SUVA > 3.0 mg $m^{-1}L^{-1}$			
PAC and coagulation	SUVA: 3.1 mg $m^{-1}L^{-1}$ DOC: 4.4mgL^{-1} UV_{254}: 13.6m^{-1} THM-FP: 301µgL^{-1}	31 % increased TOC removal 21% increased UV_{254} removal 25% reduced THM-FP potential			Uyak *et al.* 2007
		Water with a SUVA < 3.0 mg $m^{-1}L^{-1}$			
PAC and coagulation	SUVA: 1.4 mg $m^{-1}L^{-1}$ DOC: 2.8mgL^{-1} UV_{254}: 4.0m^{-1}	68 % lower THM-FP			Najm *et al.* 1998
	SUVA: 0.8 mg $m^{-1}L^{-1}$ DOC: 5.7mgL^{-1} UV_{254}: 4.7m^{-1}				

Treatment option	Raw water characteristics	Increased removal compared with conventional coagulation	Advantage over conventional coagulation	Disadvantage compared with conventional coagulation	Reference
Water with SUVA > 3.0 mg $m^{-1}L^{-1}$					
Fenton's reagent and coagulation	SUVA: 5.1mg $m^{-1}L^{-1}$ DOC: 7.5mgL^{-1} UV_{254}: 38.1m^{-1} THM-FP:140µgL^{-1}	5% increased DOC removal 1% increased UV_{254} removal	>90% removal of organic matter with MW <3kD		Murray and Parsons, 2004a
Photo Fenton's reagent and coagulation	SUVA: 5.1mg $m^{-1}L^{-1}$ DOC: 7.5mgL^{-1} UV_{254}: 38.1m^{-1} THM-FP:140µgL^{-1}	1% increased DOC removal 3% increased UV_{254} removal	>90% removal of organic matter with MW <3kD		Murray and Parsons, 2004a
TiO_2/UV and coagulation	SUVA: 5.1mg $m^{-1}L^{-1}$ DOC: 7.5mgL^{-1} UV_{254}: 38.1m^{-1} THM-FP:140µgL^{-1}	7% reduced DOC removal 5% increased UV_{254} removal	>90% removal of organic matter with MW <3kD		Murray and Parsons, 2004a
Water with SUVA < 3.0 mg $m^{-1}L^{-1}$ and unknown SUVA					
Preozonation and coagulation	SUVA[a]:1.8mg $m^{-1}L^{-1}$ TOC: 6.5mgL^{-1} UV_{254}: 11.6m^{-1} TMH-FP: 407µgL^{-1}	4% increased TOC removal 15% increased UV_{254} removal 8% reduced THM-FP	Enhanced biodegrability of organic material		Chen *et al.* 2007
	TOC: 3.8mgL^{-1} Turbidity: 8.2NTU	1.4% increased UV_{254} removal 9 % increased turbidity removal		Increased UV_{254} after coagulation when ozone was overdosed	Yan *et al.* 2007

3.5.6 Summary of treatment options for enhanced NOM removal

MIEX® has been shown to be effective as a pretreatment before coagulation for NOM removal. The resin removes more DOC and reduces the THM and HAA-FP of the water than traditional coagulation. MIEX® used as a pre-treatment was able to reduce the coagulant demand (Singer and Bilyk, 2002; Fearing *et al.,* 2004; Boyer and Singer, 2005; Boyer and Singer, 2006; Kitis *et al*., 2007; Mergen *et al.*, 2008). Large MW hydrophobic UV_{254} absorbing organic material was preferably removed by MIEX® (Kitis *et al*., 2007, Boyer and Singer, 2005) although it was also reported to remove non UV_{254} absorbing NOM (Jonhson and Singer, 2004). Treatment of high SUVA waters at full scale with a 10 % regeneration rate eventually reduced the removal capacity of the resin because large MW organics clog the pores of the resin and saturates the resin (Mergen *et al.*, 2008).

Oxidation changes the character of the NOM by breaking down large organic material into smaller substances and ultimately to CO_2. A shift in the NOM make-up towards smaller MW hydrophilic material can lead to reduced coagulation efficiency following that coagulation is relatively poor at removing low MW hydrophilic material (Yan *et al.,* 2007; Fearing et al., 2004). Using coagulation prior to oxidation with TiO_2 photocatalysis resulted in breakdown of small MW hydrophilic NOM which was still in the water after coagulation (Shon *et al.,* 2005). At low concentrations of dissolved organic matter with a large amount of particles with adsorbed organic material, oxidation by preozonation aids in the coagulation process by reducing the stability of the particles (Becker and O'Melia, 2001). A disadvantage with AOPs is the unspecific reactive nature of the hydroxyl radical which can lead to the possible production of by-products with unknown toxicity. The UV light required for photocatalytic treatment results in high operating costs (Murray and Parsons 2004a; Murray and Parsons, 2004b). Advances in lamp technology should make the treatment economically feasible in the future but until then, the treatment is too expensive (Murray and Parsons 2004a; Murray and Parsons, 2004b).

Adding cationic polyelectrolytes to the coagulation process can improve removal and reduce coagulant demand. (Edzwald and Tobiason, 1999; Bolto *et al.*, 1999; Bolto *et al.*, 2001). The efficiency increases with increased CD (Bolto *et al.*, 1999; Kam and Gregory, 2001) and in the presence of particles which serve as both an adsorbent for NOM as well as a nucleating species for precipitating the NOM-polymer complex (Bolto *et al.*, 2001). When cationic polymer is added to coagulation with Fe, the flocs formed were smaller and less compact, most likely because of increased charge neutralisation.

Using activated carbon together with coagulation can increase NOM removal performance (Tomaszewska *et al.*, 2004; Uyak *et al.*, 2007). Activated carbon had the ability to remove small MW organic substances which are difficult to remove with coagulation (Uyak *et al.*, 2007). Coagulation easily removed large MW organic substances which out-competed smaller substances for adsorption on activated carbon (Hooper *et al.*, 1996; Nowack *et al.*, 1999). The combination of coagulation and activated carbon therefore complement one another. The combination of activated carbon was also found to be more cost effective then coagulation alone (Najm *et al.*, 1998).

3.6 A novel coagulant as a treatment option for enhanced NOM removal

An additional treatment option for enhanced NOM removal has been proposed in the form of a novel highly charged coagulant based on the tetravalent Zr ion (Zr^{4+}).

Zr occurs widely over the earth's crust and comprises 0.016% (162 ppm) of the earth's crustal rocks (Greenwood and Earnshaw, 1998; Cotton et al., 1999b). This makes Zr the fourth most abundant transition metal after Fe, Ti and Mn (Greenwood and Earnshaw, 1998). The main mineral forms of Zr are zircon ($ZrSiO_4$) and baddeleyite (ZrO_2) which are mainly mined in the USA, Russia, Australia and the republic of South Africa (Greenwood and Earnshaw, 1998). Due to its corrosion resistance and mechanical stability Zr has many uses in industry, for example in superconducting alloys, alternatives to stainless steel and as cladding for uranium dioxide fuel rods in water cooled nuclear reactors (Greenwood and Earnshaw, 1998).

The aqeous chemistry of Zr is complex and more research is needed to reach a complete understanding of all mechanisms involved (Ekberg *et al.*, 2003; Cho *et al.*, 2005; Kobayashi *et al.*, 2007). Most research on the water chemistry of Zr has focused on the polymeric species formed at low pH levels (Richens, 1997; Cotton *et al.*, 1999b; Ekberg *et al.*, 2003). In aqueous solutions, Zr^{4+} is the only stable valency state and tends to be extensively hydrolysed (Kroschwitz and Howe-Grant, 1999). It is a relatively large and spherical ion which shows high coordination numbers (up to eight) and a multitude of coordination polyhedral (Cotton *et al.*, 1999b). Zr has a strong tendency towards hydrolysis and both hydroxylation and precipitation of Zr^{4+} occurs at pH levels below 2 (Baes and Mesmer, 1976; Ekberg *et al.*, 2003; Cho *et al.*, 2005). Free Zr^{4+} ions only exists under highly acidic conditions ($[H^+]$ of 1-2 M) at very low concentrations ($[Zr^{4+}]$ of 10^{-4} M) (Cotton *et al.*, 1999b). Upon reducing the acidity of the solution to pH levels between 0.5 - 1.5 the tetranuclear species $Zr_4(OH)_8(H_2O)_{16}^{8+}$ and the octanuclear species $Zr_8(OH)_{20}(H_2O)_{24}^{12+}$ are formed (Toth *et al.*, 1996; Matsui and Ohgai, 2002). The polynuclear $Zr_4(OH)_8(H_2O)_{16}^{8+}$ has a μ-hydroxy bridged tetranuclear form where each Zr ion binds to eight other atoms (Richens, 1997). The existence of mononuclear species such as $Zr(OH)^{3+}$, $Zr(OH)_2^{2+}$ and $Zr(OH)_3^{+}$ as well as of dimers such as $Zr_2(OH)_6^{2+}$ and $Zr_2(OH)_7^{+}$ and trimers

such as $Zr_3(OH)_4^{8+}$ and $Zr_3(OH)_5^{7+}$ have also been postulated (Baes and Mesmer, 1976; Veyland *et al.*, 1998; Ekberg *et al.*, 2003). The mononuclear species are only considered to exist in solutions with Zr concentrations below 10^{-6} M (Kobayashi *et al.*, 2007). The formation of the dimer $Zr_2(OH)_6^{2+}$ varies greatly with zirconium concentration in the pH range from 0-3 while neither $Zr_3(OH)_4^{8+}$ or $Zr_4(OH)_8(H_2O)_{16}^{8+}$ are condisered to exist in solution above pH 2 (Ekberg *et al.*, 2003). Tetrameric structures have been found to form oligomeric structures during an increase in pH from 0.2 to 3 (Cho *et al.*, 2005). This could explain the removal of $Zr_4(OH)_8(H_2O)_{16}^{8+}$ from solution. Also, precipitated hydrolysis species have been found to contain tetrameric units of with $Zr_4(OH)_8(H_2O)_{16}^{8+}$ hydroxyl bridges (Fryer *et al.*, 1970).

There is a wide variation in the solubility data for Zr species obtained by different researchers depending on the method used and wether or not polymeric species have been considered (Cho *et al.*, 2005; Kobayashi *et al.*, 2007). This prevents the compilation of a reliable speciation diagram to describe the solubility of Zr species as a function of pH (Cho *et al.*, 2005). Solubility of Zr species is to a large extent controlled by equilibrium with aqueous $Zr(OH)_4$ which did not reach equilibrium during a period of four months in laboratory tests (Ekberg *et al.*, 2003; Kobayashi *et al.* 2007). It has been suggested that aqueous $Zr(OH)_4$ species account for 99 % of dissolved Zr at pH levels around 4 with the other 1 % being in the $Zr(OH)_3^+$ form (Lowalekar *et al.*, 2006). However, it has also been suggested that solid $Zr(OH)_4$ dominates in solution from pH 3 up to around pH 12 with $Zr_2(OH)_7^+$ and $Zr(OH)_3^+$ simultanously being present between pH 3 and 8 (Veyland *et al.*, 1998). Above pH 9 those species have been replaced by the negatively charged $Zr(OH)_5^-$ which dominates in solution at pH levels at around 13 and above (Veyland *et al.*, 1998). At pH levels above 12.5, the solubility of solid $Zr(OH)_4$ is reduced due to the formation of the the zirconate ion according to the following reaction (Ekberg *et al.*, 2003):

$$Zr(OH)_{4(s)} + 2OH^- \rightarrow ZrO_3^{2-} + 3H_2O$$

$ZrO_2 \cdot nH_2O$ can also form under alkaline conditionson (Kroschwitz and Howe-Grant, 1999). This dioxide is considered virtually insoluble in excess base and there is no convincing evidence for the existence of a ZrO^{2+} ion (Cotton et al., 1999b). Dudeney *et al.* (1991) showed that alkyl carboxylate surfactants can be removed from the

aqueous phase by adsorption onto growing particles of $ZrO_2.nH_2O$ by rendering the resulting particles hydrophobic. Precipitates of complex acids of Zr can also be separated from solutions of Zr salts after addition of α–hydroxycarboxylic acids because of the formation of insoluble chelates (Blumenthal, 1963). Zirconium compounds have a high affinity for carboxyl groups in various compounds. This has been shown by the irreversible adsorption of proteins in HPLC packings and the chemical bonding to organic acids in metal oxide surface adsorption applications, which was superior to both Fe and Al (Sun and Carr, 1995; Purvis *et al.*, 1998; Vanderkam *et al.*, 1998). Results from adsorption experiments SiO_2 wafers have also shown that Si-O-Zr bonds can form by reaction between neutral $Zr(OH)_4$ species and surface silanol groups (Lowalekar *et al.*, 2006).

The novel coagulant presented in this thesis consists of the oxychloride salt of Zr which is prepared by hydrolysation of the tetrahalide $ZrCl_4$ (Cotton *et al.*, 1999b). The structure of $ZrCl_4$ consists of zigzag chains of $ZrCl_6$ octahedra and is hydrolysed in water according to the following reaction (Cotton *et al.*, 1999b):

$$ZrCl_4 + 9H_2O \rightarrow ZrOCl_2 \cdot 8H_2O + 2HCl$$

The tetravalent Zr^{4+} ion has a higher charge per mole than traditionally used coagulants based on Fe^{3+} and Al^{3+}. Charge neutralisation is a fundamental mechanism by which NOM is removed during coagulation and optimum NOM removal occurs between the iso-electric point (i.e.p.) of the coagulant and the NOM (Sharp *et al.*, 2006a, Sharp *et al.*, 2006b). The higher charge of Zr^{4+} is therefore hypothesised to improve charge neutralisation and subsequent NOM removal. Zr has also shown high affinity for organic material (Blumenthal, 1963; Dudeney *et al.*, 1991; Sun and Carr, 1995; Purvis *et al.*, 1998; Lowalekar *et al.*, 2006). Zr can also reach high coordination numbers resulting in a large number of chemical bonds (Cotton *et al.*, 1999b). The proposed Zr based coagulant is therefore hypothesised to induce complexation and adsorption mechanisms to a high degree. The size the Zr^{4+} is also relatively large resulting in a higher surface area of Zr compounds compared to Fe and Al based compounds (Cotton *et al.*, 1999b). Further, zirconium is a heavy compound, having an atomic mass unit of 91.224 compared to 55.845 and 26.981 for Fe and Al respectively.

The use of Zr as a coagulant can be implemented at a WTP without any additional capital investment because existing dosing equipment can be used and has therefore an advantage over other treatment options that have been discussed in this review. It is also easy to handle and has no known toxicity (Blumenthal, 1976; Kroschwitz and Howe-Grant, 1999). However it is not approved for use in drinking water, so further toxicological studies are needed before Zr can be considered for use as a coagulant.

3.7 Summary of literature review

- The destabilisation of NOM during coagulation occurs as a result of several mechanisms: double layer compression, adsorption, charge neutralisation, complexation, sweep flocculation and inter particle bridging.
- Aggregation is a balance between floc growth and breakage meaning that large flocs are stronger than small flocs. Aggregation is favoured by reduced electrostatic repulsion between particles.
- A coagulant needs to have a high charge and a strong affinity for organic material in order to destabilise NOM efficiently.
- For efficient solid-liquid separation, the aggregates formed after addition of the coagulant needs to have favourable characteristics and high strength. Favourable characteristics are large and dense flocs in the case of sedimentation and low density flocs in the case of flotation.

  Several treatment options are available to enhance the NOM removal process. These can work by adding additional charge, improve floc properties, increase the area of possible adsorption sites or break up the NOM using free radicals.
- Zr is regarded as a strong candidate as a treatment option for enhanced NOM removal due to its high charge, strong affinity for organic substances and prospects of simple implementation.

4. Materials and methods

4.1 Bench scale jar testing

4.1.1 Raw water sampling for bench scale experiments

Raw water was sampled from Albert WTP in Halifax, UK on the 25th of March and on the 16th of May 2008. The water was collected in 25 L plastic containers and stored at 5º C. The containers were placed at room temperature over night prior to jar testing to reach room temperature (20º C).

4.1.2 Bench scale jar testing materials

The equipment used was a Phips & Bird PB-900 six paddle jar tester (Camlab Ltd, UK), and a pH-meter (Jenway 2300 with an epoxy pH electrode, Scientific Laboratory Supplies, UK). HCl and NaOH (Anlytical reagent grade, Fisher scientific, UK) was used for pH adjustment. Samples produced during jar testing were analysed for turbidity using a HACH 2100 turbidimeter (Camlab Ltd, UK) and zeta potential using a Zetasizer 2000HSA (Malvern instruments, UK). Samples from jar testing were filtered using glass fibre filters with a pore size of 1.2 µm in diameter (Munktell Filter AB, Sweden) and analysed for dissolved organic carbon (DOC) using a Shimadzu 5000A TOC analyser coupled to a Malvern ASI 5000A autosampler (Malvern instruments, UK). The UV absorbance of filtered samples at 254 nm was measured using a Jenway 6505 UV/Vis Spectrophotometer (Originally from Patterson Scientific, UK now Camlab Ltd, UK) with a 40 mm quartz cell supplied by Starna Brand, UK. HPSEC analysis on filtered water was carried out using a Kontron HPLC system (Scitech instruments, UK) consisting of a 525 pump module, 565 autosampler module, 535 UV detector module, degasser and communications module, used together with a Thermasphere column heater (Phenomenex, UK).

4.1.3 Bench scale NOM removal

Bench scale testing for determination of optimum coagulation conditions for a novel zirconium coagulant and a conventional Fe coagulant was carried out using bench scale jar testing on water sampled on the 25th of March 2008. The Fe coagulant was Ferripol XL (EA West, UK) and will henceforth be referred to as Fe-Coag. The zirconium coagulant was zirconium oxychloride (MEL Chemicals, UK) and will henceforth be referred to as Zr-OCl. For each coagulant, a series of jar tests were performed with increasing coagulant doses ranging from between 2 and 16 mgL^{-1} as Fe and Zr respectively in increments of 2 mgL^{-1} at coagulation pH of between 3 and 6 in increments of 1 pH unit. For each jar test, a 1 L sample of raw water was added to a 1 L rectangular container from. The jar test procedure consisted of a 75 s fast stir phase at 200 rpm and a 15 min flocculation phase at 30 rpm. The sample was then left to settle for an additional 15 min. Coagulant was added using a 20-200 µl automatic pipette (Thermo Life Sciences, UK) after 15 s of the fast stir phase. The pH was adjusted within 30 s of the addition of coagulant (the jar test would be terminated if the correct pH was not reached within 30 s). After settling, 100 ml of unfiltered water for turbidity and zeta potential measurements were taken from the sampling tap. An aliquot of the remaining water was filtered using glass fibre filters (pore size of 1.2 µm) and measured for residual DOC, UV_{254} absorbance and HPSEC analysis.

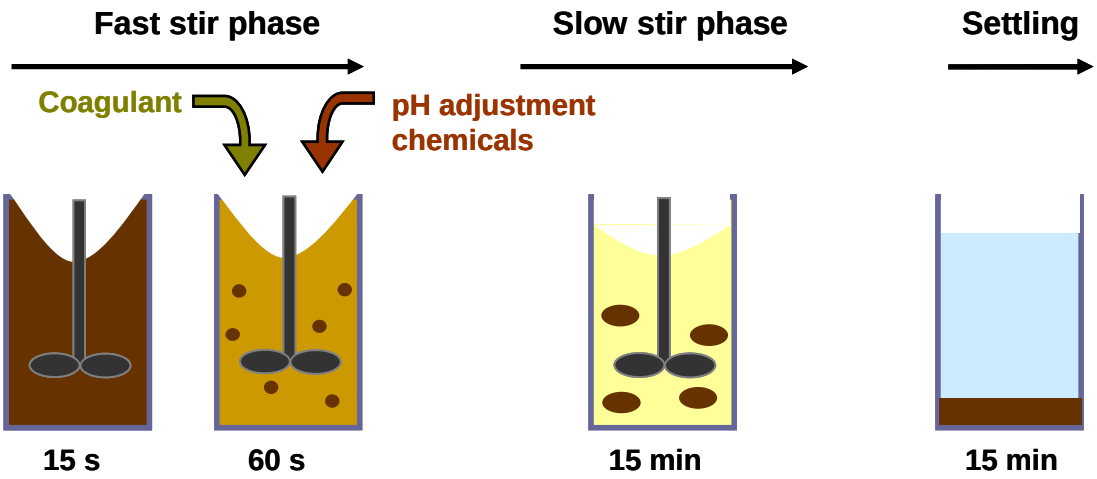

Figure 4.1: Schematic of jar test experiment

4.1.4 Blending

Preliminary jar tests identified that optimum coagulation performance was achieved at a dose of 8 mgL^{-1} as both Fe and Zr at pH 5. The same jar test procedure, equipment and chemicals as described in sections 4.1.2 and 4.1.3 were used on water sampled on the 16th of May 2008. Fe-Coag and Zr-OCl were first used separately and in subsequent tests, the coagulants were dosed together. This was carried out using two separate solutions of Fe-Coag and Zr-OCl. The solutions were added simultaneously using automatic pipettes and the volumes added were adjusted to produce blends of 20, 40, 60 and 80% of Zr by weight for a total coagulant dose (as Fe and Zr) of 8 mgL^{-1}. Samples were taken as before to determine zeta potential, turbidity residual DOC and UV_{254} absorbance.

4.2 Floc size and breakage

Floc size and breakage profiles were determined for water treated by only Fe and Zr and formed from coagulant blends containing 20 and 80 % Zr by weight. The experiment setup consisted of a Phips and Bird two paddle jar tester (Virginia, USA), a 505S peristaltic pump (Watson & Marlow, UK) and a Malvern Mastersizer 2000 laser diffraction instrument (Malvern instruments, UK) (Figure 4.2). During the jar test sequence, the water sample was continuously introduced to the laser diffraction instrument using the peristaltic pump at a flow rate of 25 ml min^{-1}. A one L cylindrical glass beaker was used for the jar tests. The tubing was kept in place in the jar by two holding parts at the side of the jar above the stirrer. Particle size measurements were taken every minute for the length of the jar test sequence. The results were logged on to a PC. The same jar test procedure as described above was used with the addition of a third 15min stir phase with increasing shear rates of 30, 40, 50, 75, 100, 150 and 200 rpm. This was carried out to investigate floc breakage. For the sequence with a 200 rpm breakage shear stir phase, a fourth 15min rate phase at 30 rpm was added to monitor floc re growth. The sequence was repeated three times for every increased stirrer speed. The mean value of the median equivalent diameter (d_{50}) that was logged for each replicate was used to give the floc size for each data point. Before analysis, the Mastersizer optical cell was cleaned, first with tap water and then twice with de-ionised water. If needed, the cell was removed from the

Mastersizer and cleaned using ethanol and lens wipes. The computer software was restarted before every analysis to avoid software crashes.

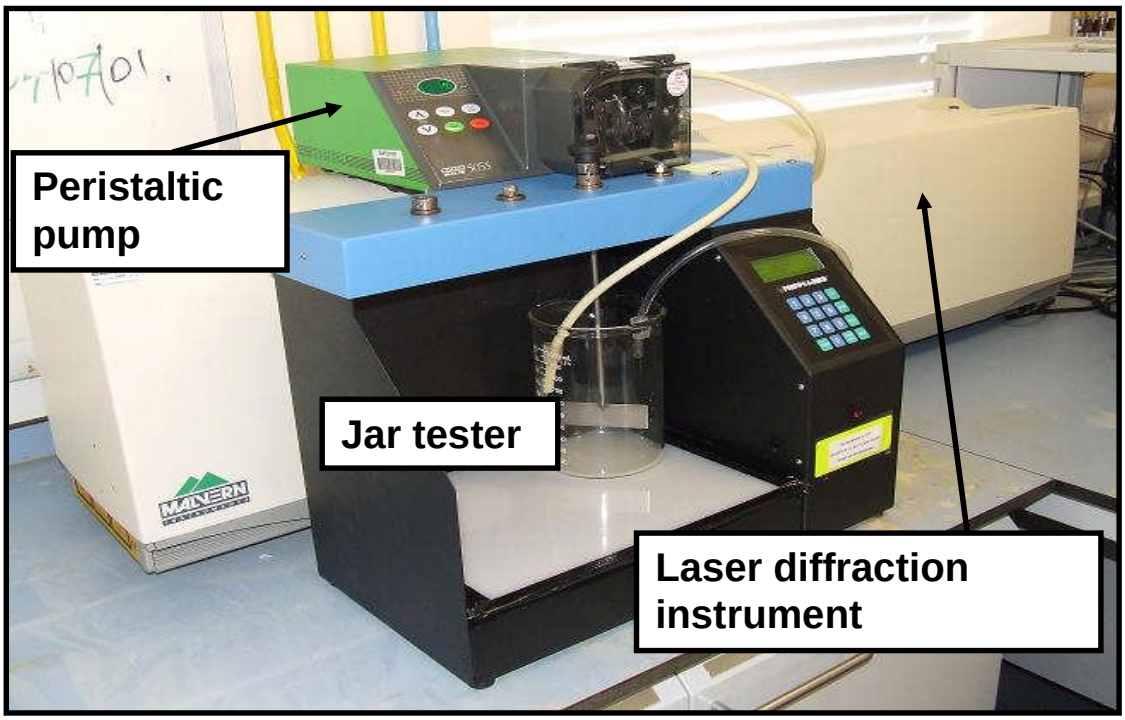

Figure 4.2: Experiment setup for measurements of floc size and breakage.

4.3 Pilot plant experiment

4.3.1 Raw water sampling for pilot plant experiments

Three sets of pilot plant experiments were conducted to benchmark the performance of Zr-OCl against Fe-Coag under optimum NOM-removal conditions and to evaluate the use of a blend of Zr-OCl and Fe-Coag in continuous operation at pilot scale. Water was sampled on the 14th of July, the 6th of October and the 26th of November 2008 from Albert WTP in Halifax, UK and transported to Cranfield University's pilot plant hall using a 30 m^3 tanker. Water was stored in the tanker between runs, and was fed directly from the tanker to the pilot plant during runs.

4.3.2 Determination of optimum coagulation conditions

To begin investigation of NOM removal in continuous operation at pilot scale, an aliquot of raw water was taken from the tanker after sampling and subjected to the same jar test procedure as described in section (4.1.3). Measurements of UV_{254} were used to find optimum coagulation conditions by increasing the coagulant dose in increments of 2 mgL^{-1} between 2 and 16 mgL^{-1}. UV_{254} as a function of dose reached a plateau. The lowest dose to reach the plateau was regarded as the optimum. The pH at which optimum dose was the lowest was regarded as the optimum.

4.3.3 Preparation of chemicals

Fresh solutions of coagulant(s) were prepared before the start of each run. Stock solutions of Zr-OCl and Fe-Coag were diluted with de-ionised water. The concentrations of the coagulant solutions were adjusted according to the flow rate of the raw water through the pilot plant and the pump speed of the peristaltic pump used for coagulant dosing. Since dilution of the coagulants can lead to precipitation of various species which would impact on the coagulation process, the peristaltic pump speed was kept as low as possible in order to keep the coagulant concentration as high as possible. NaOH solutions of 0.5 and 0.25 molar concentrations were prepared by diluting NaOH pellets (Anlytical reagent grade, Fisher scientific, UK) in de-ionised water.

4.3.4 Pilot plant used for pilot-scale experiments

The pilot plant used in the experiment consisted of a rapid mixing tank, two flocculator tanks, a DAF unit and a sand filter (Figure 4.3). The rapid mixing tank was cylinder shaped and had a height of 25 cm and a diameter of 30 cm. The feed water was mixed at 200 RPM, and the contact time was 2 minutes. The two flocculator tanks where 36 cm high, 45 cm wide and 46 cm deep. The feed water was mixed at 5 RPM and the contact time was 10-12 min in each tank. Raw water was pumped through the plant at 200 Lh^{-1} using a submersible pump lowered in a 1 m^3 container filled with raw water from the tanker. The flow through the plant was controlled using a flow meter coupled to a valve positioned before the rapid mixing tank. The flow was calibrated prior to pilot scale testing.

The coagulant and pH adjusting chemical(s) were pumped into the coagulation tank using peristaltic pumps (Watson and Marlow, UK). Coagulant chemical doses were calibrated prior to pilot plant experimentation. This was done by adjusting the coagulant chemical concentration based on the flow rates of the peristaltic pump(s) and the pilot plant flow rate. The pH was monitored with a Jenway 2300 pH meter (Fisher scientific, UK) with an epoxy pH electrode (Fisher scientific, UK). The pH probe was kept submerged in the coagulation tank during the experiment, held by a clamp. The coagulation pH was recorded every 5 min and the pH adjusting chemical dosing was adjusted if necessary to keep the pH at the desired level.

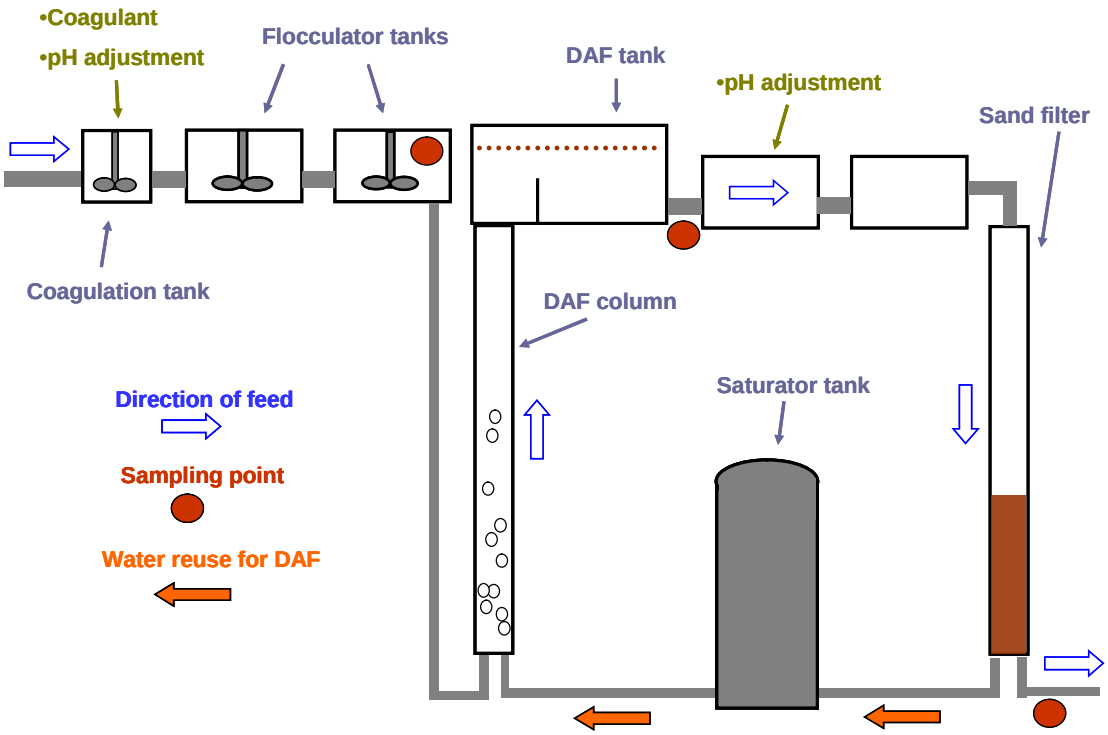

Figure 4.3: Schematic of pilot plant

The DAF unit consisted of a saturator system, an air saturator pump and a cylindrical DAF column leading to an open water tank with a bottom valve the DAF column. The open water tank was 44 cm high, 30 cm wide and 25 cm deep. . The surface overflow of the DAF unit was 0.2 $Lh^{-1}cm^{-2}$ and the recycle ratio was 18 %. The pressurised water tank was first depressurised and filled with treated water. The tank was pressurised to 5 bars and then saturated with air using the air saturation pump. Saturated water from the pressurised water tank was then fed into the bottom of the DAF column upwards together with water being fed into the column from the second flocculator tank. This caused flocs to float to the surface of the water column. When the open water tank was filled up, water was led out from the open water tank with the bottom valve, such that the water level was kept level.

The DAF saturator system needed to be refilled every 45 min. During refill, water from the flocculator tank was fed directly to the drain, the DAF column was emptied and the open water tank bottom valve was closed. The flow through the sand filter was minimised so that it could run continuously during refill. The refill took 15 min and included the procedure described above. This way the pilot plant was run

continuously with the exception of the DAF unit which ran for 45 with a 15 min restart.

After the DAF the water was fed into a mixing container where the pH was adjusted to > 6.7 using NaOH which was added using a peristaltic pump. The water was then fed to another container in which the pH was monitored every 5 min using a pH meter. Water was pumped from the pH monitoring container onto the sand filter using a submersible pump. The diameter of the sand filter column was 19 cm and the depth of the sand filter was 36 cm. The surface overflow rate was 0.8 $Lh^{-1}cm^{-2}$.

For every pilot plant experiment, the plant was run in continuous operation for 6h. In July, samples were taken hourly. By November, a more efficient schedule had been developed, allowing samples to be taken twice every hour. Samples were taken in the second flocculation tank, after the DAF unit and after sand filtration. Samples were taken for UV_{254}, (DOC), turbidity, zeta potential and THM-FP according to Table 4.1.

Table 4.1: Overview of samples taken for pilot plant experiment.

Sampling point	**Samples analysed for**
Flocculator tank	UV_{254} absorbance, zeta potential
Post DAF	UV_{254} absorbance, DOC, turbidity, zeta potential
Post Filter	UV_{254} absorbance, DOC, turbidity, zeta potential, THM-FP

The following set of runs where performed:

14^{th} of July

- Fe and Zr under optimum conditions
- Blends of Fe and Zr of 20 and 80% as Zr by weight

26^{th} of November

- Fe and Zr under optimum conditions
- Blends of Fe and Zr of 20 and 80% as Zr by weight

4.4 Analytical techniques

4.4.1 Trihalomethane formation potential (THM-FP)

4.4.1.1 Chlorination

Samples taken for THM-FP were first measured for DOC (details in section 4.4.3). The exact chlorine concentration of a sodium hypo chlorite solution was determined using a titration (described below). The volume needed to achieve a chlorine concentration 5 times the DOC in a total of 100 ml was calculated for each sample. Sodium hypo chlorite and 2 ml pH 7 phosphate buffer (Fisher Scientific, UK) was added to a 100 mL screw neck borosilicate glass reagent bottle with a black phenolic 25 mm cap (Fisher Scientific, UK). It was important to ensure that the water sample filled the bottle completely. Otherwise the THMs would volatilise into any air pocket present inside the bottle. To make sure the bottle was filled completely, it was turned upside down and inspected for air bubbles. The sample was then put in the dark at room temperature (20º C) for 7 days. The THM-FP was then determined as sum of the concentration of trichloromethane, dichlorobromomethane, dibromochloromethane and tribromomethane.

4.4.1.2 Extraction

The extraction of THM-FP samples into methyl-tert-butyl-ether (MTBE) for analysis with gas chromatography was done accordingly: A powder buffer (pH 5) was prepared by mixing 99 g of Na_2HPO_4 and 1 g KH_2PO_4 (both of laboratory reagent grade, supplied by Fisher scientific, UK). To quench the chlorination process, a 120 gL^{-1} solution of sodium sulphite (anhydrous, VWR International inc. UK) was prepared. Sodium chloride (laboratory reagent grade, Fisher Scientific, UK) was put in a glass beaker covered with aluminium foil in an oven set to 100º C over night to dry. 500 µl of sodium sulphite was added to the sample. 50 g of the sample was then put in a 60 ml (140 · 28 mm) glass screw vial (Kinesis, UK) together with 1 g powder buffer and 10 g sodium chloride and mixed gently until the mix was homogenised and the salt and the buffer had dissolved as much as it could. 3 ml of MTBE (HPLC analytical grade, Fisher Scientific, UK) was added and the bottle was shaken for 4 min. The sample was then allowed to settle for another 2 min. The MTBE top layer

was removed using a disposable plastic pipette and added to a vial for gas chromatography analysis.

4.4.1.3 Gas chromatography quantification

THMs (trichloromethane, dichlorobromomethane, dibromochloromethane, tribromomethane,) were quantified on an Agilent technologies 6890N gas chromatograph with a micro electron capture detector (Agilent 6890 GC-ECD). A capillary column (Phenomen ZB-1MS – 30 m × 250 µm id × 0.25 µm) was used with helium carrier gas at a flow rate of 0.9 $mlmin^{-1}$. The split ratio was set at 10:1. A volume of 1 µL was injected using an Agilent technologies 768313 series injector. The initial oven temperature was 35º C held for 9 minutes followed by a 10º C per minute temperature ramp to 40º C and held for 3 minutes. The temperature was increased to 77º C at a rate of 6º $Cmin^{-1}$ and held for 1.5 minutes followed by an increase to 225º C at a rate of 30º $Cmin^{-1}$ and held for 1 minute. The temperature of the injector was set at 200º C and the detector at 300º C. The rate of data collection was 20 Hz. Standards for the calibration curve was produced using trihalomethanes calibration mix (Sigma-Aldrich, UK).

4.4.2 High performance size exclusion chromatography (HPSEC)

The Kontron HPLC system was compiled of a 525 pump module, a 565 autosampler module, a 535 UV detector module, Thermasphere column heater, degasser, communications module and PC. The mobile phase was 0.01M sodium acetate solution, prepared from HPLC grade sodium acetate trihydrate (Fisher Scientific, UK) and ultrapure water (Purelab Ultrapure water unit, ELGA Process water, UK). This was pumped at 1 mL/min (isocratic) through a Phenomenex BioSep SEC 3000 column, 300x7.8 mm, held at 30º C. The detector was set at 254 nm with a run time of 15 minutes. 475 µL of sample was used for each analysis. A 1.5ml glass vial was filled to the neck with filtered sample and placed in the autosampler. The above described programme was run to retrieve chromatograms showing UV absorbance over time for UV absorbing material present in the sample separated by size.

4.4.3 Dissolved organic carbon (DOC)

4.4.3.1 Calibration of Shimadzu 5000A TOC analyser

Before measurement of DOC, the Shimadzu 5000A TOC analyser was calibrated using 2.5, 5 and 10 mgL^{-1} standards of inorganic and total carbon. The standards were prepared by diluting a stock solution of standard using a volumetric flask and a pipette. The inorganic carbon stock solution was prepared using anhydrous sodium hydrogen carbonate (BDH laboratory supplies, UK). The total carbon stock solution was prepared using analytical reagent grade potassium hydrogen phthalate (BDH Prolabo Brand, VWR International, UK). The calibration of the pipette was checked by weighing the amount of ultrapure water it extracted. Calibration standards of 10 mgL^{-1} were prepared in a volumetric flask. Aliquots of this standard were diluted to 5 and 2.5 mgL^{-1} using a pipette and ultrapure water. Before calibration of the instrument, a blank sample consisting of ultrapure water was run as a sample. If the concentration was measured to be above 0.5 mgL^{-1}, a wash program would precede the calibration to clean the machine from residual carbon. During analysis, 2.5mgL^{-1} standards were measured every 10-15 samples to check that the calibration was stable.

4.4.3.2 Handling of samples to be analysed for DOC

Samples were filtered using glass fibre filters (pore size of 1.2 µm). They were then placed in vials which were covered with laboratory film (Parafilm “M”, Pechiney Plastic packaging, Illinois, USA) to avoid the intrusion of additional carbon from the surrounding air. Vials used for DOC measurements were acid washed between runs to remove all remaining carbon. This was carried out by rinsing them with de- ionised water before submerging them in a 5 % HCl solution for a minimum of 24 hours. Finally the vials were rinsed again with de-ionised water before being used for another run.

4.4.4 UV_{254} absorbance

Before measurement of UV_{254} absorbance, the Jenway 6505 UV/Vis spectrophotometer was calibrated using ultrapure water. The 40 mm quartz cell was rinsed with ultrapure water between every sample. For bench scale experiments, every sample was measured once. For pilot plant experiments, every sample was measured in triplicate. All measurements were performed on samples at room temperature (20º C).

4.4.5 Zeta potential

4.4.5.1 Maintenance of Malvern Zetasizer 2000HSA

Samples from pilot plant experiments were left at room temperature over night prior to determination of zeta potential. This would cause the samples to settle and reach room temperature prior to measurement. Zeta potential is affected by temperature, such as the distribution of ions in the diffuse region is depends on thermal (and electrical) forces. Settling was allowed because it was found that the cell was easier to keep clean when settled samples were used. Zeta potential is independent of particle size. For this reason the use of settled samples was not considered to affect the quality of the results. 10 mL of sample was injected using a 10 mL syringe (central nozzle, BD Plastipak). The Zetasizer was set to take three measurements. All three measurements were recorded to calculate the standard deviation of the results. For bench scale samples, 20 mL of sample was injected using a 10 mL central nozzle BD Plastipak syringe. The Zetasizer was set to take three measurements and display the average which was recorded.

4.4.5.2 Handling of samples to be measured for zeta potential

The cell was cleaned between samples by injecting de-ionised water through the cell. The count rate was checked occasionally, on average every 5 samples. The cell was considered clean. If the count rate was below 30 Kcps (Kilo counts per second). Before analysis of a sample, the cell was checked for air bubbles. If an air bubble was found in the cell, it was washed with ethanol and then with de-ionised water before the sample was put back in the cell. If the Zetasizer 2000HSA had not been used for a week or more, the cell was taken out and cleaned using a pipe cleaner drenched in

ethanol. The outside of the cell was then wiped with soft paper sprayed with ethanol. When the cell was placed back in the Zetasizer, it was rinsed with de-ionised water. The count rate was checked when the cell was filled with de-ionised water. Finally, a standard was used to check the calibration.

4.4.6 Turbidity

The HACH 2100 turbidimeter (Colorado, USA) calibration was checked before analysis using a set of solid standards. The cells used during analysis were washed with ultrapure water between every measurement and wiped clean to avoid light scattering of any water in the outside of the cell. The sample was checked for air bubbles before being inserted into the turbidimeter. If air bubbles were in the sample, the cell was left on the bench until the air bubbles had left the water column. Room tempered samples from bench scale experiments were gently shaken and measured once. The turbidimeter was set to take one measurement every second and display the average. The average result after 10 s from the time the sample cell was inserted was recorded.

For pilot plant experiments, samples were left at room temperature over night. The samples were homogenised by gently turning the sample bottle upside down 10-12 times. The turbidimeter was set to display the result once every second. The sample was left for 30 s after being inserted. One reading was taken after 30 s and then three more readings were then taken every 10 seconds.

4.4.7 pH

The pH meter was calibrated hourly during jar testing using three standards of pH 4, 7 and 10 (Fisher Scientific, UK). When not in use, the pH probe was kept submerged in a pH 4 buffer. During bench scale experiments, recalibration was performed once every hour. The pH probes were used for a maximum of 6 months before being replaced by a new probe. This was done to ensure fast response times to changing pH were monitored correctly.

4.4.8 Measurements of residual Zr

Zr measurements were carried out using a Perkin-Elmer Elan 9000 ICP-MS. (Perkin-Elmer, Seer Green, Beaconsfield, BUCKS, UK). Sample flow rate was approximately 1 ml/ min. The MS was set at m/z =90 for Zr. Samples were analysed against a commercially available Zr standard solution (Fisher Scientific), diluted down to the range of interest. Rhodium (m/z = 103) standard was used as an internal standard for both samples and Zr standards. Due to memory effects of Zr, a prolonged sample line wash of 20 minutes with 3 % HCl + 1 % HNO_3 was used between samples and standards.

4.5 Statistical analysis of data

Samples retrieved from pilot plant treatments were processed accordingly for analysis of difference between treatments. Any observations that were at least 1.5 times the interquartile range (Q3 – Q1) above the third quartile or below the first quartile were considered outliers and subsequently removed. Samples were tested for normality using the Anderson-Darling test. In the case of two normal samples; homogeneity of variance between them was tested using the F-test. The student's t-test was subsequently used assuming equal variance or not assuming equal variance depending on the result from the F-test. In the case of at least one sample not being normal, the Mann-Whitney nonparametric test was used. A significance level of 0.05 was applied for statistical analysis of samples taken during pilot plant testing and a significance levels of 0.01 was applied for statistical analysis of floc.

5. Results and discussion

5.1 Fe vs Zr

5.1.1 Introduction

The removal efficiency of NOM from moorland source waters using zirconium as a coagulant was tested at both bench and pilot scale on water from Albert WTPs in Halifax, UK. This was a typical moorland source water of high colour, high DOC and low turbidity (Table 5.1). The results were benchmarked against the ferric based coagulant used at Albert WTPs at the time.

5.1.2 Raw water characteristics

Bench scale experiments were carried out on water sampled on the 25th of March and on the 16th of May which had similar characteristics. The DOC was 8.4 and 8.6 mgL^{-1}, the UV_{254} was 39.6 and 38.9 m^{-1} and the SUVA was 4.7 and 4.5 mg $m^{-1}L^{-1}$ for water sampled on the 25th of March and the 16th of May respectively (Table 5.1). The turbidity was 2.4 and 3.5 NTU respectively (Table 5.1). Pilot scale treatment was carried out on waters sampled on the 14th of July and on the 26th of November. In July, the water had a DOC of 8.7 mgL^{-1} with a UV_{254} of 45.1 m^{-1} resulting in a SUVA of 5.2 mg $m^{-1}L^{-1}$ indicating that the NOM was predominately hydrophobic in nature (Sharp *et al.*, 2006b) (Table 5.1). In November, the DOC of the water was 50% higher (13.1 mgL^{-1}) while the UV_{254} was similar (44.7 m^{-1}). This resulted in a much lower SUVA of 3.4 mg $m^{-1}L^{-1}$. The hydrophobic fraction of the NOM typically consist of large MW humic and fulvic acids containing functional groups which absorb visible light (Sharp, 2005). A high SUVA therefore indicates a high proportion of hydrophobic NOM. The lower SUVA of the water sampled in November indicated that the NOM content was less hydrophobic, i.e. containing a smaller fraction of humic and fulvic acids in relation to hydrophilic components. Low SUVA water is more difficult to treat because coagulation preferably removes hydrophobic organic compounds but is relatively poor at removing low molecular weight hydrophilic material (Fearing *et al.*, 2004). The DOC shows a variation from March to November (Table 5.1). This variation has been observed earlier in moorland waters and has been attributed to several factors such as changes in precipitation and snowmelt which can cause additional organic material to be flushed into the water (Sharp, 2005).

Table 5.1: Characteristics of raw water sampled from Albert water treatment works for bench and pilot scale experiments.

Properties	Bench scale		Pilot scale	
	25 March	16 May	14 July	26 Nov
DOC (mg L^{-1})	8.4	8.6	8.7	13.1
UV_{254} (m^{-1})	39.6	38.9	45.1	44.7
SUVA (mg $m^{-1}L^{-1}$)	4.7	4.5	5.2	3.4
Zeta potential (mV)	-16.6	-19.3	-18.9	-16.8
Turbidity (NTU)	2.4	3.5	1.3	3.9

5.1.3 Bench scale treatment

The jar test procedure described in section (4.1.3) was applied to water sampled on the 25th of March (Table 5.1). This water had a SUVA value of 4.7 mg $m^{-1}L^{-1}$. Waters with SUVA values greater than 4 mg $m^{-1}L^{-1}$ are regarded as being predominantly hydrophobic in nature (Sharp *et al.*, 2006a). The hydrophobic fraction carries a majority of the charge load of the water (Sharp *et al.*, 2006a) which is negative at pH levels of natural moorland source waters (Duan *et al.*, 2002). During coagulation with metal salts, charge neutralisation and charge complexation mechanisms are believed to dominate for NOM removal (Duan and Gregory, 2003). As a result, optimum coagulation occurs around the iso electric point of the coagulant and the NOM (Sharp, 2005). The measurement of surface charge of suspended and dissolved NOM is therefore an important tool for assessing coagulation performance. This is carried out in the present study by measuring the zeta potential of samples that have not been filtered (details in section 4.4.5).

5.1.3.1 Performance vs. zeta potential

Plotting performance with regards to DOC removal, UV_{254} and turbidity vs. zeta potential revealed a u-shaped relationship between coagulation performance and zeta potential. This is in agreement with findings reported by Sharp *et al.* (2005; 2006b) for both ferric sulphate and alum coagulation. For both coagulants in the present study, NOM removal performance improved with increased zeta potential going from negative values around -20 mV towards zero. Removal then deteriorated with positive zeta potential values, leaving a window of optimum performance. The operational window for Zr-OCl was found to be wider than for Fe-Coag. The operational window for Fe-Coag was between -10 and +5 for turbidity. For DOC and UV_{254} removal, performance deteriorated below -10 mV and the upper end of the operational window was around 0 for DOC and +5 for UV_{254} (Figure 5.1). This is in agreement with Sharp *et al.* (2005; 2006b) who reported operational windows for a Fe based coagulant around -10 to +5 mV on a similar water. The operational window for Zr-OCl stretched between -15 and 15 mV for DOC and UV_{254} removal and between -10 and + 10 mV for turbidity (Figure 5.1). UV_{254} results after treatment with Fe-Coag shows high values around a zeta potential of zero (Figure 5.1) These data points correlate to the UV_{254} measurements taken after treatment with Fe-Coag at pH 3 (Figure 5.2). At pH levels around 2-3 the hydrolysed species formed by Fe (like for example $[Fe(H_2O)_5(OH)]^{2+}$, $[Fe(H_2O)_4(OH)_2]^{+}$) give the solution a yellow colour (Greenwood and Earnshaw, 1998b). This is likely to have caused the high UV_{254} absorbance coupled with charge neutralisation.

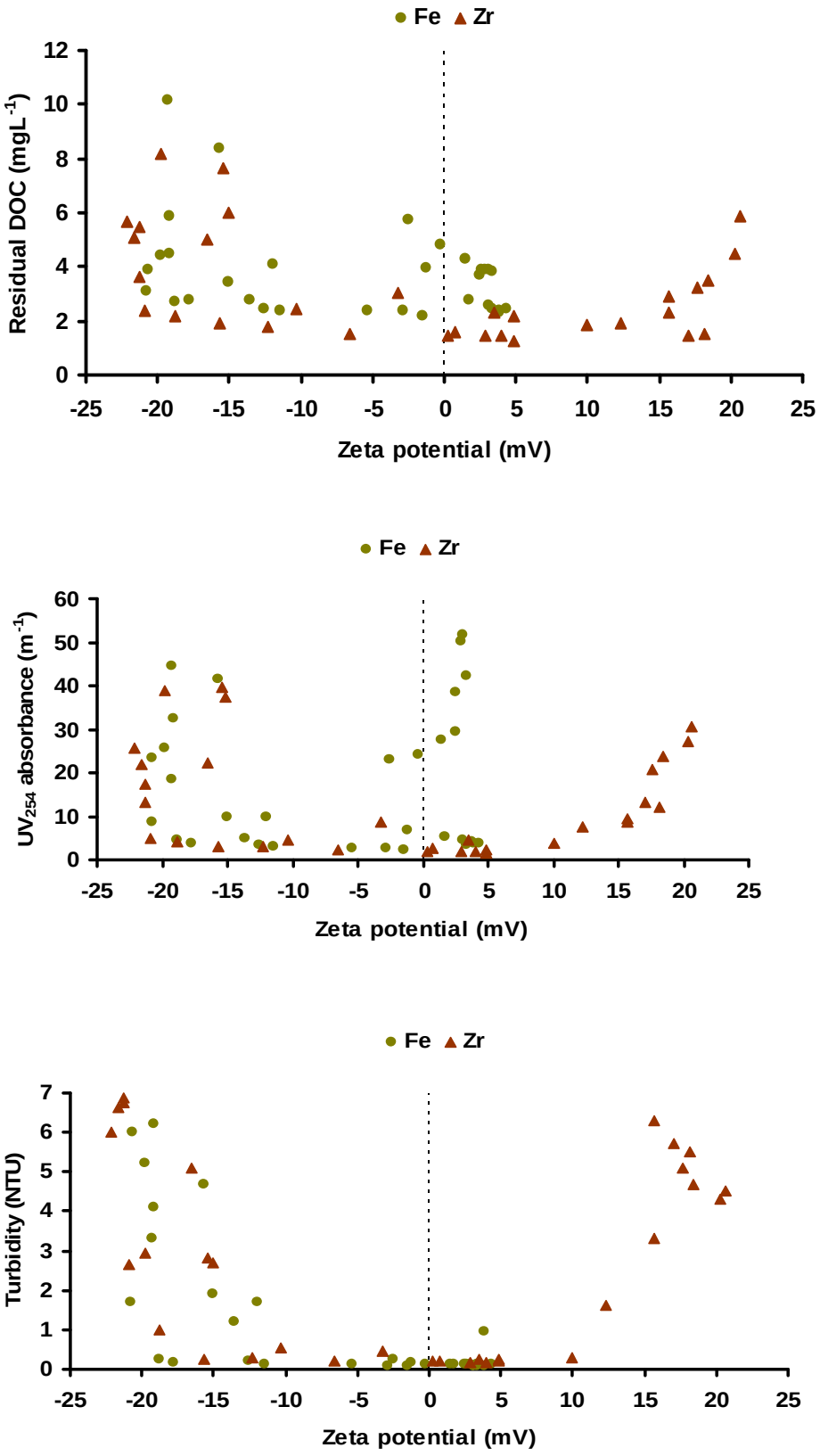

Figure 5.1: Residual DOC, UV_{254} and turbidity with zeta potential after treatment with Fe-Coag and Zr-OCl at bench scale on water sampled on the 25th of March for all doses and pH levels tested.

5.1.3.2 UV_{254} removal

Optimum removal of NOM was reached at doses of 8 mgL^{-1} as Fe and Zr (0.14 and 0.09 mM as Fe and Zr respectively) for both coagulants. The optimum pH for removal was 4 for Fe-Coag and 5 for Zr-OCl. After treatment with Fe-Coag under optimum conditions the UV_{254} was 4.7 m^{-1}, while Zr-OCl treatment resulted in a UV_{254} of 2.3 m^{-1} (Figures 5.2 and 5.3). This was equal to a 6 % lower UV_{254} in water treated with Zr-OCl compared to water treated with Fe-coag which cannot be considered significant.

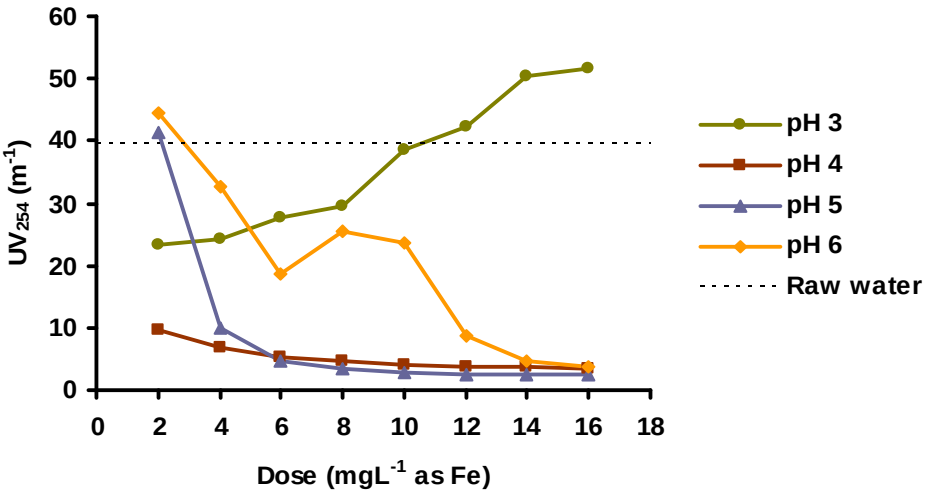

Figure 5.2: UV_{254} after treatment at bench scale for doses between 2-16 mgL^{-1} as Fe on water sampled on the 25th of March at pH levels of 3, 4, 5 and 6.

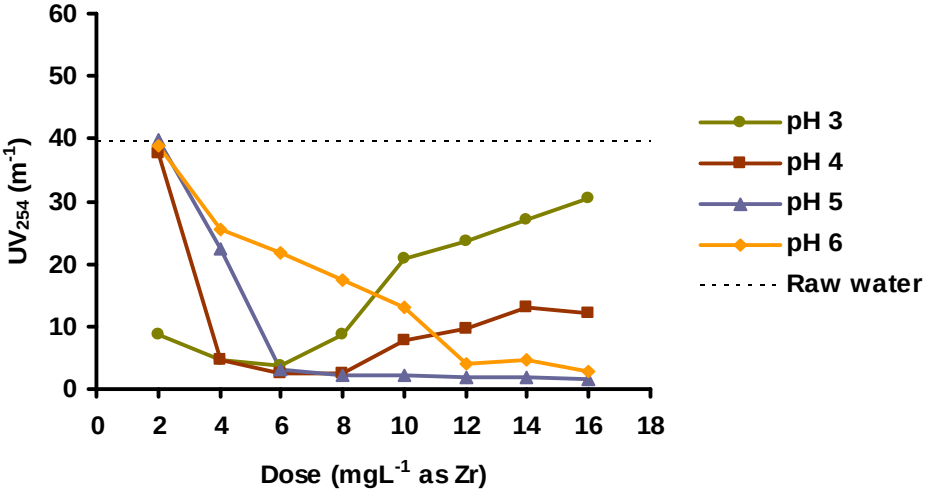

Figure 5.3: UV_{254} after treatment at bench scale for doses between 2-16 mgL^{-1} as Zr on water sampled on the 25th of March at pH levels of 3, 4, 5 and 6.

5.1.3.3 DOC removal

Residual DOC in water treated under optimum conditions were 2.6 mgL^{-1} vs. 1.5 mgL^{-1} for Fe-Coag and Zr-OCl respectively (Figures 5.4 and 5.5). This was equal to a 10 % lower residual DOC in water treated with Zr-OCl compared to water treated with Fe-Coag.

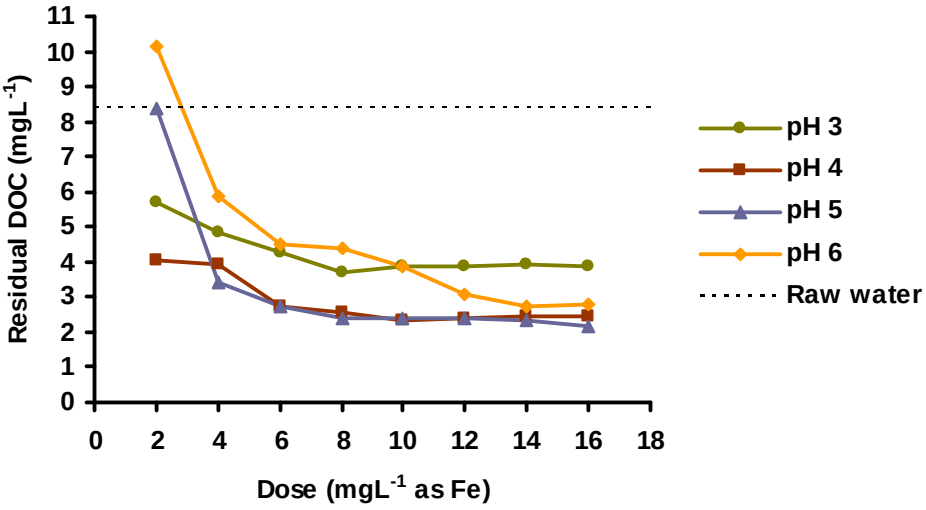

Figure 5.4: Residual DOC after treatment at bench scale for doses between 2-16 mgL^{-1} as Fe on water sampled on the 25th of March at pH levels of 3, 4, 5 and 6.

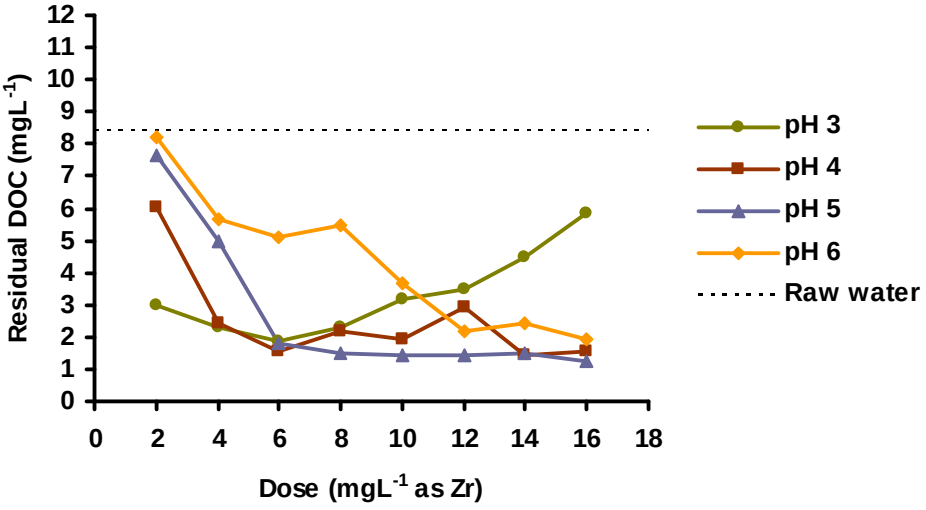

Figure 5.5: Residual DOC after treatment at bench scale for doses between 2-16 mgL^{-1} as Zr on water sampled on the 25th of March at pH levels of 3, 4, 5 and 6.

5.1.3.4 Turbidity removal

For the optimum conditions found for DOC and UV_{254}, treatment with Fe-Coag and Zr-OCl resulted in residual turbidity of 0.1 and 0.2 NTU respectively (Figures 5.6 and 5.7) which was not a significant difference. At pH 6, treatment with Fe-Coag caused high turbidity (Figure 5.6). This indicated the formation of small flocs which did not settle well. At pH 6 the mole fraction of the $Fe(OH)^{2+}$ ion becomes negligible compared to the $Fe(OH_2)^{+}$ and the uncharged $Fe(OH)_3$ ions which will dominate in solution (Duan and Gregory, 2003). Zr-OCl also showed high turbidity at pH 6 (Figure 5.7). In the case of Zr, increasing the pH from 3-6 continuously strengthens the dominance of the uncharged $Zr(OH)_4$ ion over the charged $Zr_2(OH)^{7+}$ and $Zr(OH_3)^{+}$ species (Veiland *et al.*, 1998; Lowalekar *et al.*, 2006). This will cause a reduction in zeta potential with subsequent reduced coagulation (Sharp, 2005). At pH levels of 3 and 4 (where the $Zr_2(OH)_7^{+}$ and $Zr(OH)_3^{+}$ and $Zr(OH)_6^{2+}$ ions are more prevalent), treatment with Zr-OCl resulted in increased turbidity at higher doses (Veiland *et al.*, 1998; Ekberg, 2004). Flocs formed with charge neutralisation have been found to be smaller and less compact than flocs formed with sweep flocculation (Kim *et al.*, 2001). Small flocs with low compaction could have caused increased turbidity seen after treatment with Zr-OCl seen at pH 3 and 4.

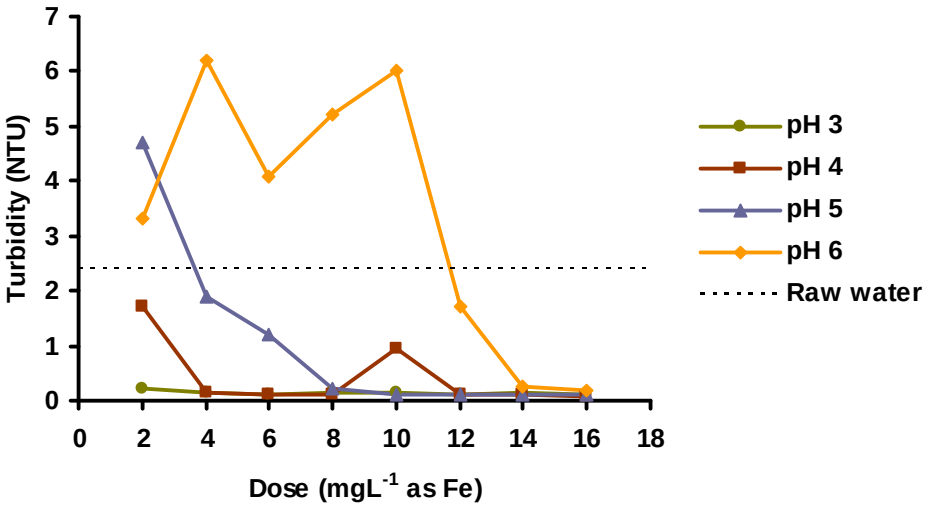

Figure 5.6: Turbidity after treatment at bench scale for doses between 2-16 mgL^{-1} as Fe on water sampled on the 25th of March at pH levels of 3, 4, 5 and 6.

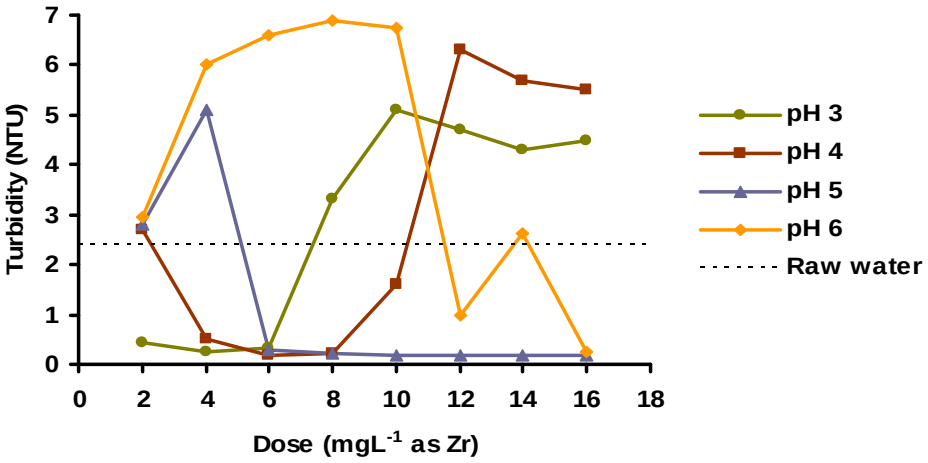

Figure 5.7: Turbidity after treatment at bench scale for doses between 2-16 mgL^{-1} as Zr on water sampled on the 25th of March at pH levels of 3, 4, 5 and 6.

5.1.3.5 Zeta potential

Treatment with Zr-OCl resulted in a higher zeta potential than for Fe-Coag for the same dose applied (2 - 16 mgL^{-1}) under all pH conditions tested (Figures 5.8 and 5.9). The molecular weight of Zr is higher than Fe (91.2 vs. 55.8 $gmol^{-1}$ for Zr and Fe respectively). Consequently, the differences in zeta potential for the same dose were even larger when molar concentrations were considered as opposed to mass concentrations. For example, molar concentrations of 0.11 mM resulted in zeta potentials of +1.7 and +12.3 mV for Fe-Coag and Zr-OCl respectively at pH 4, and -13.6 and +0.3 mV respectively at pH 5. Optimum pH and dose by mass for both coagulants had proved to be similar for all waters tested; leading to the conclusion that Zr-OCl performs optimally at higher zeta potentials. At pH levels of 3 and 4, the highest zeta potentials were observed for both Fe-Coag and Zr-OCl. It was also where the largest differences in zeta potential between Fe-Coag and Zr-OCl were observed. For example, the zeta potential at a dose of 12 mg L^{-1} was -5.4 and +2.9 mV for Fe-Coag and Zr-OCl respectively at pH 5 and +3.9 and +15.7 mV for Fe-Coag and Zr-OCl respectively at pH 4. This showed a big potential for Zr-OCl to add positive charge to the coagulation process. Between pH 3 and 5, the $Fe(OH)^{2+}$ and $Fe(OH)^{+}$ species dominate in solutions with Fe (Duan and Gregory, 2003). $Zr_2(OH)_7^{+}$, $Zr(OH)_3^{+}$ and $Zr(OH)_4$ have been proposed in different compositions in solutuions with Zr (Veyland *et al.*, 1998; Lowalekar *et al.*, 2006). This does not explain the

higher charge added by Zr-OCl in terms of the charge of the species formed in solution. However, Lowalekar *et al.* (2006) reported a shift in zeta potential despite a high dominance of $Zr(OH)_4$. This was explained by the formation of Si-O-Zr bonds after reaction between $Zr(OH)_4$ and silanol groups. Also, the highly charged $Zr_4(OH)_8(H_2O)_{16}^{8+}$ species have been found in precipitated tetrameric units (Fryer *et al.*, 1970). If such precipitated units were present they would have a strong influence on zeta potential.

At pH 6 the zeta potential was reduced as a result of treatment with both Fe-Coag and Zr-OCl (Figure 5.8 and 5.9). This is likely to have been caused by negatively charged species of Fe and Zr. Negatively charged species ($Fe(OH_4)^-$ and $Zr(OH_5)^-$) begins to form in solution at pH levels around 6.5 for Fe and around 8.5 for Zr (Veiland *et al.*, 1998; Duan and Gregory, 2003). Measurement of pH during the jar testing procedure was discontinued after the end of the fast stir phase (Section 4.1.3). Treatment at pH 6 involved the most significant addition of NaOH to raise the pH sufficiently within the fast stir phase. It is clear from the results that the pH continued to rise after the fast stir phase to above 6.5 and 8.5 after treatments at pH 6 with Fe-Coag and Zr-OCl respectively, causing a reduction in zeta potential.

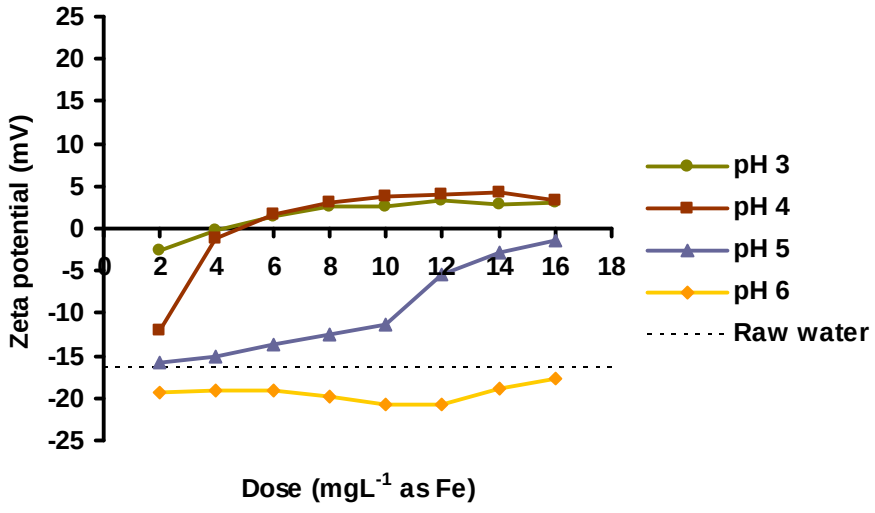

Figure 5.8: Zeta potential response of changing coagulant dose from 2-16 mgL^{-1} as Fe from bench scale jar tests on water sampled on the 25th of March at pH levels of 3, 4, 5 and 6.

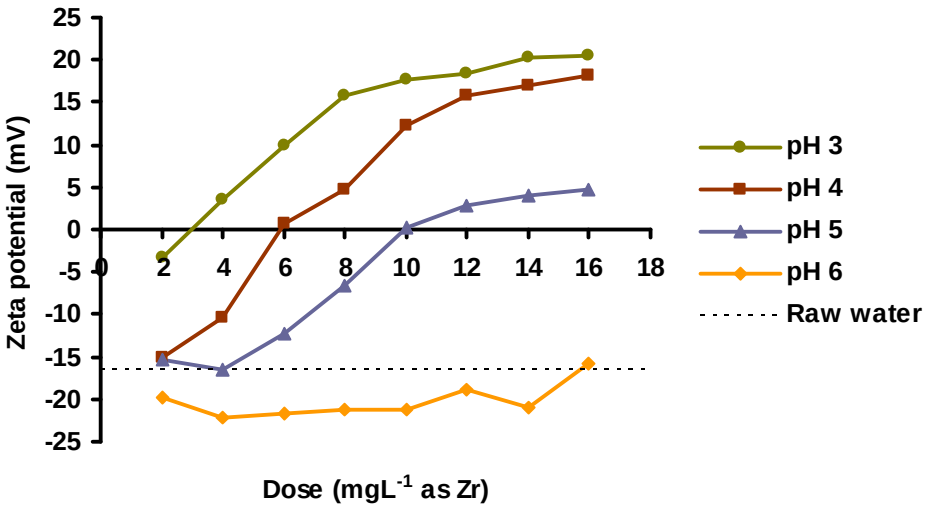

Figure 5.9: Zeta potential response of changing coagulant dose from 2-16 mgL^{-1} as Zr from bench scale jar tests on water sampled on the 25th of March at pH levels of 3, 4, 5 and 6.

5.1.3.6 HPSEC traces

Both coagulants readily removed UV_{254} absorbing material eluted before 8 min when separated using HPSEC (Figures 5.10 and 5.11). This corresponded to material with molecular weight > 5000 Da (Fearing *et al.*, 2004). Zr showed lower HPSEC traces between 8 and 11 min (Figure 5.11). For example, the peak heights after 9.5 min were 1200 and 1140 mAU for Fe-Coag and Zr-OCl respectively corresponding to an 8 % lower UV_{254} absorbance for Zr-OCl. HPSEC traces with elution times between 8 and 11 min have been shown to correspond with organic material of MW between 2000 and 5000 Da (Fearing *et al.*, 2004). Goslan (2003) reported that the humic acid fraction (HAF) and the fulvic acid fraction (FAF) of the NOM had elution times between 5.3 and 11.2 minutes and 6.5 and 11.2 minutes respectively showing an overlap in the size distribution. The MW of the HAF has been found to be >3000 Da while the MW of the FAF was between 1000 and 3000 Da (Goslan *et al.*, 2004). This implied that Zr-OCl was more effective than Fe-Coag at removing the low MW, UV_{254} absorbing HAF and the mid to high MW FAF of the NOM.

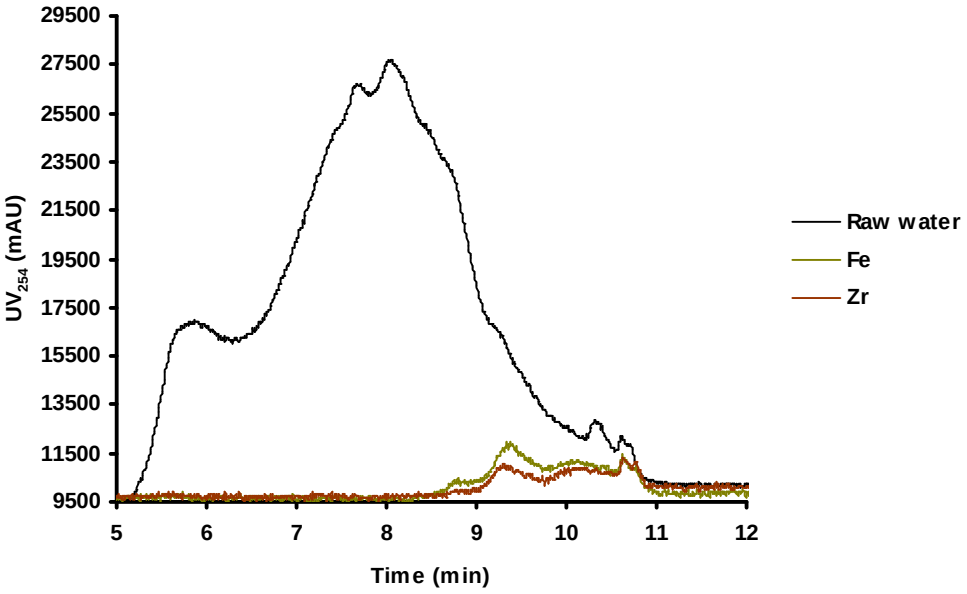

Figure 5.10: HPSEC traces of raw water and water treated under optimum conditions (8 mgL^{-1} as Fe at pH 4 and 8 mgL^{-1} as Zr at pH 5) at bench scale using Fe-Coag and Zr-OCl on water sampled on the 25th of March.

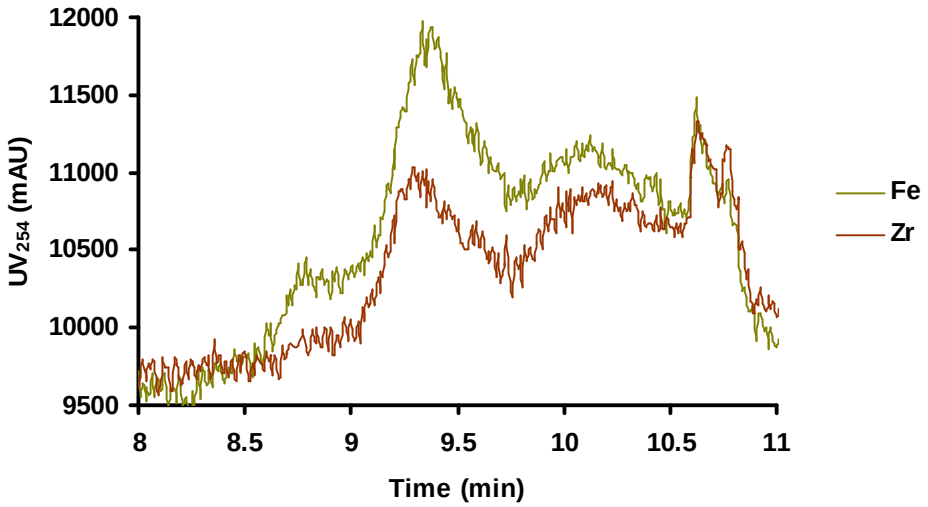

Figure 5.11: HPSEC traces from elution time between 8 and 11 min from water treated under optimum conditions (8 mgL^{-1} as Fe at pH 4 and 8 mgL^{-1} as Zr at pH 5) at bench scale using Fe-Coag and Zr-OCl.

5.1.4 Floc properties

5.1.4.1 Floc size

The flocs formed when Zr-OCl was used reached a steady state d_{50} of 958 ± 49 µm (Figure 5.12). This was significantly higher than the steady state d_{50} of 667 ± 64 µm for Fe ($T_{(308)}$ = -45.84, $p < 0.01$). The results correlated well with previous work (Jarvis *et al.*, 2005b) and demonstrated the ability of Zr-OCl to form larger flocs then Fe-Coag.

5.1.4.2 Floc growth

The results showed a clear difference in growth pattern between Fe-Coag and Zr-OCl flocs (Figure 5.12). The Zr-OCl floc growth rate increased from 69 µm min^{-1} (between 3 and 6 minutes of the experiment) to 150 µm min^{-1} after 6 minutes until the point of steady state after 10 min. Fe-Coag flocs grew quickly in the early stages of the experiment (197 µm min^{-1} between 2 and 4 min), before the growth rate slowed down (56 µm min^{-1} between 4 and 7 min) before reaching steady state after 7-8 min. The same difference in growth pattern was observed between MIEX® pretreated water and raw water during treatment with a Fe based coagulant (Mergen, 2008). The MIEX® pretreated water had a reduced presence of NOM of low MW which would imply a larger incorporation of high MW NOM in the flocs with subsequent improvements in floc properties (Jefferson *et al.*, 2004; Mergen, 2008).

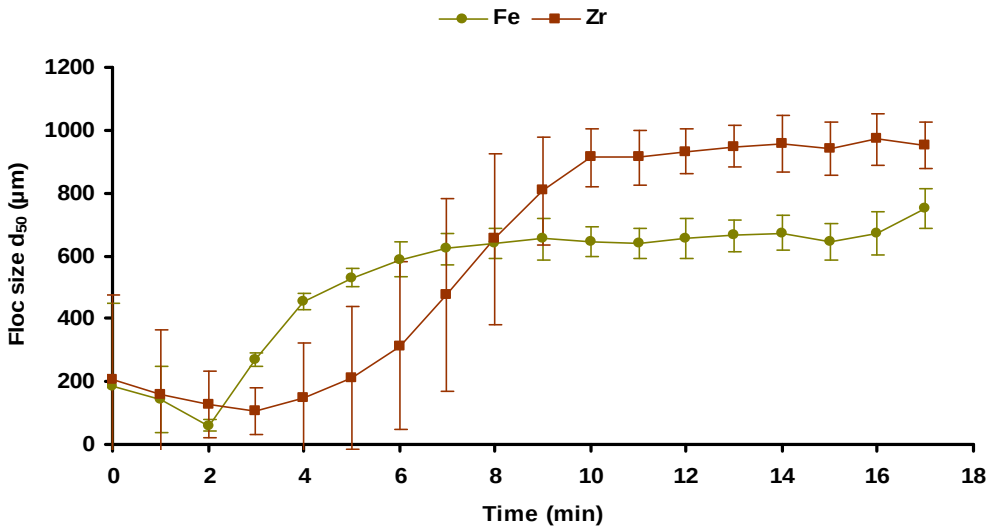

Figure 5.12: Floc growth and steady state size for treatment with Fe-Coag and Zr-OCl under optimum conditions (8 mgL^{-1} at pH 4.5 for both Fe and Zr) at bench scale on water sampled on the 16th of May. Floc growth was induced by subjecting the system to a shear rate of 30 rpm.

5.1.4.3 Floc breakage

Typical breakage profiles of coagulant-NOM flocs exhibit a gradual decrease in floc size at low shear rates, while high shear rates cause a rapid drop in size (Jarvis *et al.*, 2005b; Jarvis *et al.*, 2005c; Sharp *et al.*, 2006c). The same was observed for the flocs formed using Fe-Coag and Zr-OCl in this study (Figures 5.13 and 5.14). The principal difference between Fe-Coag and Zr-OCl treatment was that the characteristic rapid drop in floc size occurred at a higher shear rate for Zr-OCl. Flocs formed during treatment with Fe-Coag showed a gradual decrease in floc size over time until 50 rpm, after which a rapid decrease in size was observed. For the Zr-OCl flocs, a rapid decrease in size was only observed for shear rates of 150 and 200 rpm. For shear rates of 75 and 100 rpm the flocs showed a gradual decrease in size, while at shear rates below this there was no breakage at all. For example, at 50 rpm the Zr-OCl flocs remained at an average size of 969 ± 53 µm throughout the jar test sequence. The Fe-Coag flocs however were significantly reduced from a steady state size of 702.2 ± 53 µm to a size of 479 ± 15 µm at the end of the 50 rpm shear rate phase ($T_{(34)} = -22.26$, $P < 0.01$).

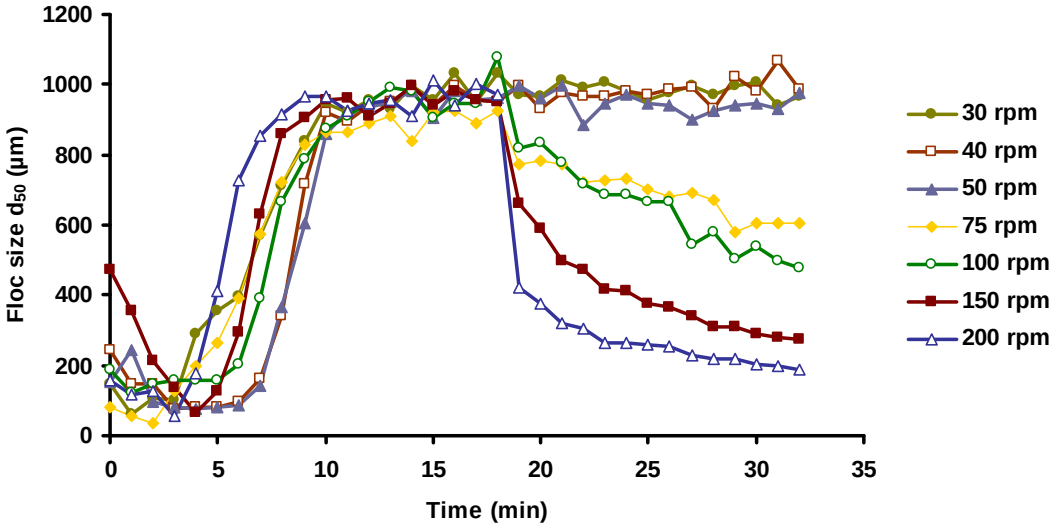

Figure 5.13: Floc breakage profile for treatment with optimum coagulant dose of Zr-OCl (8 mgL^{-1} as Zr at pH 4.5) at bench scale on water sampled on the 16th of May.

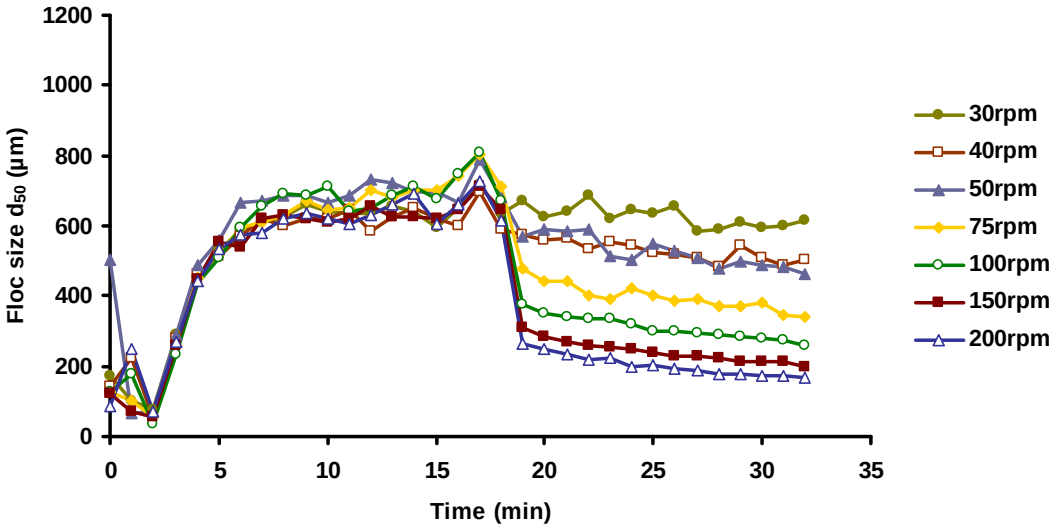

Figure 5.14: Floc breakage profile for treatment with optimum coagulant dose of Fe-Coag (8 mgL^{-1} as Fe at pH 4.5) at bench scale on water sampled on the 16th of May.

When resulting floc size after breakage with increased shear rate was considered, the Zr-OCl flocs were seen to retain the same size until 50 rpm, followed by a decrease in size with increasing shear rate. There was a linear relationship on a log log scale between broken floc size and shear rate (Figure 5.15). The Fe-Coag flocs exhibited a gradual decrease in size throughout all shear rates tested (R^2 = 0.99, as supposed to 0.93 for Zr-OCl). The resulting degradation slope for Zr-OCl was steeper than for Fe-Coag (0.91 vs. 0.70 respectively), indicating a faster decline in floc size with

increased shear rates for Zr-OCl. This was regarded as the result of a larger initial size for Zr-OCl, which converged on a similar floc size for both coagulants after a shear rate of 200 rpm (189 ± 7.3 vs.168 ± 0.8 µm for Zr-OCl and Fe-Coag respectively). The Zr-OCl flocs were bigger than the Fe-Coag flocs after breakage for all shear rates tested (Figure 5.15). Floc size is connected with floc strength since the size of a floc is the result of a balance between growth and breakage (Biggs and Lant, 2000). In this context a larger floc is considered stronger for a given shear rate condition. Therefore, the Zr-OCl flocs were regarded as being stronger than the Fe-Coag flocs.

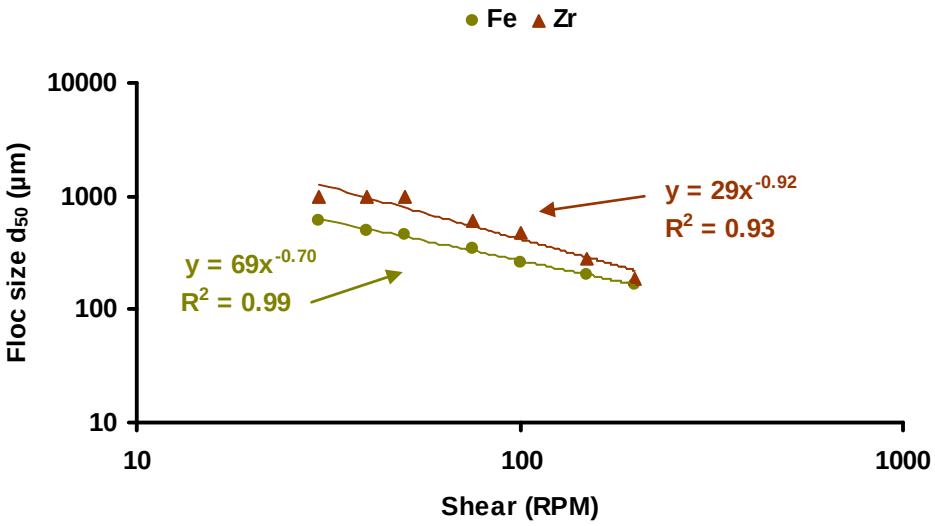

Figure 5.15: The floc breakage profile with increasing rpm for Fe-Coag and Zr-OCl under optimum conditions at bench scale on water sampled on the 16th of May.

An alternative way of evaluating the floc strength is using the following equation adapted from Francios (1987):

$$\text{Strength factor} = \frac{d(2)}{d(1)} \times 100$$

Equation 5.1

Where $d(1)$ is the floc size before breakage and $d(2)$ is the floc size after breakage. The strength factor describes a flocs relative decrease in size as the result of increased shear rate.

The resulting strength factors for Zr-OCl at shear rates of 30, 40 and 50 rpm were 94, 104 and 102 respectively meaning that little or no breakage occurred (Table 5.2). The strength factors for Zr-OCl were reduced with increasing shear rate correlating with the fast decline in floc size observed in Figure 15. The strength factors for Fe-Coag flocs were steadily reduced with increased shear rate (Table 5.2). Zr-OCl and Fe-Coag flocs showed similar strength factors at 150 and 200 rpm. After breakage at these shear rates, the flocs formed using Zr-OCl were larger than the ones formed using Fe-Coag, indicating stronger flocs for the given shear rates conditions. The similarities in strength factor were derived from the larger initial floc size for Zr-OCl.

Table 5.2: Strength factor for flocs formed after treatment with Zr-OCl and Fe-Coag under optimum conditions at bench scale on water sampled on the 15th of March for shear rates between 30 and 200 rpm.

Coagulant	**Strength factor**						
	30rpm	40rpm	50rpm	75rpm	100rpm	150rpm	200rpm
Zr	94	104	102	65	44	29	19
Fe	86	72	59	42	32	28	23

5.1.4.4 Floc re-growth

After floc growth at 30 rpm and breakage at 200 rpm, floc re-growth was induced by an additional phase with a shear rate of 30 rpm (Figure 5.16). During this phase the flocs grew quickly and reached a new steady size after 2 - 3 min of re-growth. The Zr-OCl flocs were larger before and after breakage as well as after re-growth. Compared to the size before breakage, the new steady state floc size was much lower (331 ± 7 µm and 265 ± 9 µm for Zr-OCl and Fe-Coag compared to 959 ± 58 µm and 645 ± 71 µm for Zr-OCl and Fe-Coag respectively). This indicated the occurrence of irreversible breakage in both Fe-Coag and Zr-OCl systems (Jarvis *et al*., 2005a).

Floc re-growth was determined by the recovery factor, which is calculated as follows:

$$\text{Recovery factor} = \frac{d(3)-d(2)}{d(1)-d(2)} \times 100$$

Equation 5.2

Where $d(1)$ is defined as the average floc size before breakage, $d(2)$ is floc size after breakage and $d(3)$ is the floc size after re-growth (Francois, 1987). This makes a higher recovery factor an indication of better re-growth ability. Recovery factors for Zr-OCl and Fe-Coag were 18 and 20 respectively indicating little difference in the re-growth capacity for Fe-Coag and Zr-OCl flocs. The recovery factor is a relative measure of re-growth. The smaller initial size of the Fe-Coag flocs therefore explained the higher recovery factor for Fe-Coag. The larger Zr-OCl flocs also broke more extensively at 200 rpm. This was shown by the lower strength factor (Table 5.2). Zr-OCl Consequently gives a lower recovery factor, despite producing larger flocs both before and during breakage as well as after re-growth.

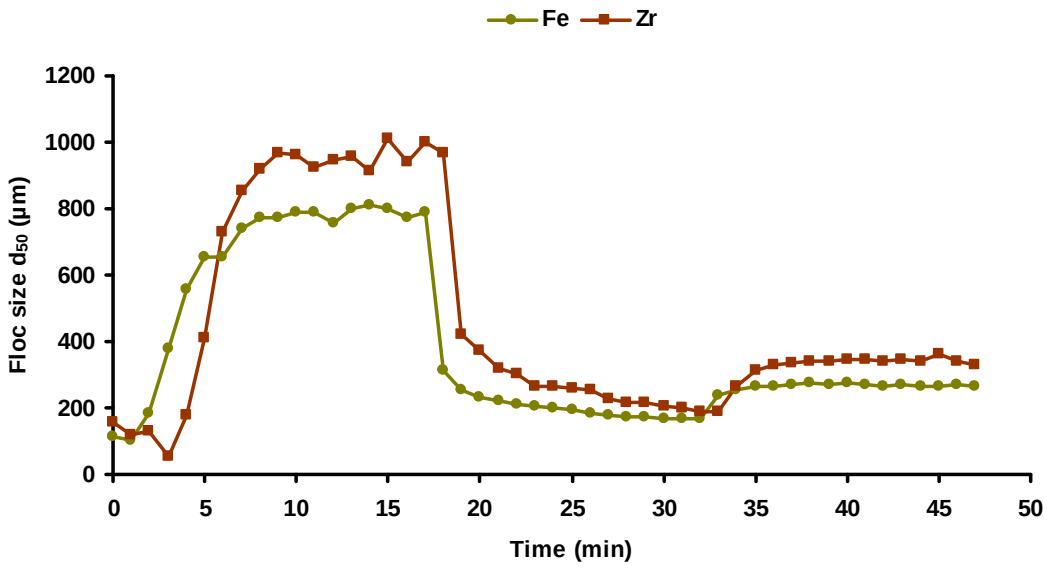

Figure 5.16: Re-growth of flocs formed using Fe-Coag and Zr-OCl under optimum conditions at bench scale on water sampled on the 16th of May. Breakage was induced using a shear rate of 200 rpm for 15 min and re-growth was induced by a shear rate of 30 rpm for 15 min.

5.1.5 Pilot scale

5.1.5.1 Pilot scale treatment of water sampled on the 14th of July

Optimum coagulation conditions were determined using the procedure described in section (4.3.1). The optimum conditions were 9 mgL^{-1} as Fe and Zr at pH 4.5 in July and 10 mgL^{-1} as Fe and Zr at pH 4 in November. Zr-OCl outperformed Fe-Coag for turbidity and NOM removal on the high SUVA water sampled in July. Statistical analysis of the data from the pilot plant experiments were carried out according to section (4.5). Residual turbidity, residual DOC and UV_{254} were found to be significantly lower, and the zeta potential was significantly higher at a confidence level of 0.05 during treatment with Zr-OCl at all stages of the treatment process (Table 5.3). The THM-FP was also found to be significantly lower in water treated with Zr-OCl at a confidence level of 0.05.

5.1.5.1.1 Flocculator tank

Zeta potential measured in the flocculator tank was and -6.4 ± 4.5 and +2.7 ± 0.6 mV during treatment Zr-OCl and Fe-Coag respectively (Figure 5.17). UV_{254} was 3.1 ± 0.1 m^{-1} for Fe and 1.6 ± 0.1 m^{-1} for Zr-OCl corresponding to UV_{254} removal of 92.3 and 95.6 % for Fe-Coag and Zr-OCl respectively (Figure 5.18). These results were similar to what was observed at bench scale on a similar water under optimum conditions (section 5.1.3), showing a higher zeta potential during treatment with Zr-OCl as well as a better removal of UV_{254} absorbance.

5.1.5.1.2 DAF

After passing through the DAF unit, the zeta potential decreased and the UV_{254} of the water increased compared with the results from the flocculator tank for both treatments. The zeta potential was -14.4 ± 1.8 mV for Fe-Coag which was outside the optimum range for coagulation with Fe based coagulants of -10 to + 5 mV as seen in section 5.1.3.1 and in previous studies (Sharp *et al.*, 2006a; Sharp *et al.*, 2006c; Sharp *et al.*, 2006d). Zeta potential for Zr-OCl was -0.6 ± 3.0 mV which was inside the optimum zeta range for Zr-OCl of between -10 to +15 mV found in section 5.1.3.1. The treated water that was used in the saturator for the DAF had a zeta potential of -18.3 mV during treatment with Fe-Coag and -15.5 mV during treatment with Zr-OCl

as a result of the pH adjustment to > 6.7 before the filter (Section 4.3.2). Increased pH causes a decrease in zeta potential following the adsorption of OH^- ions on particle surfaces. This was shown by Huang *et al.* (1999) who measured the surface charge of kaolin particles in water. When the pH was increased, the OH^- ions were absorbed until they were in excess resulting in a negative zeta potential. The UV_{254} after DAF was 3.5 ± 0.4 m^{-1} for Fe-Coag and 2.0 ± 0.1 m^{-1} for Zr-OCl which corresponded to removals of 92.3 and 95.6 % for Fe-Coag and Zr-OCl respectively. DOC removal was 80.5 % (residual DOC of 1.7 ± 0.3 mgL^{-1}) during treatment with Fe-Coag and 86.2 % (residual DOC of 1.2 ± 0.1 mgL^{-1}) during treatment with Zr-OCl, which were better results than what was achieved at bench scale on similar water for both coagulants (Section 5.1.3). Turbidity was 6.4 ± 4.8 NTU during treatment with Fe-Coag while Zr-OCl treatment resulted in a 65 % lower turbidity of 2.3 ± 0.3 NTU (Figure 5.19). During removal using DAF, the flocs formed are exposed to high shear rates. Fukushi *et al.* (1995) reported effective mean energy dissipation rates (ε) in a DAF unit of about 0.006 Wcm^{-3} for a batch experiment and 0.06 Wcm^{-3} for continuous flow. This was equivalent to velocity gradients (*G)* of 2400 s^{-1} and 7600 s^{-1} respectively. Shear rates such as this can cause flocs to break up into smaller particles (Jarvis *et al.*, 2005). Zr-OCl flocs have been shown in this study to produce larger (and hence stronger flocs) then Fe-Coag. The more robust Zr-OCl flocs resisted breakage through the DAF unit resulting in a lower particle concentration after DAF. The large variation in turbidity during treatment with Fe-Coag was due to a technical problem with the DAF unit. The flow of saturated water was reduced sporadically for a short time with subsequent loss of particle removal. This caused a large amount of flocs to remain in the water. The flocs themselves increased the turbidity of the samples taken shortly after the flow had been temporarily reduced.

The decision to adjust the pH after DAF was to more closely mirror the conditions at a full scale WTP using a ferric coagulant where the pH is normally adjusted in a similar way to remove aluminium from the water. The minimum solubility of aluminium is around pH 6 (Duan and Gregory, 2003). This means that most of the aluminium in the water will be removed from the liquid phase during filtration at this pH. It was clear that the procedure applied in this study reduced the removal efficiency of both coagulants.

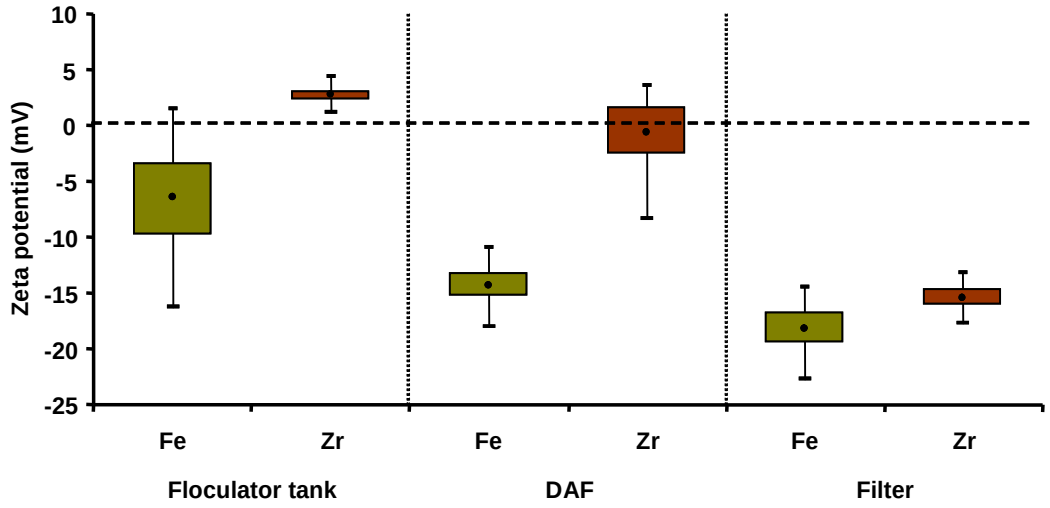

Figure 5.17: Zeta potential measured in the flocculator tank, after DAF and after the filter; during pilot plant treatment with Fe-Coag and Zr-OCl under optimum conditions on water sampled on the 14th of July (the bars represent the maximum and the minimum values, the box the 25th to 75th percentile values and the data point the mean).

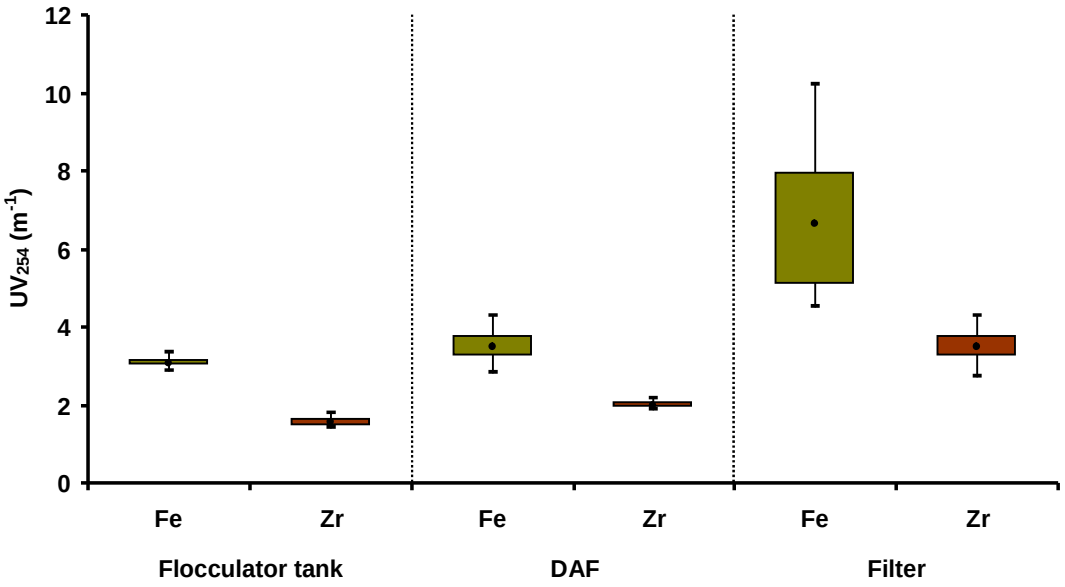

Figure 5.18: UV_{254} measured in the flocculator tank, after DAF and after the filter; during pilot plant treatment with Fe-Coag and Zr-OCl under optimum conditions on water sampled on the 14th of July (the bars represent the maximum and the minimum values, the box the 25th to 75th percentile values and the data point the mean).

5.1.5.1.3 Filter

Turbidity was further removed during sand filtration resulting in final turbidity after pilot scale treatment of 1.2 ± 0.5 NTU for Fe-Coag. Zr-OCl produced a 63 % lower final turbidity of 0.4 ± 0.1 NTU, showing superior turbidity removal over Fe-Coag (Figure 5.20). Final UV_{254} was 6.6 ± 1.9 and 3.5 ± 0.4 m^{-1} for Fe-Coag and Zr-OCl respectively, which corresponded to removals of 85.3 % for Fe-Coag and 92.3 % for Zr-OCl (Figure 5.17). Residual DOC of 2.1 ± 0.3 mgL^{-1} for Fe-Coag and 1.5 ± 0.1 mgL^{-1} for Zr-OCl was equal to DOC removal of 75.5 and 82.3 % for Fe-Coag and Zr-OCl respectively (Figure 5.19). Both UV_{254} and residual DOC, increased from before the filter to after the filter (Figures 5.18 and 5.19). This correlated with a large decrease in zeta potential in water sampled before the filter and after the filter (Figure 5.17).

The zeta potential in water sampled after the filter was -18.2 ± 2.0 and -15.5 ± 1.0 mV for Fe-Coag and Zr-OCl respectively. This was attributed to the increased pH to ≥ 6.7 before filtration (Section 4.3.2). The pH of the water before the filtration stage fluctuated over time and it could at times reach as high as 10. This was due to the change in flow rate through the pre filter pH adjustment tank following the restart process needed for the DAF unit (Section 4.3.2). An increase in pH will promote hydrolysis of metal cations according to the sequence in Section 3.4 were the charge of the species decrease with increasing pH. Ultimately, negatively charged species will form (Duan and Gregory, 2003). The negatively charged species of Fe and Zr begins to form in solution at pH levels around 6.5 for Fe and around 8.5 for Zr and at high pH levels of 10-12 the negatively charged species $Fe(OH_4)^-$ and $Zr(OH_5)^-$ dominate in solution (Veiland *et al.*, 1998; Duan and Gregory, 2003). These species will not destabilise NOM which will stay dissolved in water. The increased DOC and UV_{254} after the filter can therefore be explained by a change in composition of hydrolysed species of Fe and Zr towards species with less charge causing re-stabilisation of NOM. This would have increased the amount of DOC and UV absorbing organic material in the water after the filtering which was applied before measurements of DOC and UV_{254} (Sections 4.4.3.2 and 4.4.4).

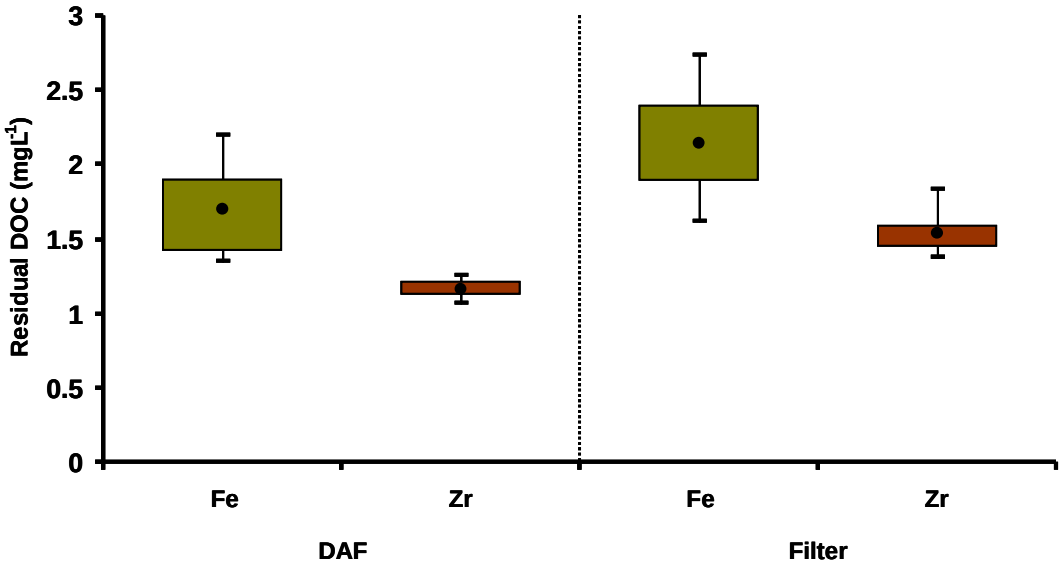

Figure 5.19: Residual DOC measured after DAF and after the filter during pilot plant treatment with Fe-Coag and Zr-OCl under optimum conditions on water sampled on the 14th of July (the bars represent the maximum and the minimum values, the box the 25th to 75th percentile values and the data point the mean).

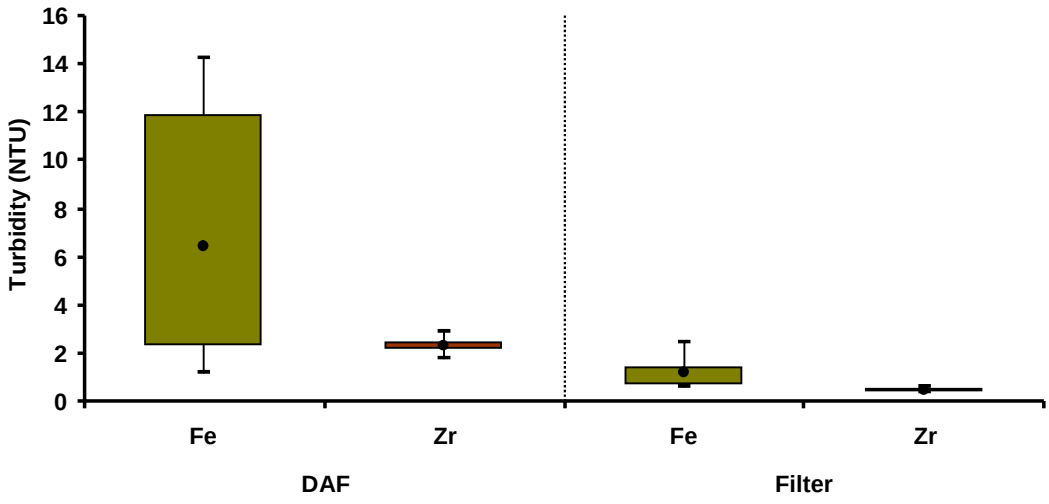

Figure 5.20: Turbidity measured after DAF and after the filter during pilot plant treatment with Fe-Coag and Zr-OCl under optimum conditions on water sampled on the 14th of July (the bars represent the maximum and the minimum values, the box the 25th to 75th percentile values and the data point the mean).

5.1.5.1.4 THM-FP

The THM-FP of water sampled after the filter was 163.1 ± 36.7 μgL^{-1} after treatment with Fe-Coag and 100.7 ± 15.0 μgL^{-1} after treatment with Zr-OCl (Figure 5.21). The amount of THMs formed per mg DOC was 75.6 ± 5.5 μgmg^{-1} and 68.2 ± 8.2 μgmg^{-1} for Fe-Coag and Zr-OCl respectively (Figure 5.21). HPSEC traces showed a better removal in the 2000 to 5000 Da MW region consisting of humic and fulvic acids by Zr-OCl compared to Fe-Coag (Figures 5.10 and 5.11). A lower amount of THMs formed per mg of DOC following lower HPSEC traces in the 2000 – 5000 Da region was also reported by Mergen (2008) who compared the THM-FP in water treated with MIEX resin with a Fe based coagulant. The humic and fulvic acids represent the hydrophobic fraction of the NOM which is regarded as the main precursor for THMs (Goslan *et al.*, 2002). This explaines the lower amount of THMs formed per mg DOC.

The reduction of THM-FP by coagulation is the result of removal of DBP precursors (Goslan *et al.*, 2002). As a result, a reduction in THM-FP follows a reduction in DOC (Chen *et al.*, 2007; Uyak *et al.*, 2007). The lower THM-FP of water treated with Zr-OCl was therefore also attributed to the lower residual DOC with a subsequent lower concentration of DBP precursors.

The results demonstrated that Zr-OCl reduced the THM-FP more than Fe-Coag both because of a better DOC removal and because of a better removal of the main DBP precursors. Raw water data could not be obtained.

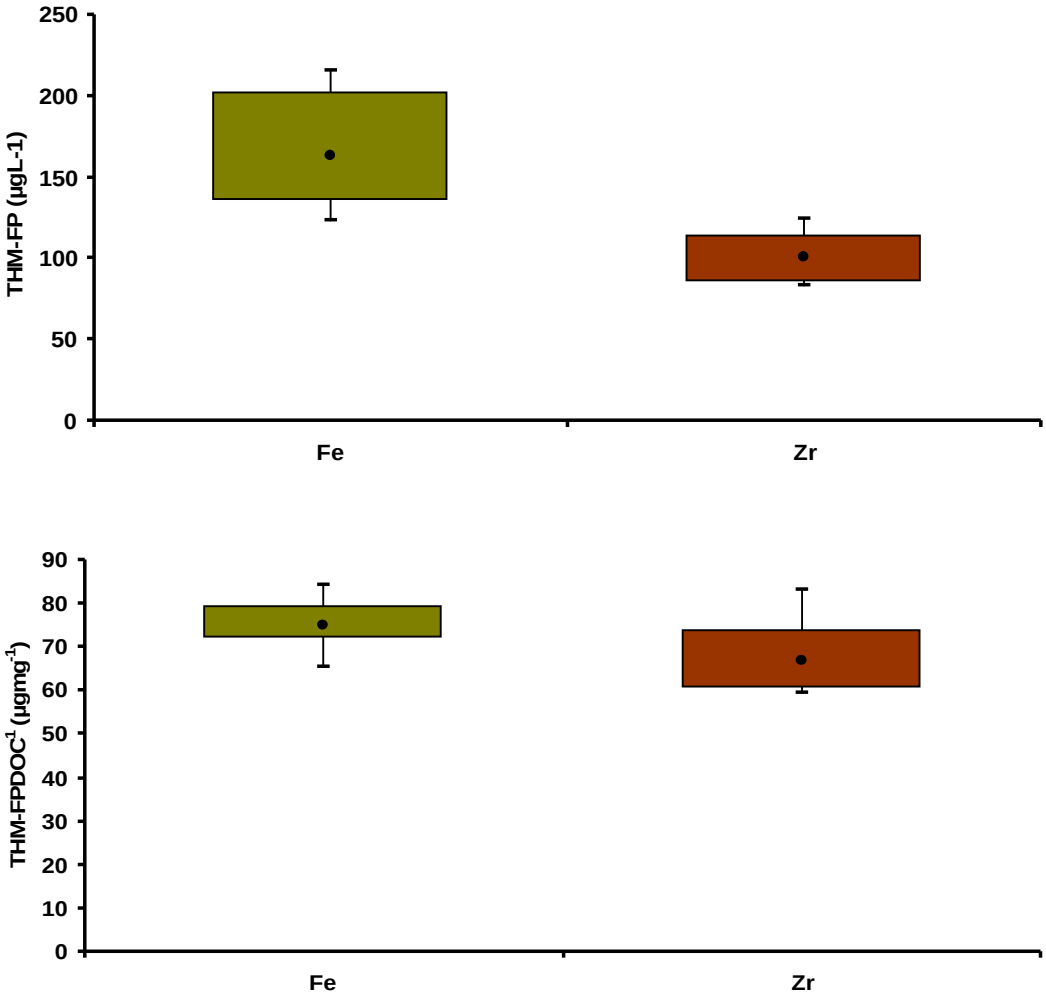

Figure 5.21: THM-FP and THM-FP per mg of DOC of final treated water after pilot scale treatment with Fe-Coag and Zr-OCl under optimum conditions on water sampled on the 14th of July (the bars represent the maximum and the minimum values, the box the 25th to 75th percentile values and the data point the mean).

Table 5.3: Summary of statistical analysis carried out on data from pilot plant treatment on water sampled on the 14th of July.

	Test	Test statistic	N-Value (Fe-Coag + Zr-OCl)	P-value
Flocculator tank				
UV_{254}	Mann-Whitney	W = 666	32 + 36	<0.05
Zeta potential	One tail T-test	T = 14.19	51 + 42	<0.05
DAF				
UV_{254}	Mann-Whitney	W = 465.0	27 + 30	<0.05
DOC	Mann-Whitney	W = 45.0	11 + 9	<0.05
Turbidity	Mann-Whitney	W = 587.0	36 + 26	<0.05
Zeta potential	Mann-Whitney	W = 2184.0	36 + 39	<0.05
Filter				
UV_{254}	Mann-Whitney	W = 666.0	36 + 36	<0.05
DOC	One tail T-test	T = -7.35	20 + 24	<0.05
Turbidity	Mann-Whitney	W = 528.0	28 + 32	<0.05
Zeta potential	One tail T-test	T = 7.74	39 + 39	<0.05
THM-FP	Mann-Whitney	W = 67.0	12 + 11	<0.05
THM-FP/ DOC	One tail T-test	T = -2.54	12 + 11	<0.05

5.1.5.2 Pilot scale treatment of water sampled on the 26th of November

During treatment of the water sampled in November, turbidity and UV_{254} was significantly lower across all of the processes during treatment with Zr-OCl (Table 5.4). THM-FP was significantly lower in water treated with Zr-OCl compared with Fe-Coag. All differences in zeta potential were found to be statistically significant. DOC was significantly lower after DAF while no difference was observed in the final water sampled after the filter. This was confirmed using the Mann-Whitney nonparametric test.

5.1.5.2.1 Flocculator tank

The zeta potential in the flocculator tank during treatment with Fe-Coag and Zr-OCl was similar (3.9 ± 0.4 mV for Fe-Coag compared to 3.4 ± 1.1 mV for Zr-OCl). Previous experiments have consistently shown a higher zeta potential for Zr-OCl compared to Fe-Coag for the same dose (Figures 5.8, 5.9 and 5.17. From bench scale experiments the expected zeta potential for Zr-Coag at pH 4 and a dose of 10 mgL^{-1} was 12.3 mV (Figure 5.9). The zeta potential observed at bench scale that most closely mirrored that found at pilot scale in November was 4.8 mV, which was observed after treatment with a dose of 8 mgL^{-1} as Zr. This indicated under dosing of Zr-OCl during the pilot plant trials in November and the actual dose added was estimated to be 8 mgL^{-1} as Zr. The UV_{254} was 5.6 ± 0.6 and 2.5 ± 0.2 m^{-1} during treatment with Fe-Coag and Zr-OCl respectively. This corresponded to removals of 87.4 % for Fe-Coag and 94.4 % for Zr-OCl which was lower then what was observed in July where the UV_{254} of 3.1 ± 0.1 and 1.6 ± 0.1 resulted in removals of 92.3 and 95.6 % for Fe-Coag and Zr-OCl respectively (Figure 5.23). The biggest difference was for Fe-Coag (4.9 %), while Zr-OCl the difference was relatively small for Zr-OCl (1.2 %) despite the underdosing.

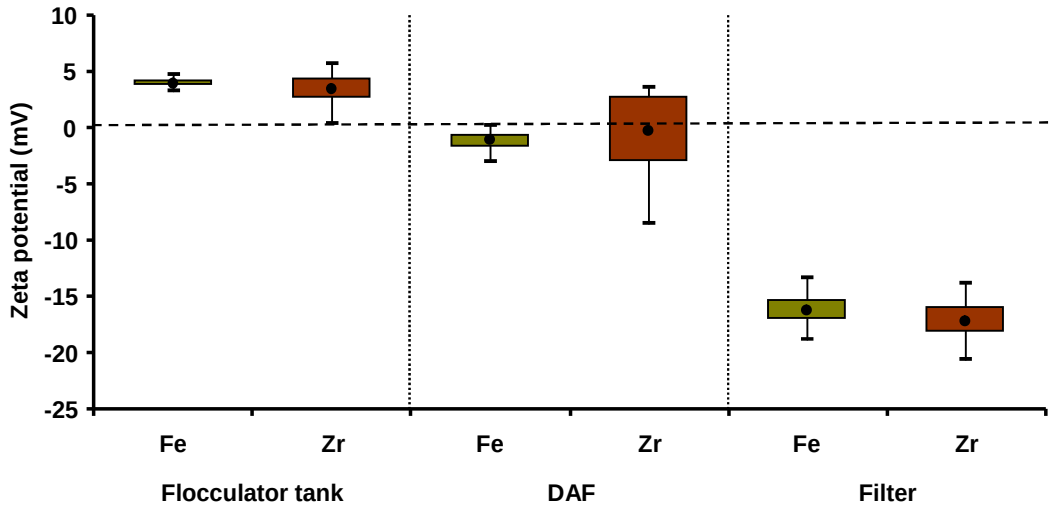

Figure 5.22: Zeta potential measured in the flocculator tank, after DAF and after the filter; during pilot plant treatment with Fe-Coag and Zr-OCl under optimum conditions on water sampled on the 26th of November (the bars represent the maximum and the minimum values, the box the 25th to 75th percentile values and the data point the mean).

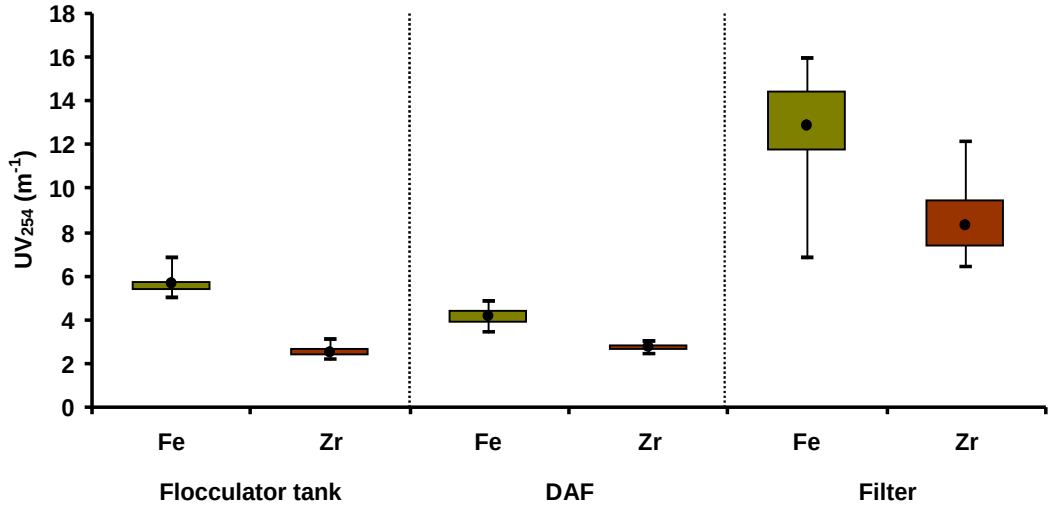

Figure 5.23: UV_{254} measured in the flocculator tank, after DAF and after the filter during pilot plant treatment with Fe-Coag and Zr-OCl under optimum conditions on water sampled on the 26th of November (the bars represent the maximum and the minimum values, the box the 25th to 75th percentile values and the data point the mean).

5.1.5.2.2 DAF

The zeta potential was higher for Zr-OCl than for Fe-Coag after DAF following a decrease for both treatments down to -1.2 ± 0.8 mV for Fe-Coag and -0.4 ± 3.4 mV for Zr-OCl (Figure 5.22). The reason for the decrease in zeta potential from the flocculator tank is outlined in Section 5.1.2.1.2. UV_{254} absorbance was 4.1 ± 0.4 m^{-1} for Fe-Coag and 2.7 ± 0.2 m^{-1} for Zr-OCl (Figure 5.23). This corresponded to 90.7 % removal for Fe-Coag and 93.9 % removal for Zr-OCl which was lower than the 92.3 and 95.6 % removal which was observed in July for Fe-Coag and Zr-OCl respectively. DOC removal was 87.0 % (residual DOC of 1.7 ± 0.1 mgL^{-1}) for Fe-Coag and 88.5 % (residual DOC of 1.5 ± 0.3 mgL^{-1}) for Zr-OCl (Figure 5.24). The residual DOC in July was 1.7 ± 0.3 and 1.2 ± 0.1 mgL^{-1} for Fe-Coag and Zr-OCl respectively. Since the raw water DOC was higher in November then in July, the removals were better in November than in July where they were 80.5 and 86.2 % for Fe-Coag and Zr-OCl respectively. However UV_{254} removal was worse even though raw water UV_{254} was higher in July. The UV_{254} removal in July was 92.3 and 95.6 % for Fe-Coag and Zr-OCl respectively. Turbidity after DAF was 12.1 ± 3.3 NTU and 5.4 ± 1.4 NTU for Fe-Coag and Zr-OCl respectively (Figure 5.25) which was higher compared to in July. It was also higher than the raw water turbidity. This is likely to be due to the technical problem with the DAF unit detailed in Section 5.1.5.1.2. Flocs formed during coagulation increased the turbidity of the water. When these were not removed during DAF the turbidity of the samples taken after DAF had a higher turbidity than the raw water.

The mass ratio of DOC to coagulant was higher in November. In July there was less than 1 mg DOC to 1 mg coagulant (8.7 mgL^{-1} DOC and a coagulant dose of 9 mgL^{-1}), while there was more than 1.3 mg DOC to 1 mg coagulant in November (13.1 mgL^{-1} DOC and a coagulant dose of 10 mgL^{-1}). A NOM to coagulant mass ratio above 1:1 has been shown to negatively impact the characteristics of flocs in terms of size and strength, even when NOM removal was high (Jarvis *et al.*, 2005d). The higher turbidity after DAF in November was therefore attributed to differences in raw water characteristics which impacted floc properties and subsequently reduced DAF performance.

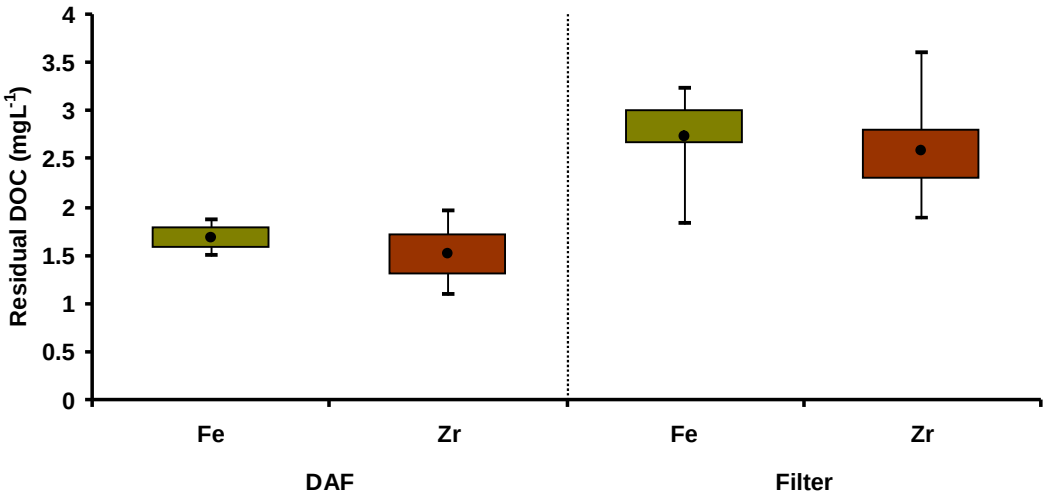

Figure 5.24: Residual DOC measured after DAF and after the filter, during pilot plant treatment with Fe-Coag and Zr-OCl under optimum conditions on water sampled on the 26th of November (the bars represent the maximum and the minimum values, the box the 25th to 75th percentile values and the data point the mean).

5.1.5.2.3 Filter

After the filter, most of the turbidity had been removed. The turbidity was reduced by 73 % to 3.2 ± 0.6 NTU for Fe and by 62 % to 2.0 ± 0.7 NTU for Zr (Figure 5.25). The final UV_{254} after treatment was 12.8 ± 2.5 m^{-1} (71 % removal) and 8.3 ± 1.5 m^{-1} (81 % removal) for Fe and Zr respectively (Figure 5.23). On the high SUVA water sampled in July, the differences in removal of UV_{254} and DOC were the same (7 %), but no significant difference in DOC removal was observed between Fe and Zr treatments on the low SUVA water in November (Table 5.4) despite the 10 % difference in UV_{254} removal. Residual DOC was 2.6 ± 0.5 and 2.7 ± 0.4 mgL^{-1} corresponding to DOC removals of 79 and 80 % for Fe and Zr respectively (Figure 5.24). NOM levels were again higher after the filter then before the filter and this observation again correlated with a decrease in zeta potential to a level outside the optimum window for coagulation (-16.1 ± 1.3 and -17.2 ± 1.6 mV for Fe and Zr respectively) which had re-dissolved some of the organic material and reduced particle capture by the filter media as described in Section 5.1.5.1.3.

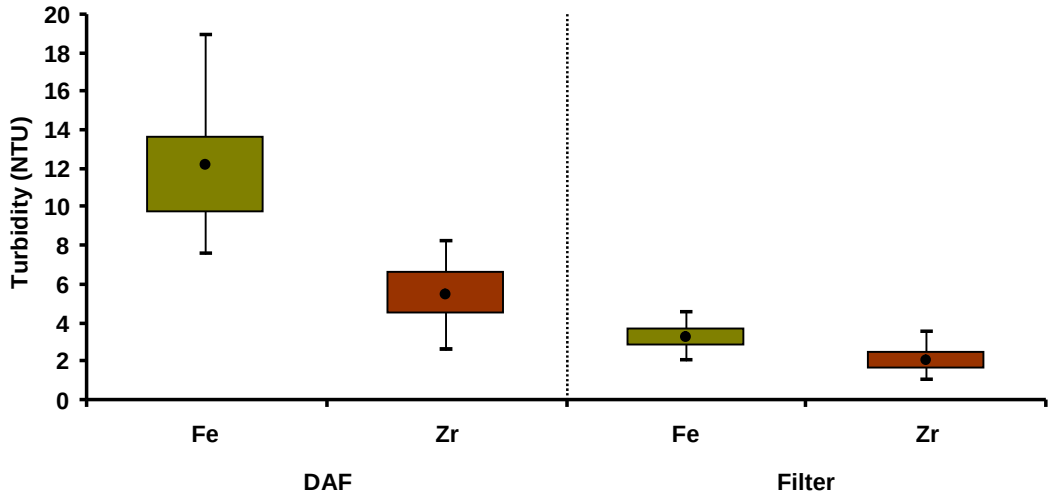

Figure 5.25: Turbidity measured after DAF and after the filter during pilot plant treatment with Fe-Coag and Zr-OCl under optimum conditions on water sampled on the 26th of November (the bars represent the maximum and the minimum values, the box the 25th to 75th percentile values and the data point the mean).

5.1.5.2.4 THM-FP

Although the residual DOC in the final water was not different THM formation was reduced for Zr-OCl. The THM-FP in final water treated with Fe-Coag was 194.6 ± 24 μgL^{-1}. Zr-OCl treated water had a THM-FP of 150.5 ± 30 μgL^{-1} which was significantly lower (Table 5.3). The THM-FP per mg of DOC was also significantly lower for Zr (67.0 ± 2.0 μgmg^{-1} and 59.9 ± 8.1 μgmg^{-1} for Fe-Coag and Zr-OCl respectively).

The THM-FP after treatment with both Fe-Coag and Zr-OCl was higher in November than in July. The SUVA of the water sampled in November was significantly lower than in July and a low SUVA is known to reduce the effectiveness of coagulation for DBP precursors (Krasner and Amy 1995, White *et al.*, 1997). The THM-FP after treatment with Zr was lower than after treatment with Fe-Coag despite the fact that the residual DOC was the same (Figure 5.25). Zr-OCl removed 10 % more of the UV_{254} than Fe-Coag indicating superior removal of the hydrophobic fraction of the NOM, which is the main cause of the UV_{254} of the raw water (Sharp *et al.*, 2006b). The hydrophobic fraction is regarded as the main precursor for THMs (Goslan *et al.*,

2002). This implied that the lower THM-FP after treatment with Zr-OCl was due to a more effective removal of THM precursors. Raw water data was not obtained.

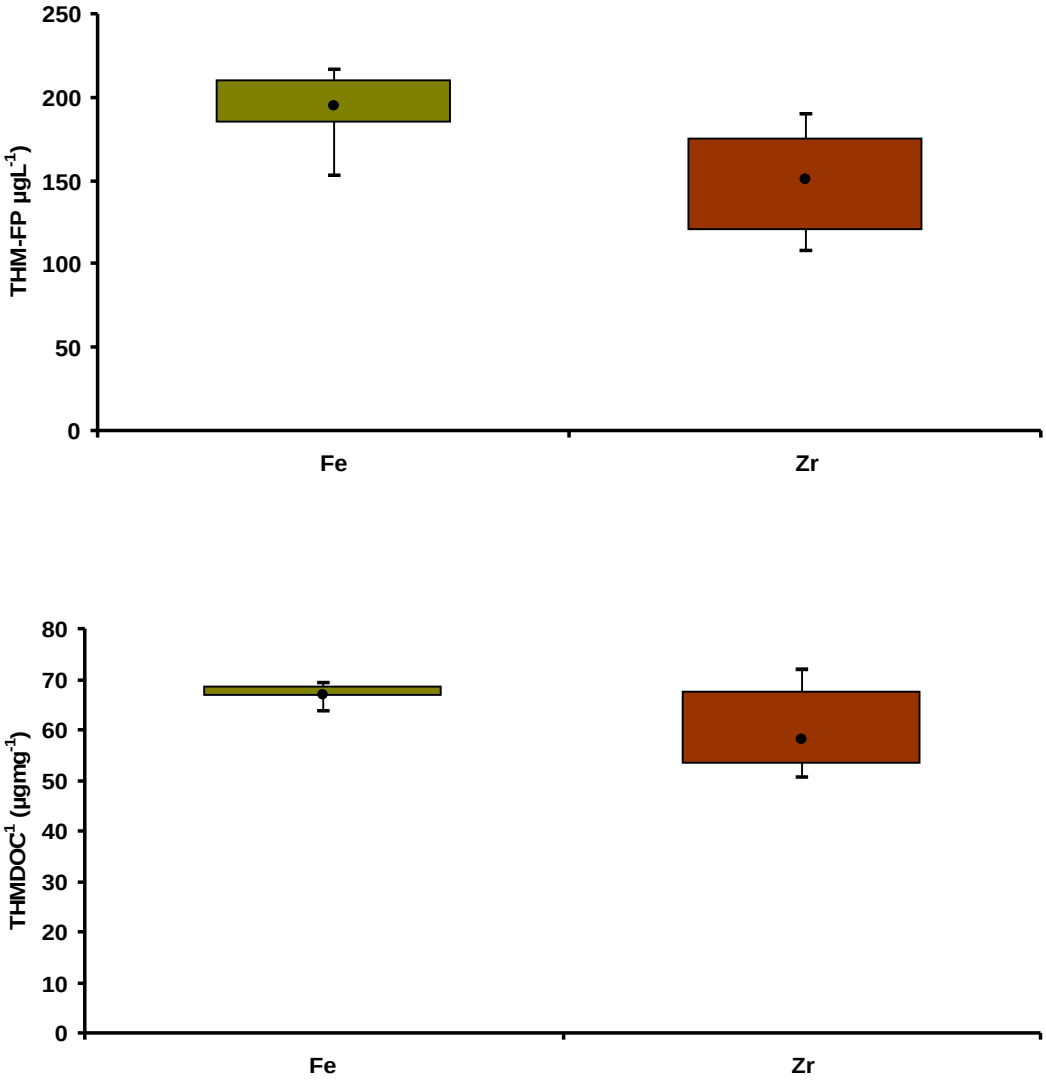

Figure 5.26: THM-FP and THM-FP per mg of DOC of final treated water after pilot scale treatment with Fe-Coag and Zr-OCl under optimum conditions on water sampled on the 26th of November (the bars represent the maximum and the minimum values, the box the 25th to 75th percentile values and the data point the mean).

Table 5.4: Summary of statistical analysis carried out on data from pilot plant treatment on water sampled on the 26th of November.

	Test	Test statistic	N-Value (Fe-Coag + Zr-OCl)	P-value
Flocculator tank				
UV_{254}	Mann-Whitney	W = 2628	36 + 72	<0.05
Zeta potential	One tailed T-test	T = -2.57	35 + 71	<0.05
DAF				
UV_{254}	Mann-Whitney	W = 1830	36 + 60	<0.05
DOC	One tailed T-test	T = -2.18	12 + 19	<0.05
Turbidity	Mann-Whitney	W = 4678	48 + 96	<0.05
Zeta potential	Mann-Whitney	W = 3513.5	31 + 66	<0.05
Filter				
UV_{254}	Mann-Whitney	W = 2668	36 + 69	<0.05
DOC	Mann-Whitney	W = 779	18 + 33	>0.05
Turbidity	Mann-Whitney	W = 5138.5	48 + 96	<0.05
Zeta potential	One tailed T-test	T = -2.90	36 + 71	<0.05
THM-FP	One tailed T-test	T = -3.07	6 + 11	<0.05
THM-FP/ DOC	One tailed T-test	T = -2.67	6 + 11	<0.05

5.2 Blending

5.2.1 Introduction

Blends of Fe-Coag and Zr-OCl were used for treatment of water containing NOM at bench scale and pilot scale according to section (4.1.4). The blends will be referred to by their weight% of Zr and Fe-Coag and Zr-OCl will be referred to as 0 and 100 weight% of Zr. The water sampled on the 16th of March was used to carry out a new set of bench scale treatments with both a set of blends and with 0 and 100 weight% of Zr used separately. For the pilot scale studies and the floc size measurements, results from treatment with blends of 0 and 100 weight% of Zr were compared to the results from treatment with 0 and 100 weight% of Zr separately on the same water. The aim was to understand the interactions between the two coagulants when they were used together in a blend with regards to NOM removal and floc properties.

5.2.2 Water characteristics

Bench scale blending experiments were carried out on water sampled on the 16th of May. This included testing of NOM removal and floc properties. The water had a UV_{254} of 38.9 m^{-1} and a DOC of 8.6 mgL^{-1} which was similar to the waters used for bench scale testing with Fe-Coag and Zr-OCl separately (Table 5.1). The resulting SUVA of the water was 4.5 mg $m^{-1}L^{-1}$ indicating that the NOM was mainly hydrophobic in nature (Sharp *et al.*, 2006b). Optimum coagulation conditions for both Fe-Coag and Zr-OCl were 8 mgL^{-1} as Fe and Zr at pH 5. These conditions were subsequently used for all blending experiments.

Pilot scale blending experiments were carried out on the same waters that were used for treatment with Fe-Coag and Zr-OCl separately sampled on the 14th of July and on the 26th of November (Table 5.1). In this section, the results from the treatments using blends will be compared to the results from the treatments with 0 and 100 weight% of Zr used separately (Section 5.1.2).

5.2.3 Bench scale blending

5.2.3.1 UV_{254} removal

The UV_{254} after treatment using coagulation under optimised conditions using 0 and 100 weight% Zr separately on the water sampled on the 16th of March (Table 5.1) was 3.4 and 2.6 m^{-1} respectively corresponding to removals of 91.4 and 93.4 %. 0 weight% of Zr performed better on this water compared to the water sampled on the 25th of March, where the UV_{254} after treatment with 0 weight% of Zr was 4.7 m^{-1} corresponding to a removal of 88.1 %. The performance of 100 weight% of Zr was similar to what was observed for the water sampled on the 25th of March, where UV_{254} after treatment was 2.3 m^{-1} corresponding to a removal of 94.2 %. An incremental increase in removal was observed when blends of 20, 40, 60 and 80 weight% of Zr resulted in UV_{254} removals of 92.3, 92.5, 93.3, and 93.1 % respectively. This increase in removal was very small but statistically significant with a R^2 value of 0.87 (Figure 5.27).

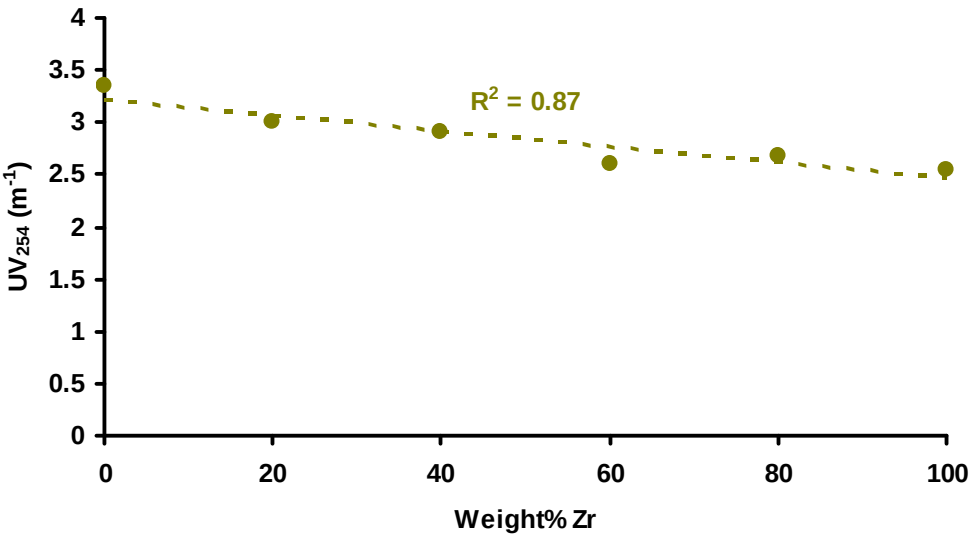

Figure 5.27: UV_{254} from water sampled on the 16th of May treated at bench scale with 6 coagulant blends of Fe-Coag and Zr-OCl with different weight% of Zr ranging from 0 to 100 % in increments of 20 % at a total dose of 8 mgL^{-1} (as Fe and/or Zr) and a pH of 5.

5.2.3.2 DOC removal

The same incremental reduction with increasing proportion of Zr was not seen for the removal of DOC. The DOC residual after treatment with 0 and 100 weight% of Zr was 2.4 and 2.3 mgL^{-1} respectively corresponding to removals of 72.3 and 72.9 %. 0 weight% of Zr performed similarly to the treatment of the water sampled on the 25th of March, where a residual DOC of 2.6 mgL^{-1} was achieved which corresponded to a removal of 69.0 %. 100 weight% of Zr performed worse than on the water sampled on the 25th of March where the residual DOC after treatment was 1.5 mgL^{-1} corresponding to a removal of 82.1 %. The sensitivity of the Shimadzu 5000 was not high enough to accurately verify any small differences in DOC concentrations between different treatments observed on the water sampled on the 16th of May. This was seen when samples with equal DOC concentration was measured several times. For example, the raw water sampled in November was measured in triplicate and the results were 12.9, 13.3 and 13.1 mgL^{-1}. This resulted in a standard deviation of 0.2 mgL^{-1}. The small difference in removal between 0 and 100 weight% of Zr (0.1 mgL^{-1}) on the water sampled on the 16th of May meant that no decreasing trend could be verified between residual DOC and weight% of Zr which can be seen from the low correlation coefficient of 0.1 (Figure 5.28).

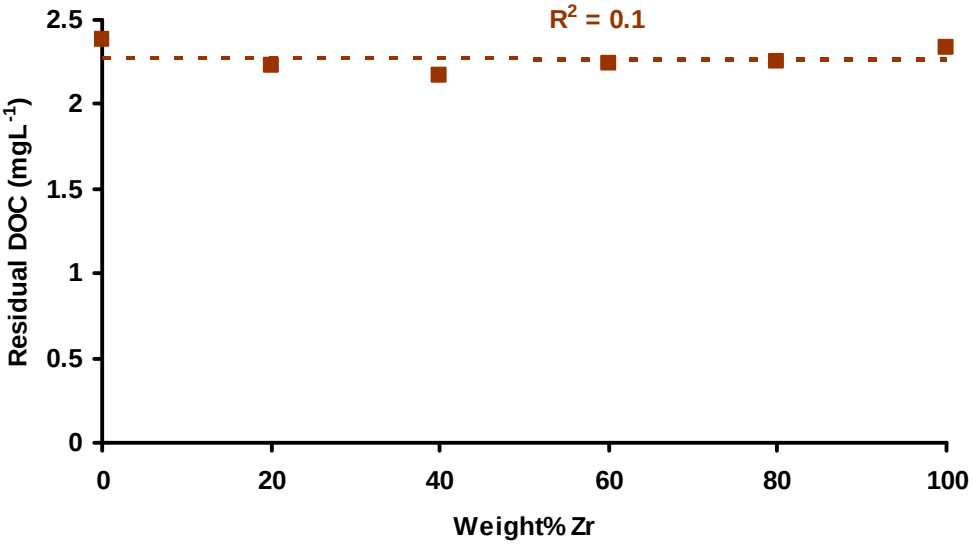

Figure 5.28: Residual DOC from water sampled on the 16th of May treated at bench scale with 6 coagulant blends of Fe-Coag and Zr-OCl with different weight% of Zr ranging from 0 to 100 % in increments of 20 % at a total dose of 8 mgL^{-1} (as Fe and/or Zr) and a pH of 5.

5.2.3.3 Turbidity removal

There was a significant improvement in residual turbidity with increasing weight% of Zr (Figure 5.29). Turbidity was reduced from 2.6 NTU after treatment with 0 weight% of Zr to 1 NTU after treatment with 100 weight% of Zr. With the exception of the 20 weight% Zr blend (which showed a turbidity of 2.9 NTU), the rest of the blends showed a turbidity between 2.6 and 1 NTU resulting in a downwards trend. Turbidity was found to decrease as a result of increased weight% of Zr with an R^2 value of 0.85 (Figure 5.29).

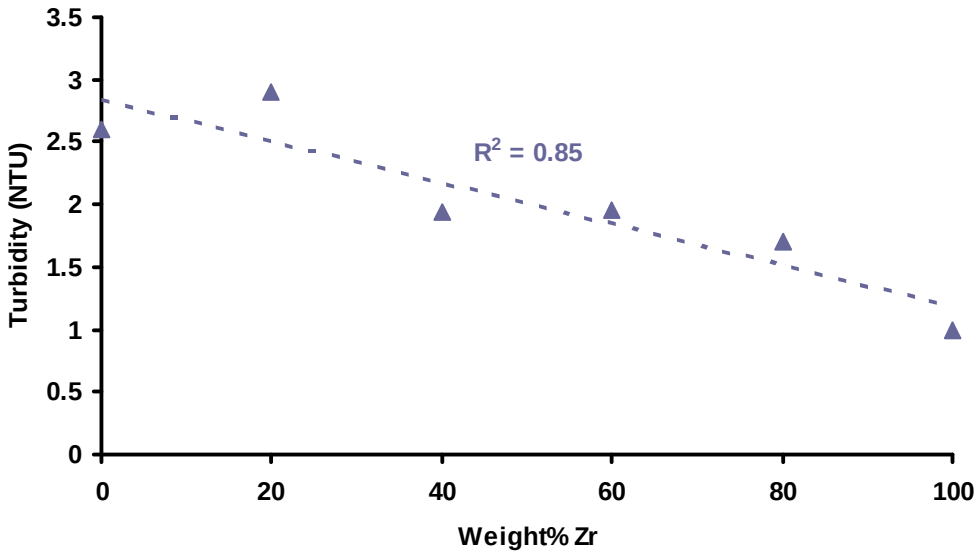

Figure 5.29: Residual turbidity from water sampled on the 16th of May treated at bench scale with 6 coagulant blends of Fe-Coag and Zr-OCl with different weight% of Zr ranging from 0 to 100 % in increments of 20 % at a total dose of 8 mgL^{-1} (as Fe and/or Zr) and a pH of 5.

5.2.3.4 Zeta potential

The zeta potential of the coagulated water became more positive with increasing weight% of Zr starting at -12.1 mV and going towards charge neutralization (Figure 5.30). The zeta potentials measured after treatment with 0 and 100 weight% of Zr were lower than the ones measured earlier after treatment with the same pH and dose conditions on other waters at both bench scale and pilot scale (Figures 5.8, 5.9, 5.22 and 5.37). This suggested that the correct zeta potentials were higher than those presented in Figure 5.30. This could be due to a calibration error or a contamination of the cell of the Malvern Zetasizer 2000HSA. However, treatment with 100 weight% of Zr still resulted in higher zeta potential compared to 0 weight% of Zr and the data was considered useful in terms of looking for changes in zeta potential as a result of changing weight% of Zr. A deviation from the above mentioned trend was the zeta potential after treatment with blends of 80 and 100 weight% of Zr which were -6.3 and -5.4 mV respectively. This was lower then what would be expected from considering the zeta potential after treatment with 0, 20, 40 and 60 weight% which were -12.1, -7.5, -4.7 and -2.9 mV respectively. Increased NOM removal with increased zeta potential going towards charge neutralization was observed when

performance was plotted against zeta potential in Section 5.1.3.1. Since performance with regards to UV_{254} and turbidity removal was improved above 60 weight% of Zr (Figures 5.27 and 5.29) other NOM removal mechanisms than charge neutralization must account for the improved performance beyond 60 weight% of Zr. Charge neutralization is not a factor for complexation by precipitation of the metal-NOM species (Gregor *et al.*, 1997). Increased removal with increased weight% of Zr between 60 and 100 % was therefore attributed to a gradual increase in the importance of complexation with increased amount of Zr in the blend.

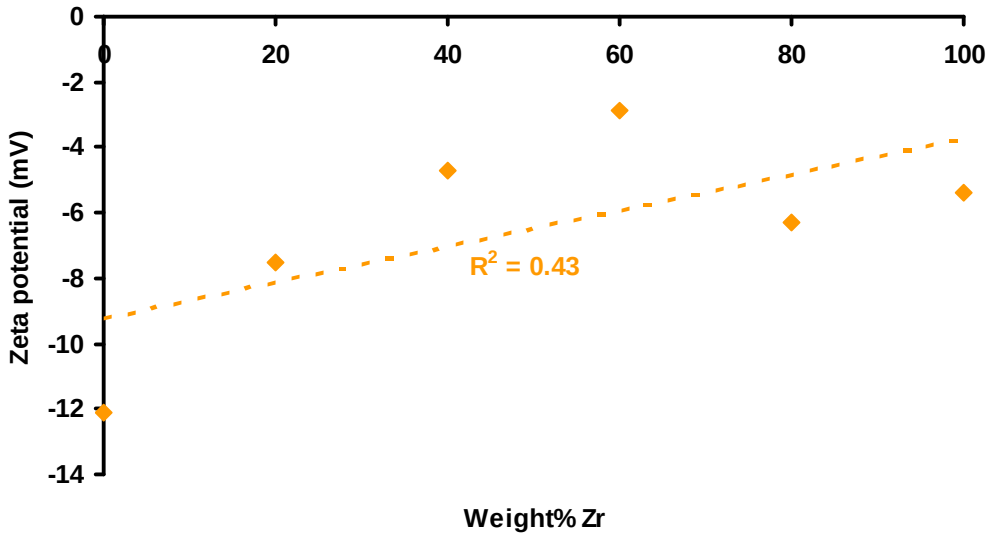

Figure 5.30: Zeta potential from water sampled on the 16th of May treated at bench scale with 6 coagulant blends of Fe-Coag and Zr-OCl with different weight% of Zr ranging from 0 to 100 % in increments of 20 % at a total dose of 8 mgL^{-1} (as Fe and/or Zr) and a pH of 5.

5.2.4 Floc properties

5.2.4.1 Floc size

The steady state size of the flocs increased with increasing weight% of Zr which explained the reduced residual turbidity with increasing weight% of Zr (Figure 5.29). The steady state size of the flocs formed during bench scale treatment with 0 – 100 weight% of Zr was in the following order (smallest to largest) (Figure 5.31): 0 weight% < 20 weight% << 80 weight% < 100 weight%. The d_{50} of the flocs were 668 ± 65, 708 ± 45, 928 ± 48 and 941 ± 81 µm for 0, 20, 80 and 100 weight% of Zr respectively. There was a significant difference in steady state size between flocs formed using 0 and 20 weight%, between 20 and 80 weight% and between 80 and 100 weight% of Zr (Table 5.5). The data showed that an increase in weight% of as little as 20 % of Zr significantly increased floc size.

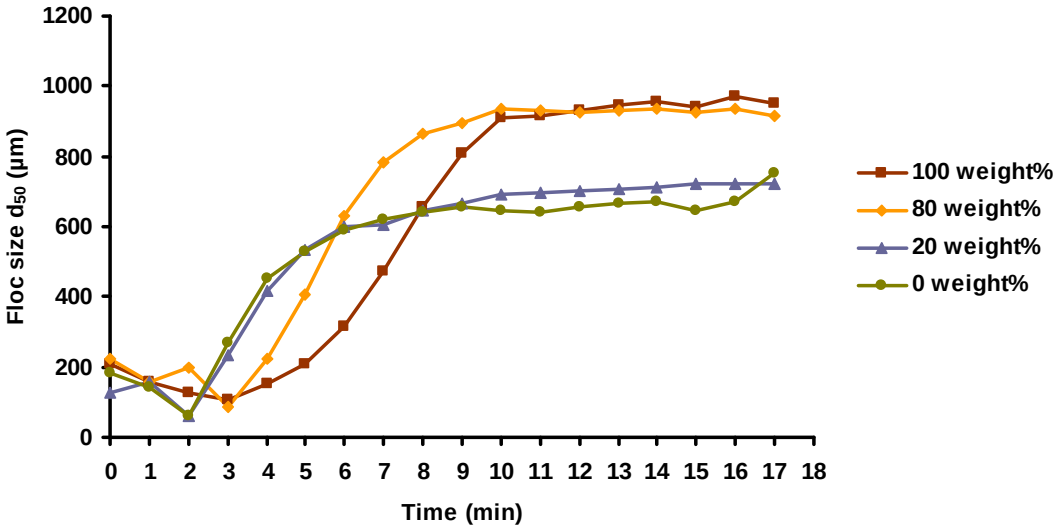

Figure 5.31: Floc growth and size for flocs formed using 0, 20, 80 and 100 weight% of Zr under optimum coagulation conditions at bench scale on water sampled on the 16th of May.

5.2.4.2 Floc growth

Treatment with 0 and 20 weight% of Zr had growth curves with a similar shape whilst growth curves observed from treatment with 80 and 100 weight% of Zr were also similar to one another (Figure 5.31). Similarities between 0 and 20 weight% of Zr and between 80 and 100 weight% of Zr were also observed for breakage profiles (Figure 5.31).

5.2.4.3 Floc breakage

The principal difference between the floc breakage profiles of 0 and 100 weight% of Zr was that the transition from a gradual decrease in floc size to a rapid drop in floc size occurred at a higher shear rate for 100 weight% of Zr (Section 5.1.4.3). A gradual decrease in floc size meant an incremental reduction in size with time as a result of increased shear rate. For treatments which experienced a rapid drop in floc size, the size of flocs were immediately reduced with increased shear rate and reached a new steady state within 1 to 2 minutes. The transition to the rapid drop in floc size occurred at shear rates of 75, 75, 100 and 150 RPM for 0, 20, 80 and 100 weight% of Zr respectively. It was apparent that the transition from a gradual decrease in floc size to a rapid drop in floc size occurred at a higher shear rate for the treatments with 80 and 100 weight% of Zr compared to the treatments with 0 and 20 weight%.

Table 5.5: Summary of statistical analysis carried out on data from floc size measurement on water sampled on the 16th of May.

Weight% Zr	Test	Test statistic	N – Value	P-value
0 vs. 20%	Mann-Whitney	W = 33583.5	167 + 166	P < 0.01
20 vs. 80%	One tailed T-test	T = 46.56	166 + 165	P < 0.01
80 vs. 100%	One tailed T-test	T = 5.50	165 + 153	P < 0.01

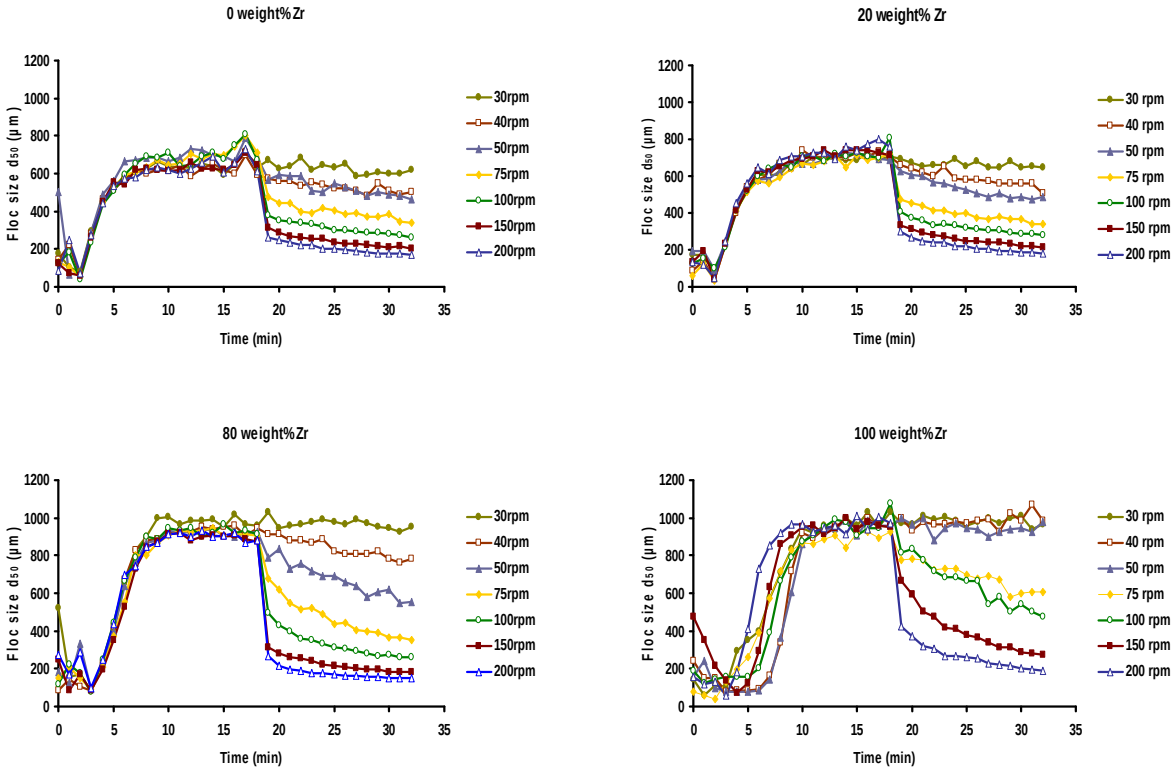

Figure 5.32: Floc breakage profiles from bench scale jar tests with 0, 20, 80 and 100 weight% of Zr under optimum conditions on water sampled on the 16th of May.

The breakage profile derived from broken floc size after increased shear rate plotted against rpm also showed similarities between 0 and 20 weight% of Zr and 80 and 100 weight% of Zr (Figure 5.33). The degradation slopes for 0 and 20 weight% of Zr was 0.70 and 0.68 and the degradation slopes for 80 and 100 weight% of Zr were 1.03 and 0.92 respectively. It was clear that the flocs formed during treatment with a high amount of Zr in the blend broke more extensively.

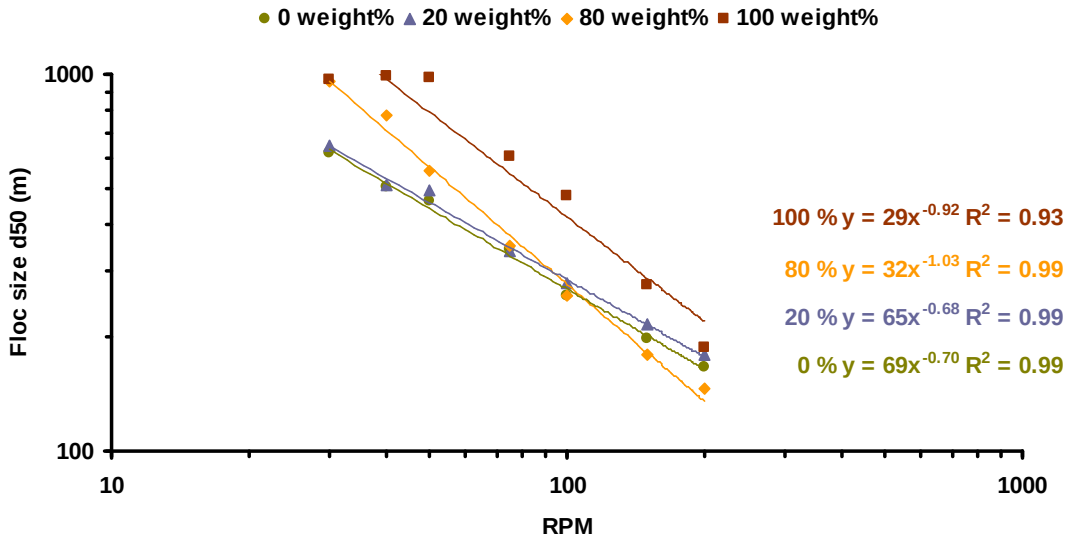

Figure 5.33: The floc breakage profiles with increasing rpm for blends with 0, 20, 80 and 100 weight% of Zr under optimum conditions at bench scale on water sampled on the 16th of May.

5.2.5 Pilot scale blending

5.2.5.1 Optimum coagulation conditions

Optimum pH and dose for both 0 and 100 weight% of Zr was 9 mgL^{-1} at pH 4.5 in July and 10 mgL^{-1} at pH 4 in November. Blending experiments were carried out under the same conditions with total metal doses of 9 mgL^{-1} (as Fe and/or Zr) at pH 4.5 in July and total metal doses of 10 mgL^{-1} (as Fe and/or Zr) at pH 4 in November.

5.2.5.2 Pilot scale blending treatment of water sampled on the 14th of July

For treatment with blends on the high SUVA water sampled on the 14th of July, statistical analysis carried out according to section (4.5) showed significant differences in removal between treatments in most cases. However, there were also instances were differences between treatments were not statistically significant (Table 5.6).

5.2.5.2.1 UV_{254} removal

A relationship between residual UV_{254} and weight% of Zr which was observed at bench scale was also observed at pilot scale across all of the treatment processes during treatment on the water sampled on the 14th of July (Figure 5.34). In the flocculator tank, the UV_{254} was 3.1 ± 0.1, 4.3 ± 0.1, 1.8 ± 0.1 and 1.6 ± 0.1 m^{-1} and after DAF, the UV_{254} absorbance was 3.5 ± 0.4, 4.8 ± 0.9, 2.7 ± 0.3 and 2.0 ± 0.1 for 0, 20, 80 and 100 weight% of Zr. UV_{254} was significantly lower during treatment with 0 weight% of Zr than with 20 weight% of Zr in the flocculator tank and after the DAF. This was the result of a dosing problem. It was discovered after the 20 weight% run that the pump used for Zr-OCl dosing was running discontinuously, causing a lower total dose with a smaller amont of Zr-OCl to be added over the course of the run. An estimate of the average dosing conditions over the course of the run suggested that the total dose could have been as low as 7.2 mgL^{-1} with a 10 weight% of Zr. After the filter, there was no significant difference between treatment with 0 weight% of Zr and treatment with 20 weight% of Zr (Table 5.6). There were however significant differences in the residual UV_{254} after treatment between the treatments with 20 and 80 weight% of Zr and between the treatments with 80 and 100 weight% of Zr (Table 5.6). The residual UV_{254} after treatment was 6.6 ± 1.9, 6.6 ± 0.4, 4.4 ± 0.7, and 3.5 ±

0.4 m^{-1} for 0, 20, 80 and 100 weight% of Zr showing increased removal with increased amount of Zr in the blend. At bench scale, the residual UV_{254} after treatment was 3.4, 3, 2.7 and 2.6 m^{-1} for 0, 20, 80 and 100 weight% of Zr. It was clear that the UV_{254} after treatment was higher at pilot scale than at bench scale. It was also clear that by increasing the proportion of Zr in the blend, the removal of UV_{254} improved.

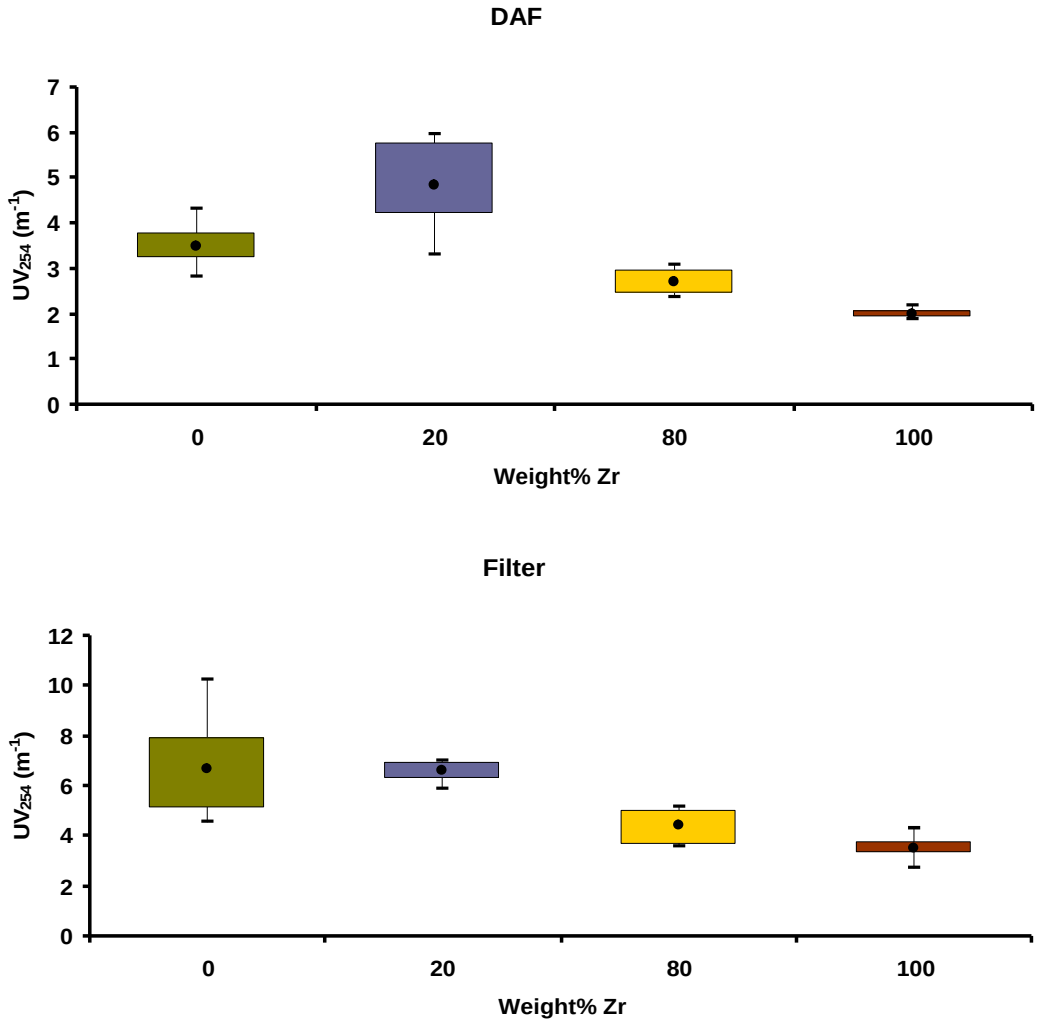

Figure 5.34: UV_{254} in the flocculator tank, after DAF and after the filter for treatment with 0, 20, 80 and 100 weight% of Zr under optimum conditions at pilot scale on water sampled on the 14th of July (the bars represent the maximum and minimum values, the box the 25th to 75th percentile values and the data point the mean).

5.2.5.2.2 DOC removal

Reductions in residual DOC with increased weight% of Zr was observed both after DAF and after the filter. After DAF, residual DOC was 1.7 ± 0.3, 2.1 ± 0.1, 1.6 ± 0.1 and 1.2 ± 0.1 mgL^{-1} for 0, 20, 80 and 100 weight% of Zr (Figure 5.35). All differences between treatments were significant (Table 5.6). However, treatment with 20 weight% of Zr resulted in the highest residual DOC following the underdosing. After the filter, residual DOC was 2.1 ± 0.3, 2.1 ± 0.1, 1.6 ± 0.2, 1.6 ± 0.1 for 0, 20, 80 and 100 weight% of Zr which corresponded to DOC removals of 75.9 % for 0 and 20 weight% of Zr and 81.6 % for 80 and 100 weight% of Zr (Figure 5.35). The only significant sequential difference in DOC was between the treatments with 20 and 80 weight% of Zr. The residual DOC after treatment was lower at pilot scale than at bench scale where treatment with 0, 20, 80 and 100 weight% of Zr resulted in DOC concentrations of 2.4, 2.2, 2.3 and 2.3 mgL^{-1} respectively. This corresponded to DOC removals of 72.3, 74.0, 73.8 and 72.9 % respectively.

It was apparent that the UV_{254} and DOC were increased from before the filter to after the filter during pilot scale treatment. This is explained in Sections 5.1.5.1.2 and 5.1.5.3.

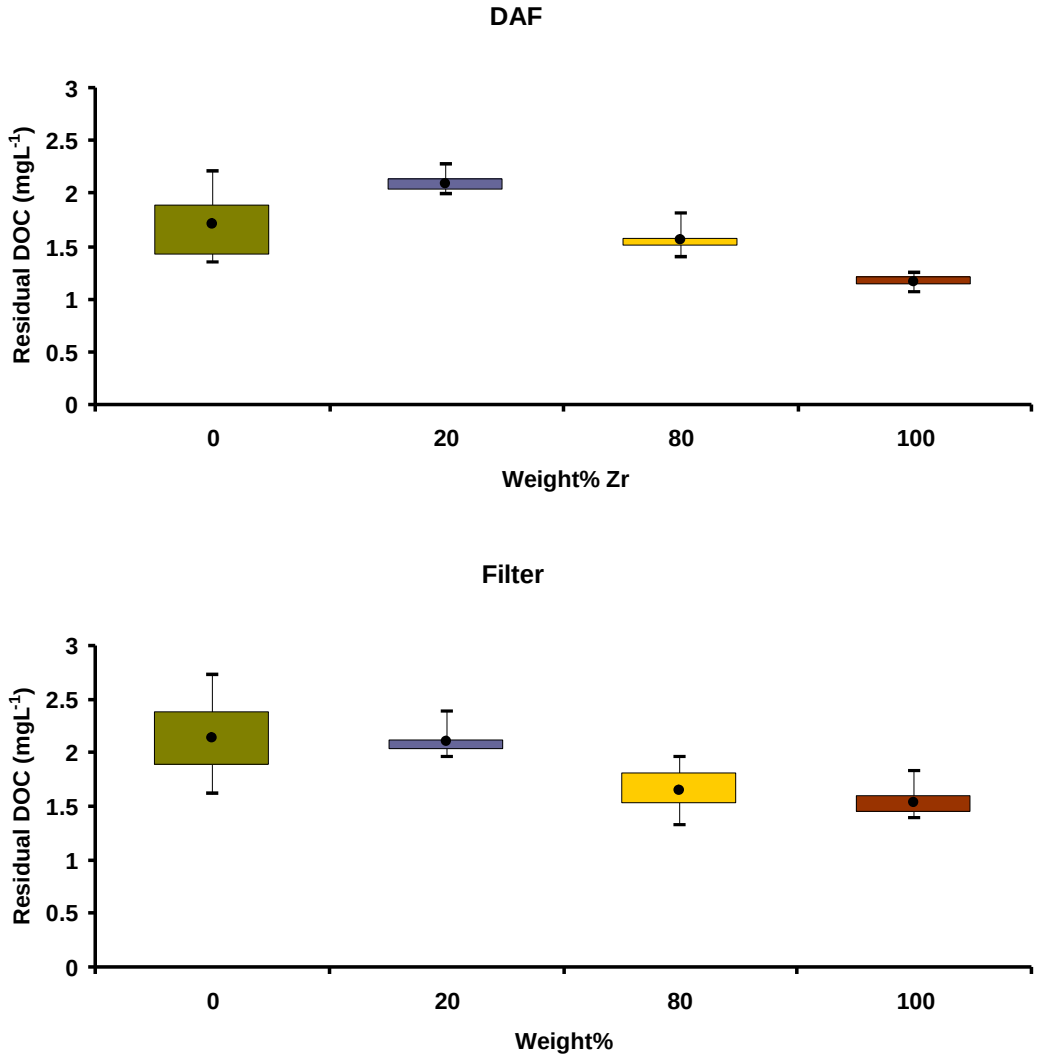

Figure 5.35: Residual DOC in the flocculator tank, after DAF and after the filter for treatment with 0, 20, 80 and 100 weight% of Zr under optimum conditions at pilot scale on water sampled on the 14th of July (the bars represent the maximum and minimum values, the box the 25th to 75th percentile values and the data point the mean).

5.2.5.2.3 Turbidity

Turbidity after DAF and after the filter was lower during treatment with 80 and 100 weight% of Zr than during treatment with 0 and 20 weight% of Zr (Figure 5.36). Turbidity after DAF was 6.4 ± 4.8, 6.0 ± 4.7, 2.9 ± 2.4 and 2.3 ± 0.3 NTU for 0, 20, 80 and 100 weight% of Zr. No significant differences were found between treatments differing significantly in weight% of Zr by less than 60 % (Table 5.6). Consequently, no reduction in turbidity was confirmed for small changes in weight% of Zr. This was the result of fluctuations in turbidity with subsequent large variance. For example, treatment with 0 and 80 weight% of Zr showed standard deviations of 76 and 83 % respectively. However, the difference between the treatments with 20 and 80 weight% of Zr was significant (Table 5.6). Unfiltered turbidity at pilot scale (i.e. turbidity after DAF) was higher than at bench scale where the unfiltered turbidity for 0, 20, 80 and 100 weight% of Zr was 2.6, 2.9, 1.7 and 1.0 NTU respectively. This indicated a higher degree of floc breakage at pilot scale, which can be attributed to shear conditions from transport over weirs and ledges and through the DAF unit (Fukushi *et al.*, 1995; Jarvis *et al.*, 2005a).

After the filter, all treatments showed smaller variance, and the turbidity was greatly reduced from before the filter (i.e. after DAF). Turbidity after the filter was 1.2 ± 0.5, 1.4 ± 0.4, 0.4 ± 0.1 and 0.4 ± 0.1 for 0, 20, 80 and 100 weight% of Zr. (Figure 5.36). Again, a significant sequential difference in turbidity was only observed between the treatments with 20 and 80 weight% of Zr showing that blends with high amount of Zr gave lower turbidity than blends with low amount of Zr but a reduction in turbidity as a result of the small change in the amount of Zr could not be verified (Table 5.6).

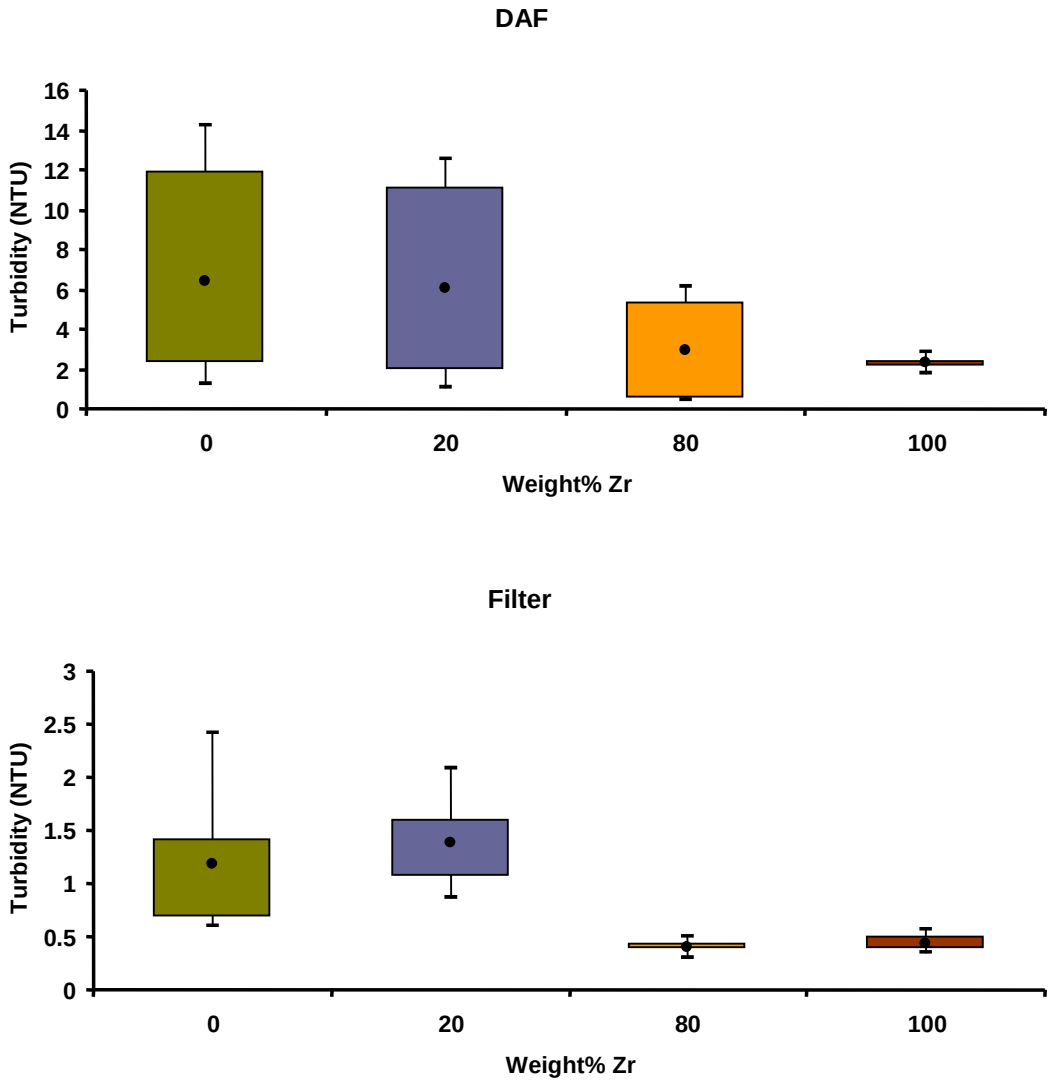

Figure 5.36: Turbidity after DAF and after the filter for treatment with 0, 20, 80 and 100 weight% of Zr under optimum conditions at pilot scale on water sampled on the 24th of July (the bars represent the maximum and minimum values, the box the 25th to 75th percentile values and the data point the mean).

5.2.5.2.4 Zeta potential

In the flocculator tank, zeta potential was increased with increased weight% of Zr, with one exception (Figure 5.37). The zeta potential during treatment with 20 weight% of Zr was -13.3 mV which was the lowest of all the treatments and outside of the optimum zeta potential range for 0 weight% of Zr (-10 to + 5 mV). This was because of underdosing of the treatment with 20 weight% of Zr (Section 5.2.3.2.1). Zeta potentials for 0, 80, and 100 weight% of Zr were -6.4 ± 4.5, 1.2 ± 1.4 and 2.7 ± 0.6 mV respectively. As a result of underdosing, treatment with 0 weight% of Zr produced a significantly higher zeta potential than for the treatment with 20 weight% of Zr, both in the flocculator tank and after the DAF (Table 5.6) where the zeta potential was -14.4 ± 1.8 mV, -15.5 ± 0.6 mV, -8.2 ± 5.5 mV and -0.6 ± 3.0 mV for 0, 20, 80 and 100 weight% of Zr respectively. There was also a difference between the treatments with 80 and 100 weight% of Zr both in the flocculator tank and after the DAF, indicating that even small changes in weight% of Zr can have a significant impact on zeta potential (Figure 5.37). The zeta potential was reduced after the DAF for all blends. After the filter, zeta potential dropped for all treatments to -18.3 ± 2.0, -18.0 ± 1.0, -15.6 ± 1.6 and -15.5 ± 1.0 mV for 0, 20, 80 and 100 weight% of Zr respectively. The reason for the changes in zeta potential between the flocculator tank and the DAF and between the DAF and the filter is outlined in sections 5.1.5.1.2 and 5.1.5.1.3.

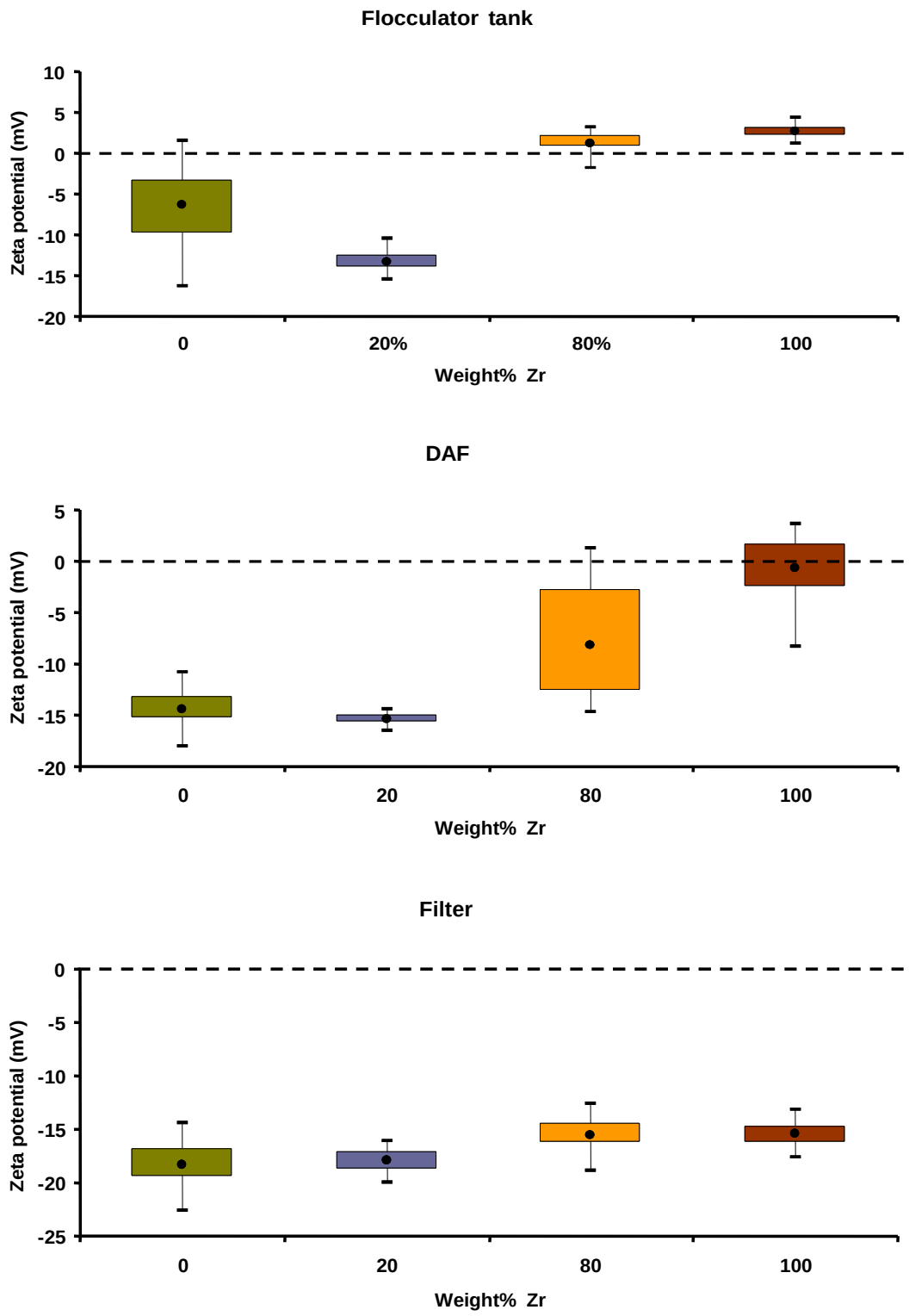

Figure 5.37: Zeta potential in the Flocculator tank, after DAF and after the filter during pilot scale treatment with 0, 20, 80 and 100 weight% of Zr under optimum conditions on water sampled on the 14th of July (the bars represent the maximum and minimum values, the box the 25th to 75th percentile values and the data point the mean).

5.2.5.2.5 THM-FP

Increased amount of Zr in the blend reduced the THM-FP of the water after treatment. The THM-FP in water sampled after the filter was 163.1 ± 34, 179. 9 ± 14, 143. 4 ± 27 and 100.7 ± 15 μgL^{-1} for 0, 20, 80 and 100 weight% of Zr respectively showing a correlation between reduced THM-FP and increased weight% of Zr (Figure 5.38). The treatment with 20 weight% of Zr deviated from this correlation as a result of underdosing of coagulant.

Reduced THM-FP follows reduced DOC (Uyak *et al.*, 2007; Chen *et al.*, 2007). This was shown by the results following that both residual DOC concentration and THM-FP after treatment was in the same order (highest to lowest) (Figures 5.35 and 5.38) 20 weight% > 0 weight% > 80 weight% > 100 weight%. However, treatment with 100 weight% of Zr gave a significantly lower THM-FP than treatment with 80 weight% of Zr despite the fact that the residual DOC was the same for the two treatments (Figure 5.35) (Table 5.6). THM formation has been found to correlate with SUVA such as more THMs are formed when the SUVA is increased (Reckhow *et al.*, 1990). The treatment with 100 weight% of Zr removed more UV_{254} than the treatment with 80 weight% of Zr after the filter and the resulting SUVA of the water was 2.7 and 2.2 mg $m^{-1}L^{-1}$ after treatment with 80 and 100 weight% of Zr respectively. This can account for the reduced THM-FP following the increase in weight% of Zr. The same observation was made when 0 and 100 weight% of Zr was used separately at pilot scale in November (Section 5.1.5.2.4). Treatment with 100 weight% of Zr produced water with lower THM-FP despite the fact that the residual DOC was the same as after treatment with 0 weight% of Zr. This was also found to be due to better UV_{254} removal. Consequently, Zr was found to reduce THM-FP both by reducing the total DOC and by reducing a larger amount of UV_{254} absorbing DBP precursors.

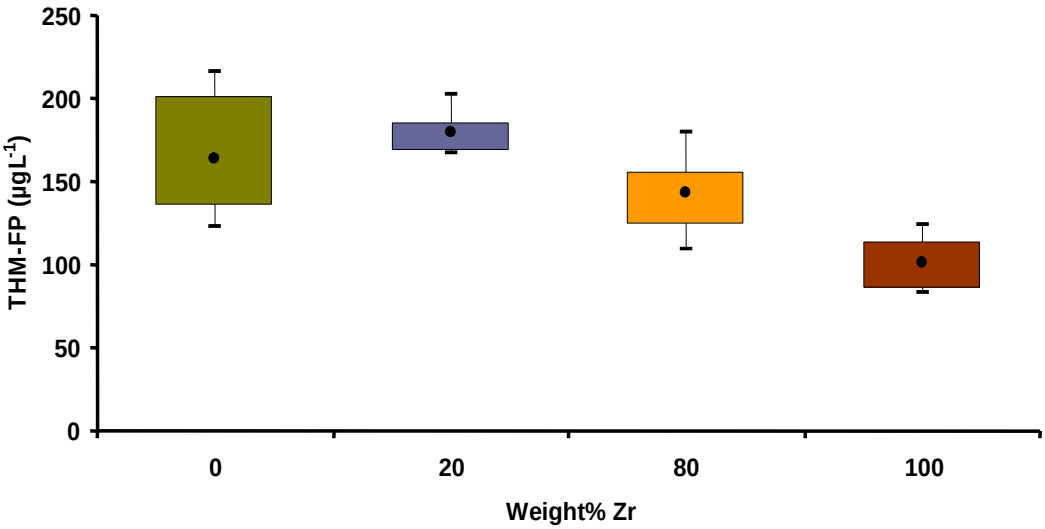

Figure 5.38:THM-FP for treatment with 0, 20, 80 and 100 weight% of Zr under optimum conditions at pilot scale on water sampled on the 14th of July (the bars represent the maximum and minimum values, the box the 25th to 75th percentile values and the data point the mean).

Table 5.6: Summary of statistical analysis of samples taken during pilot plant treatment in July

	Test	Test statistic	N-Value	P-Value
Flocculator tank				
Zeta potential				
0 vs. 20 weight%	One tailed T-test	T = 9.99	51 + 19	P<0.05
20 vs. 80 weight%	Mann-Whitney	W = 513	19 + 18	P<0.05
80 vs. 100 weight%	Mann-Whitney	W = 1537.5	18 + 42	P<0.05
UV_{254}				
0 vs. 20 weight%	One tailed T-test	T = -6.4	32 + 18	P<0.05
20 vs. 80 weight%	Mann-Whitney	W = 495	18 + 18	P<0.05
80 vs. 100 weight%	Mann-Whitney	W = 789	18 + 36	P<0.05
DAF				
Zeta potential				
0 vs. 20 weight%	One tailed T-test	T = 3.02	36 + 14	P<0.05
20 vs. 80 weight%	Mann-Whitney	W = 107	14 + 21	P<0.05
80 vs. 100 weight%	Mann-Whitney	W = 332.5	21 + 39	P<0.05
UV_{254}				
0 vs. 20 weight%	One tailed T-test	T = -5.61	27 + 18	P<0.05
20 vs. 80 weight%	Mann-Whitney	W = 441	18 + 15	P<0.05
80 vs. 100 weight%	Mann-Whitney	W = 570	15 + 30	P<0.05
Turbidity				
0 vs. 20 weight%	Mann-Whitney	W = 431	36 + 18	P>0.05
20 vs. 80 weight%	Mann-Whitney	W = 252	18 + 18	P<0.05
80 vs. 100 weight%	Mann-Whitney	W = 585	18 + 26	P>0.05
Residual DOC				
0 vs. 20 weight%	One tailed T-test	T = -3.94	11 + 6	P<0.05
20 vs. 80 weight%	One tailed T-test	T = 7.52	6 + 6	P<0.05
80 vs. 100 weight%	One tailed T-test	T = -7.68	6 + 9	P<0.05

Table 5.6: Summary of statistical analysis of samples taken during pilot plant treatment in July

	Test	Test statistic	N-Value	P-Value
Filter				
Zeta potential				
0 vs. 20 weight%	One tailed T-test	T = -0.82	39 + 21	P>0.05
20 vs. 80 weight%	One tailed T-test	T = 5.73	21 + 20	P<0.05
80 vs. 100 weight%	One tailed T-test	T = -.18	20 + 39	P>0.05
UV_{254}				
0 vs. 20 weight%	Mann-Whitney	W = 900	36 + 15	P>0.05
20 vs. 80 weight%	Mann-Whitney	W = 171	15 + 18	P<0.05
80 vs. 100 weight%	Mann-Whitney	W = 754	18 + 36	P<0.05
Turbidity				
0 vs. 20 weight%	Mann-Whitney	W = 379.5	28 + 15	P>0.05
20 vs. 80 weight%	Mann-Whitney	W 120	15 + 15	P<0.05
80 vs. 100 weight%	Mann-Whitney	W = 833.5	15 + 32	P>0.05
Residual DOC				
0 vs. 20 weight%	Mann-Whitney	W = 317.5	20 + 12	P>0.05
20 vs. 80 weight%	Mann-Whitney	W = 79	12 + 12	P<0.05
80 vs. 100 weight%	Mann-Whitney	W = 397	12 + 24	P>0.05
THM-FP				
0 vs. 20 weight%	Mann-Whitney	W = 54	12 + 5	P>0.05
20 vs. 80 weight%	Mann-Whitney	W 37	5 + 5	P<0.05
80 vs. 100 weight%	One tailed T-test	T = 4.06	5 + 11	P<0.05
THM-FP / DOC				
0 vs. 20 weight%	One tailed T-test	T = 3.91	12 + 5	P>0.05
20 vs. 80 weight%	One tailed T-test	T = -.13	5 + 5	P>0.05
80 vs. 100 weight%	One tailed T-test	T = -3.85	5 + 11	P<0.05

5.2.5.3 Pilot scale blending treatment of water sampled on the 26th of November

For treatment with blends on the low SUVA water sampled on the 26th of November, statistical analysis carried out according to section 4.5 showed significant differences in removal between treatments in most cases. However, there were also instances were differences between treatments were not statistically significant (Table 5.7).

5.2.5.3.1 UV_{254}

During treatment on the low SUVA water sampled on the 26th of November, correlations between UV_{254} and weight% of Zr were observed across all of the processes (Figure 5.39). In the flocculator tank UV_{254} during treatment was 5.6 ± 0.6, 5.1 ± 0.2, 3.5 ± 0.1, and 2.5 ± 0.2 m^{-1} for 0, 20, 80 and 100 weight% of Zr. After DAF, UV_{254} was 4.1 ± 0.4, 4.4 ± 0.4, 3.2 ± 0.4 and 2.7 ± 0.2 m^{-1} which corresponded to removals of 90.8, 90.2, 92.8 and 93.9 % for 0, 20, 80 and 100 weight% of Zr respectively. After the filter, UV_{254} was increased for all treatments to 12.8 ± 2.5, 10.6 ± 2.8, 6.9 ± 1.0 and 8.3 ± 1.5 m^{-1}, with subsequent removals of 71.3, 76.2, 84.5 and 81.4 % for 0, 20, 80 and 100 weight% Zr respectively. The removal was lower than in July (Section 5.2.5.2.1). The water sampled in November had a lower SUVA (Table 5.1) indicating that it was less hydrophobic. A low SUVA water is generally considered to be more difficult to treat then a high SUVA water (Fearing *et al.*, 2004; Sharp *et al.*, 2006a). The lower SUVA of the water sampled in November can consequently account for the lower UV_{254} removal efficiency of both coagulants in November.

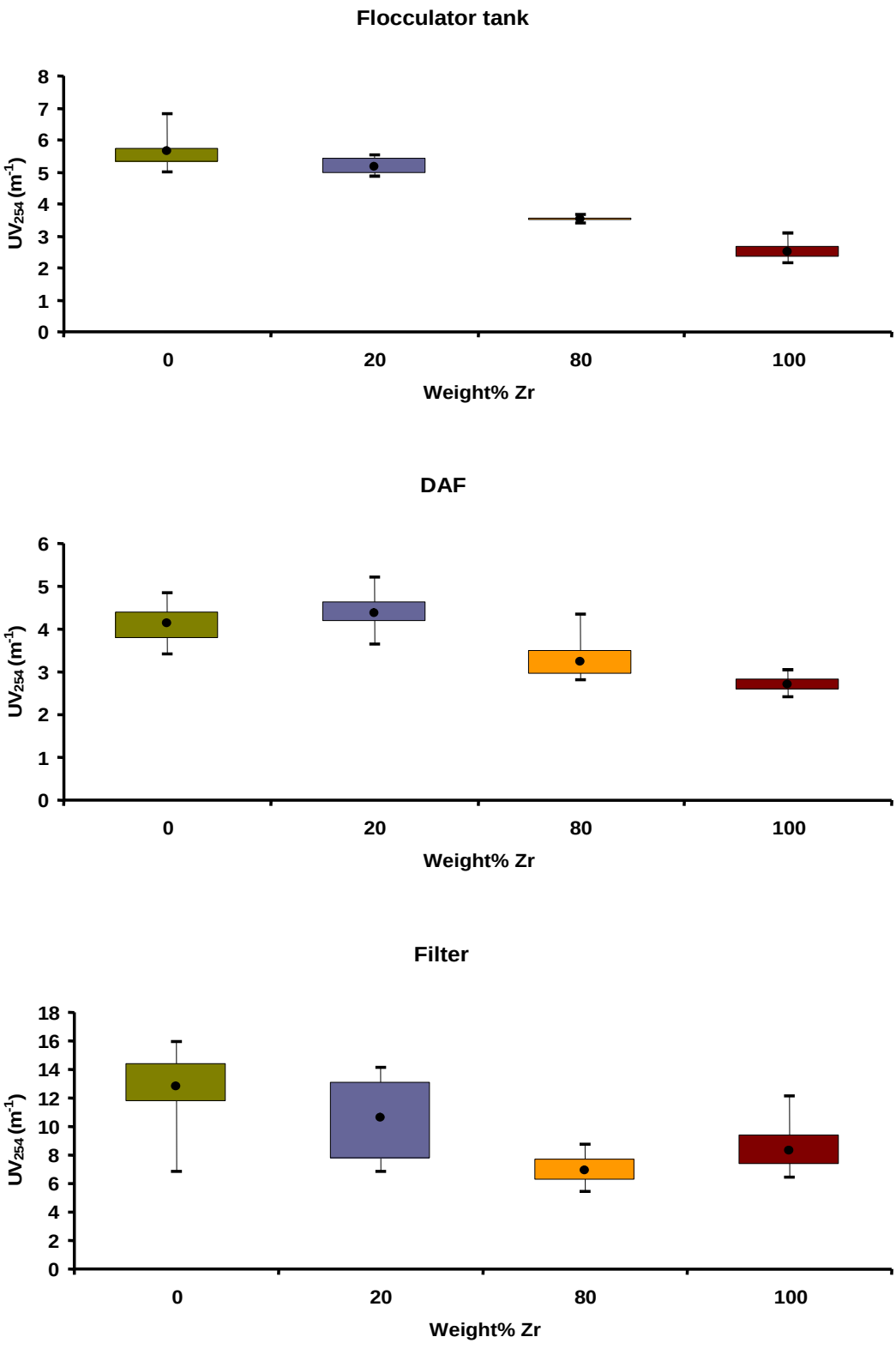

Figure 5.39: UV_{254} in the flocculator tank, after DAF during pilot scale treatment with 0, 20, 80 and 100 weight% of Zr under optimum conditions on water sampled on the 26th of November (the bars represent the maximum and minimum values, the box the 25th to 75th percentile values and the data point the mean).

5.2.5.3.2 DOC

After DAF, treatment with 0, 20, 80 and 100 weight% of Zr resulted in residual DOC of 1.7 ± 0.1, 1.7 ± 0.1, 1.6 ± 0.1 and 1.5 ± 0.3 mgL^{-1} respectively (Figure 5.40). The only significant sequential difference was observed between the treatment with 20 weight% of Zr and the treatment with 80 weight% of Zr (Table 5.7). This can be attributed to the small difference between 0 and 100 weight% of Zr. In July, there were significant differences between all treatments. This was, in part, due to the bigger differences between 0 and 100 weight% of Zr but the underdosing during treatment with 20 weight% of Zr also contributed.

After the filter, DOC increased for all treatments to 2.7 ± 0.4, 2.4 ± 0.3, 2.3 ± 0.3 and 2.6 ± 0.5 mgL^{-1} for 0, 20, 80 and 100 weight% of Zr respectively. This was higher than the DOC after the filter in July (Figure 5.35). Differences between the treatments were also increased and were all found to be significant (Table 5.7). However, the residual DOC after treatment with 100 weight% of Zr was significantly higher than after treatment with the 80 weight%. This was attributed to the underdosing of coagulant during treatment with 100 weight% of Zr (Section 5.1.2.2.1). Similar to that seen for the treatment on the high SUVA water in July, the UV_{254} and DOC was increased from before (i.e. after DAF) to after the filter. This can be attributed to the increase in pH with subsequent re-dissolving of organic material as outlined previously in Section 5.1.5.1.3.

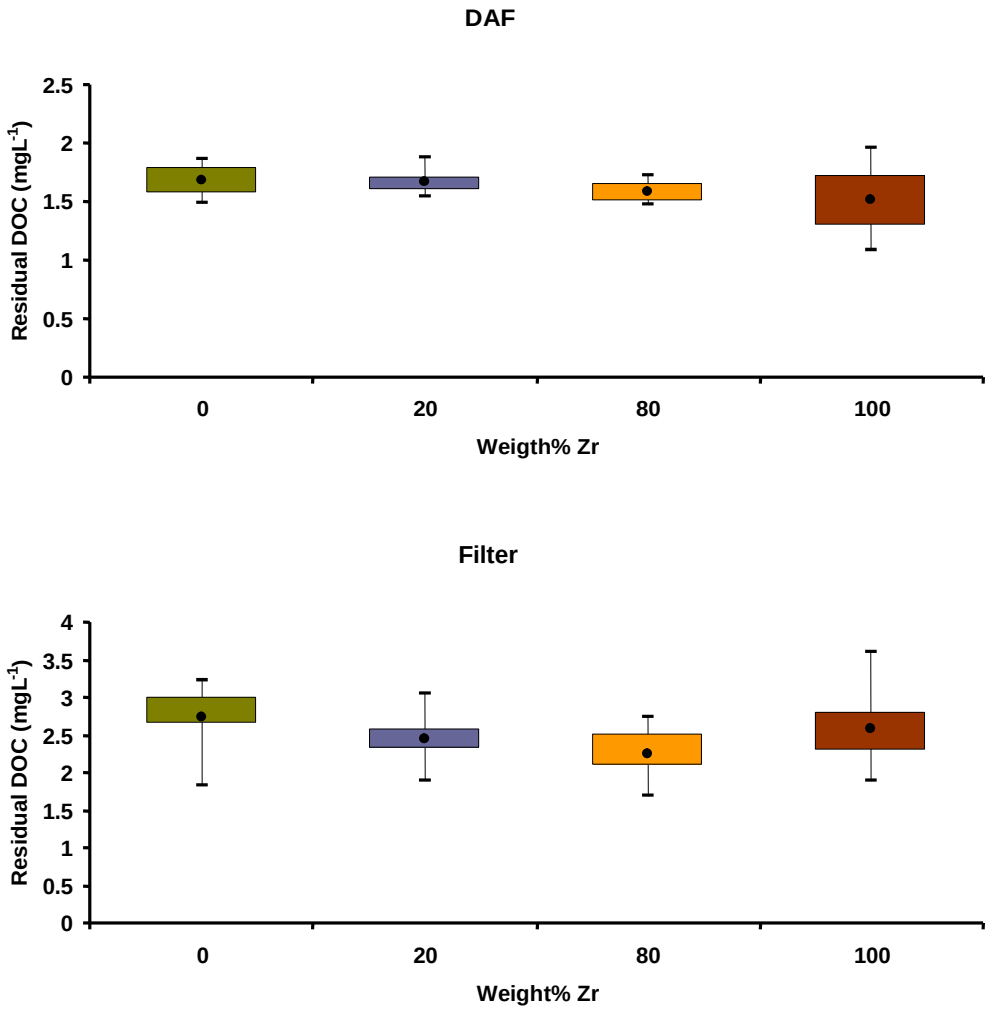

Figure 5.40: Residual DOC after DAF and after the filter during pilot scale treatment with 0, 20, 80 and 100 weight% of Zr under optimum conditions on water sampled on the 26th of November (the bars represent the maximum and minimum values, the box the 25th to 75th percentile values and the data point the mean).

5.2.5.3.3 Turbidity

Residual turbidity after DAF showed a decreasing trend with increasing weight% of Zr (Figure 5.41). Turbidity was 12.1 ± 3.3, 7.9 ± 2.0, 6.8 ± 1.8 and 5.4 ± 1.4 NTU for 0, 20, 80 and 100 weight% of Zr respectively. All differences between treatments were found to be significant (Table 5.7). After the filter, turbidity was greatly reduced for all treatments to 3.2 ± 0.6, 3.2 ± 0.8, 2.0 ± 0.5 and 2.0 ± 0.7 NTU for 0, 20, 80 and 100 weight% of Zr respectively. A decreasing trend was still observed but there was no significant difference in turbidity for treatments differing in weight% of Zr by less than 60%.

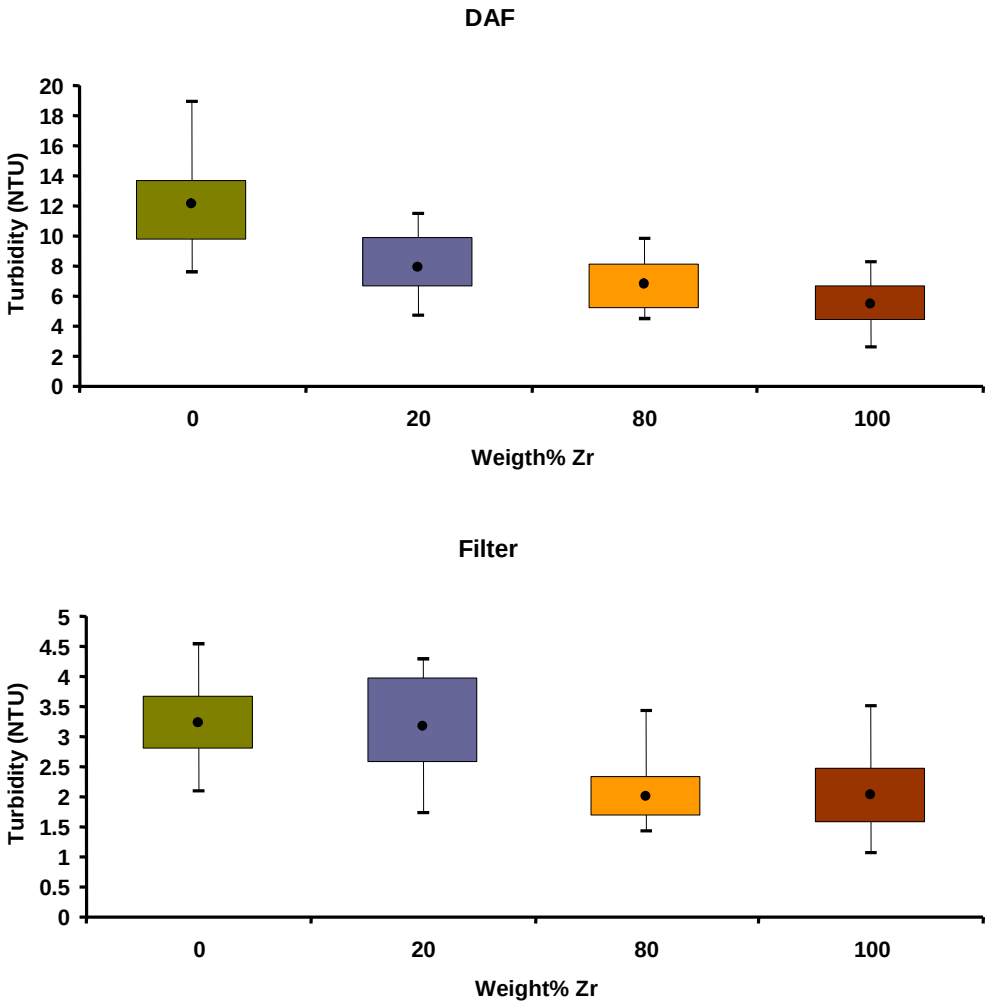

Figure 5.41: Turbidity after DAF and after the filter during pilot scale treatment with 0, 20, 80 and 100 weight% of Zr under optimum conditions on water sampled on the 26th of November (the bars represent the maximum and minimum values, the box the 25th to 75th percentile values and the data point the mean).

5.2.5.3.4 Zeta potential

In the flocculator tank, all treatments showed similar zeta potential which were all inside the optimum range for both 0 and 100 weight% of Zr which were found to be -10 to +5 mV for 0 weight% of Zr and -15 to +15 mV for 100 weight% of Zr (Section 5.1.3.1) (Figure 5.42). Treatment with 80 weight% of Zr showed the highest zeta potential of 4.6 ± 0.4 mV and treatment with 100 weight% of Zr showed the lowest of 3.4 ± 1.1 mV. Treatments with 0 and 20 weight% of Zr resulted in zeta potentials of 3.9 ± 0.4 and 3.8 ± 0.3 mV respectively. The low zeta potential for the treatment with 100 weight% of Zr is explained in Section 5.1.5.2.1).

After the DAF, zeta potential was reduced for all treatments except for the treatment with 20 weight% of Zr which showed a zeta potential of 5.1 ± 2.2 mV while treatment with 0, 80 and 100 weight% of Zr showed zeta potentials of -1.2 ± 0.8, 3.2 ± 0.9 and -0.4 ± 3.4 mV respectively (Figure 5.42). Zeta potential remained within the optimum range for all treatments. After the filter, all treatments showed similar zeta potential (-16.3 ± 1.3, -15.6 ± 1.3, -15.4 ± 1.0 and -17.9 ± 1.6 mV for 0, 20, 80 and 100 weight% of Zr respectively) which was greatly reduced from before the filter (i.e. after DAF). The treated water that was used in the saturator for the DAF had a zeta potential of -18.3 mV during treatment with 0 weight% of Zr and -15.5 mV during treatment with 100 weight% of Zr. This was a result of the pH adjustment to > 6.7 before the filter since an increase pH causes a decrease in zeta potential (Huang *et al.*, 1999). During treatment, the water from the DAF saturator was blended with the treated water causing the reduction in zeta potential after DAF.

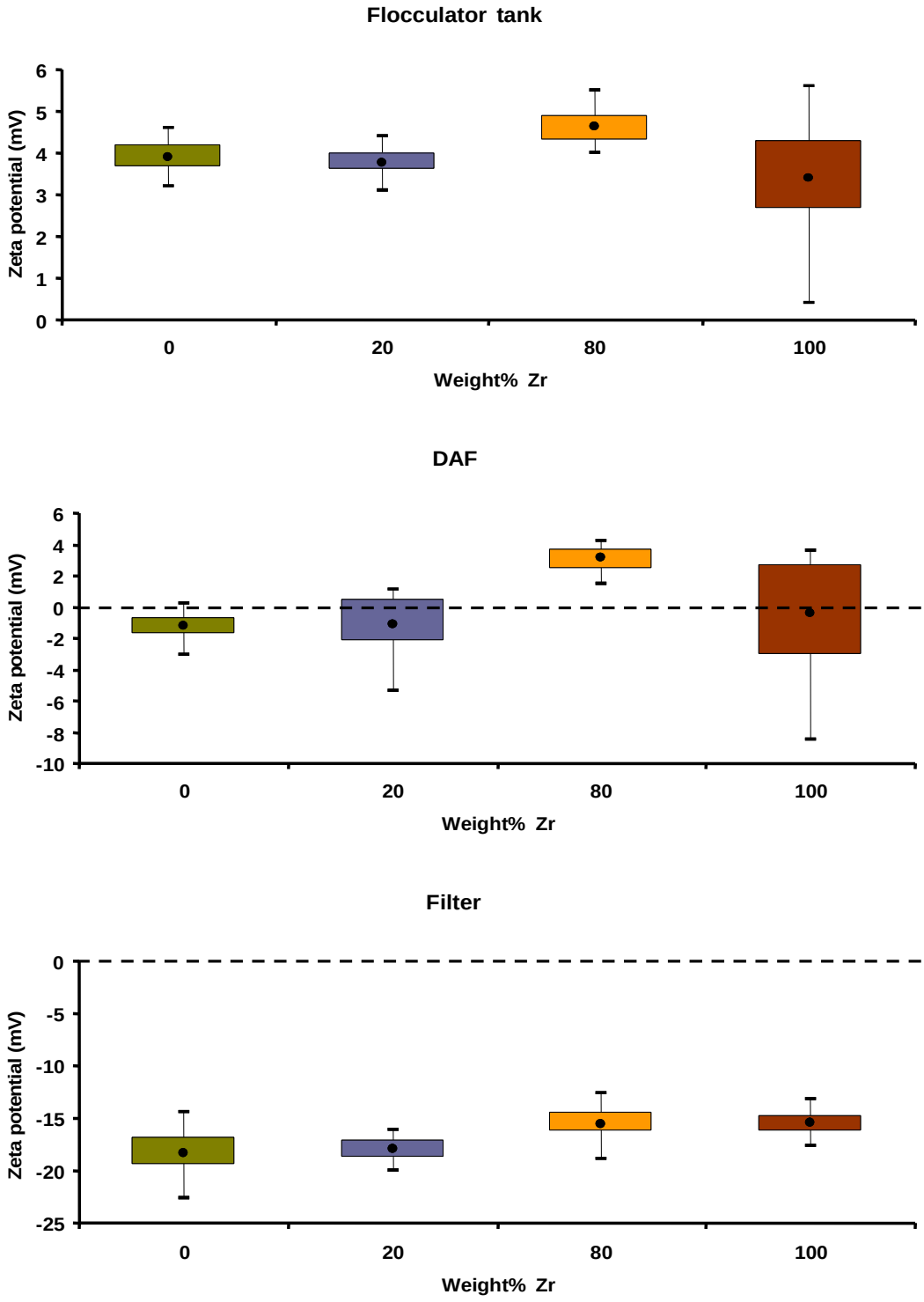

Figure 5.42: Zeta potential in the flocculator tank, after DAF and after the filter during pilot plant treatment with 0, 20, 80 and 100 weight% of Zr under optimum conditions on water sampled on the 26th of November (the bars represent the maximum and minimum values, the box the 25th to 75th percentile values and the data point the mean).

5.2.5.3.5 THM-FP

An increased amount of Zr in the blend reduced the THM-FP of the water after treatment as it did in July. The observed THM-FP of the different treatments was 194.6 ± 24, 149.4 ± 28, 131. 6 ± 23 and 150.5 ± 30 μgL^{-1} for 0, 20, 80 and 100 weight% of Zr respectively (Figure 5.43). The THM-FP of treated water was significantly lower during treatment with 20 weight% of Zr compared to treatment with 0 weight% of Zr but increasing the weight% of Zr further did not produce significantly lower THM-FP (Table 5.7).

Also, THM-FP after treatment with 100 weight% of Zr was higher than after treatment with 80 weight% of Zr. This correlated with the higher DOC after treatment with 100 weight% of Zr and supports the findings of earlier work where reduced DOC has been reported to reduce THM-FP (Uyak *et al.*, 2007; Chen *et al.*, 2007). It was previously shown in Section 5.1.5.2 that the THM-FP after treatment with 100 weight% of Zr was lower than with 0 weight% of Zr despite the fact that the residual DOC was the same. This was explained by the superior removal of UV_{254} absorbing NOM during treatment with 100 weight% of Zr indicating better removal of the hydrophobic NOM fraction which is regarded as the main THM precursor (Goslan *et al.*, 2002; Sharp *et al.*, 2006b). Consequently, bulk DOC removal will result in reduced THM-FP but for a given DOC concentration a lower fraction of hydrophobic material will result in a lower THM-FP as a result of a lower amount of THM precursors.

With the exception of the treatment with 80 weight% of Zr, the THM-FP was higher than in July where the THM-FP was 163.1 ± 34, 179. 9 ± 14, 143. 4 ± 27 and 100.7 ± 15 μgL^{-1} for 0, 20, 80 and 100 weight% of Zr respectively. This correlated with the less efficient NOM removal that was observed in November compared to in July showing that the water sampled in November was more difficult to treat following the poorer coagulation efficiency for low SUVA waters (Fearing *et al.*, 2004).

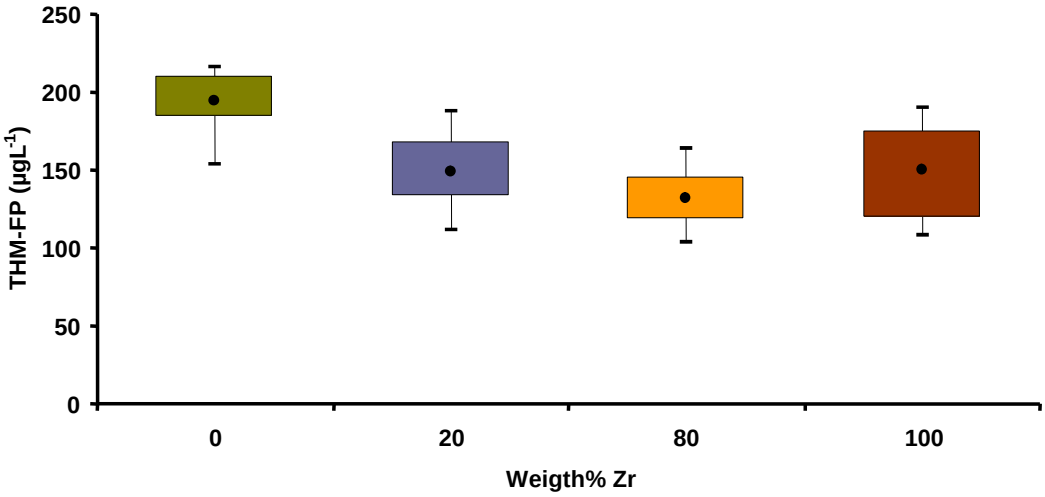

Figure 5.43: THM-FP for treatment with 0, 20, 80 and 100 weight% of Zr under optimum conditions at pilot scale on water sampled on the 26th of November (the bars represent the maximum and minimum values, the box the 25th to 75th percentile values and the data point the mean).

Table 5.7: Summary of statistical analysis of samples taken during pilot plant treatment in November

	Test	Test statistic	N-value	P-Value
Flocculator tank				
Zeta potential				
0 vs. 20 weight%	One tailed T-test	T = -1.51	35 + 36	P>0.05
20 vs. 80 weight%	One tailed T-test	T = 10.55	36 + 36	P<0.05
80 vs. 100 weight%	One tailed T-test	T = -8.38	36 + 71	P>0.05
UV_{254}				
0 vs. 20 weight%	Mann-Whitney	W = 952	36 + 36	P<0.05
20 vs. 80 weight%	One tailed T-test	T = 41.12	36 + 26	P<0.05
80 vs. 100 weight%	Mann-Whitney	W = 2628	26 + 72	P<0.05
DAF				
Zeta potential				
0 vs. 20 weight%	Mann-Whitney	W = 1393	31 + 36	P<0.05
20 vs. 80 weight%	Mann-Whitney	W = 1104	36 + 23	P<0.05
80 vs. 100 weight%	One tailed T-test	T = -7.89	23 + 66	P<0.05
UV_{254}				
0 vs. 20 weight%	Mann-Whitney	W = 1116	36 + 36	P<0.05
20 vs. 80 weight%	Mann-Whitney	W = 1793.5	36 + 33	P<0.05
80 vs. 100 weight%	Mann-Whitney	W = 2004	33 + 60	P<0.05
Turbidity				
0 vs. 20 weight%	Mann-Whitney	W = 1508.5	48 + 48	P<0.05
20 vs. 80 weight%	Mann-Whitney	W = 1955.5	48 + 48	P<0.05
80 vs. 100 weight%	Mann-Whitney	W = 5941	48 +96	P<0.05
Residual DOC				
0 vs. 20 weight%	One tailed T-test	T = -0.28	12 + 12	P>0.05
20 vs. 80 weight%	One tailed T-test	T = -2.12	12 + 12	P<0.05
80 vs. 100 weight%	One tailed T-test	T = -1.03	12 + 19	P>0.05

Table 5.7: Summary of statistical analysis of samples taken during pilot plant treatment in November

	Test	Test statistic	N-Value	P-Value
Filter				
Zeta potential				
0 vs. 20 weight%	Mann-Whitney	W = 1125	36 + 36	P<0.05
20 vs. 80 weight%	Mann-Whitney	W = 1285.5	36 + 36	P>0.05
80 vs. 100 weight%	One tailed T-test	T = 6.96	36 + 71	P<0.05
UV_{254}				
0 vs. 20 weight%	Mann-Whitney	W = 1647.5	36 + 36	P<0.05
20 vs. 80 weight%	Mann-Whitney	W = 1795.5	36 + 36	P<0.05
80 vs. 100 weight%	One tailed T-test	T = 5.64	36 + 69	P<0.05
Turbidity				
0 vs. 20 weight%	Mann-Whitney	W = 2309	48 + 48	P>0.05
20 vs. 80 weight%	Mann-Whitney	W = 1420	48 + 48	P<0.05
80 vs. 100 weight%	Mann-Whitney	W = 6895	48 + 96	P>0.05
Residual DOC				
0 vs. 20 weight%	Mann-Whitney	W = 254	18 + 18	P<0.05
20 vs. 80 weight%	One tailed T-test	T = 1.86	18 + 18	P<0.05
80 vs. 100 weight%	Mann-Whitney	W = 349	18 + 33	P<0.05
THM-FP				
0 vs. 20 weight%	One tailed T-test	T = -2.98	6 + 6	P<0.05
20 vs. 80 weight%	One tailed T-test	T = -1.21	6 + 6	P>0.05
80 vs. 100 weight%	One tailed T-test	T = 1.47	6 + 11	P>0.05
THM-FP / DOC				
0 vs. 20 weight%	One tailed T-test	T = -2.82	6 + 6	P<0.05
20 vs. 80 weight%	One tailed T-test	T = -1.36	6 + 6	P>0.05
80 vs. 100 weight%	One tailed T-test	T = 1.77	6 + 11	P>0.05

5.3 Summary of NOM removal using Fe and Zr as coagulants

It was clear that Zr-OCl could remove more NOM than Fe-Coag at both bench and pilot scale. The increased NOM removal of Zr-OCl over Fe-Coag was found to correlate with increased addition of charge to the system resulting in a higher zeta potential (Figures 5.8 and 5.9). Zr-OCl also showed a wider operational zeta potential window than Fe-Coag (Figure 5.1). The charge of a coagulation system can be increased using any positively charged coagulant by increasing the dose (Faust and Aly, 1998a). However, by increasing the coagulant dose restabilisation of NOM will occur by reversing its charge from negative to positive (Randtke, 1988; Gregor *et al.*, 1997). The wider operational zeta potential window showed that a higher charge could be added before restabilisation of NOM occurred (Figure 5.1).

Formation of robust flocs is important for high NOM removal (Jarvis *et al.*, 2005a). Zr-OCl produced larger and stronger flocs than Fe-Coag (Sections 5.1.4, 5.1.5.1.2 and 5.1.5.2.2). This improved solid-liquid removal since the Zr-OCl flocs could resist breakage to a higher degree under the high shear conditions in the DAF process (Sections 5.1.5.1.2 and 5.1.5.2.2) (Fukishi *et al.*, 1995; Jarvis *et al.*, 2005a). Charge neutralisation and double layer compression reduces the electrostatic forces between particles, increasing the aggregation rate of small particles into flocs (Amal *et al.*, 1991; Gregory, 1993). This implies that the faster growth observed for the Zr-OCl flocs as seen in Section 5.1.4.2 was due to lower electrostatic repulsion between particles during treatment with Zr-OCl. The flocs formed during treatment with Zr-OCl were stronger than the flocs formed with Fe-Coag (Sections 5.1.4.1. and 5.1.4.3). Zr is larger than Fe and can reach higher coordination numbers (Cotton *et al.*, 1999a: Cotton *et al.*, 1999b). The larger size gives a larger surface area which increases the adsorption capacity of Zr in relation to Fe (Faust and Aly, 1998b). By having higher coordination numbers, Zr has the ability to establish more chemical bonds. An increased number of chemical bonds increase the strength of flocs (Jarvis *et al.*, 2005a). Zr also reacts more readily with organic functional groups than Fe forming stronger chemical bonds (Blumenthal, 1963; Dudeney *et al.*, 1991; Sun and Carr, 1995).

The reduction of THM-FP by coagulation is the result of removal of DBP precursors (Goslan *et al.*, 2002). As a result, a reduction in THM-FP follows a reduction in DOC (Chen *et al.*, 2007; Uyak *et al.*, 2007). The hydrophobic fraction of the NOM is regarded as the main precursor for THMs and the THM-FP of the NOM has been found to increase with decreased MW (Goslan *et al.*, 2002; Goslan *et al.*, 2004). Zr-OCl removed more of the UV_{254} absorbing humic and fulvic acid fraction than Fe-Coag. This implied that treatment with Zr-OCl resulted water with lower THM-FP as a result of increased removal of DOC in general and of the humic and fulvic acid fractions in particular.

Optimum NOM for both Fe-Coag and Zr-OCl was reached at the same dose for all waters tested (Sections 5.1 and 5.2). However, Zr is heavier than Fe having an atomic mass unit of 91.224 compared to 55.845 for Fe so the molar dose for optimum NOM removal with Zr-OCl is lower than for Fe-Coag. Treatment with increasing weight% of Zr in a blend with both Zr-OCl and Fe-Coag resulted in increasing NOM removal. Blends of metal salts and polymers and blends of metal salts and activated carbon have been used earlier (Bolto *et al.*, 1999; Edwald and Tobiason, 1999; Tomaszewska *et al.*, 2004). Synergistic effects have been observed (Bolto *et al.*, 1999). However, no negative effects have been reported as a direct result of using blends.

5.4 Comparison of Zr as a coagulant with other treatment options for enhanced NOM removal

The results presented in this thesis show how the use of Zr-OCl as a coagulant for enhanced NOM removal could increase NOM removal compared to a traditionally used Ferric based coagulant. Removal of DOC was increased by 7 - 10 %, UV_{254} by 2 - 10 %, turbidity by 31 - 62 % and the THM-FP was reduced by 23 – 38 % on waters with SUVA values between 3.4 and 5.2 (Table 5.8). This section compares Zr-OCl as a treatment option for enhanced NOM removal with the other treatment options described in the literature review (Section 3.4). Waters with SUVA values below 3.0 mg $m^{-1}L^{-1}$ will not be considered since all experiments with Zr-OCl have been carried out on waters with SUVA values above 3.0 mg $m^{-1}L^{-1}$ (Table 5.8).

5.4.1 Magnetic ion exchange (MIEX®) resin pretreatment vs Zr

On waters with SUVA values above 3.0 mg $m^{-1}L^{-1}$ has MIEX resin pretreatment been reported to increase removal of TOC by 21 – 37 % and DOC by 23 %, increase removal of UV_{254} by 16 – 18 % and reduce THM-FP by 15-55 % (Table 3.1) (Singer and Bilyk, 2002; Drikas *et al.*, 2003). The increase in NOM removal relative to conventional coagulation was better than what was achieved by Zr-OCl when compared to Fe-Coag (Table 5.8). Both Zr-OCl and MIEX have shown increased removal of UV_{254} absorbing material in the MW range between 2000 and 5000 Da compared to conventional coagulants (Section 5.1.3.6) (Mergen, 2008).

5.4.2 Oxidation processes vs Zr

The oxidation process is different from the coagulation process and NOM is removed in a different way (Amirtharajah and O'Melia, 1990; Shon *et al.*, 2005). This makes a direct comparison difficult. However, oxidation by TiO_2/UV, Fentons reagent or photo Fentons reagent improved the removal of DOC by 1-7 % and removal of UV_{254} by 1-5 % (Murray and Parsons, 2004a). This is lower than what was achieved using Zr-OCl (Section 5.1). Oxidation can alter the the NOM composition towards smaller MW organic material (Yan *et al.*, 2007). This is also the case for Zr-OCl with regards to UV_{254} absorbing NOM (Section 5.1.3.6).

5.4.3 Polymers vs Zr

Addition of polymers increased DOC removal by 2- 8 % (Edzwald and Tobiason, 1999; Jarvis *et al.*, 2006). However, the removal of UV_{254} could not always be achieved (Bolto *et al.*, 1999; Bolto *et al.*, 2001). Therefore, in the case of enhanced NOM removal, Zr-OCl had a more significant effect than the addition of polymers (Tables 3.1 and 5.8). Highly charged cationic polymers can be used to remove NOM using charge neutralisation. However, when cationic polymers are used the flocs formed are small and loosely bound (Kim *et al.*, 2001; Jarvis et al., 2006). Zr-OCl can be used to add charge in coagulation, but the flocs formed are large and strong (Sections 5.1.3.5 and 5.1.4).

5.4.4 Activated carbon vs Zr

Adding activated carbon to the coagulation process increased the removal of TOC by 31 %, UV_{254} by 21 % and reduced the THM-FP by 25 % on a water with a SUVA value above 3.0 mg $m^{-1}L^{-1}$ (Table 3.1) (Uyak *et al.*, 2007). Since Zr-OCl reduced the THM-FP further than activated carbon despite reducing less UV_{254} it can be concluded that Zr-OCl was better at removing DBP precursors. Unlike Zr-OCl activated carbon has no charge neutralisation capacity and removes NOM by adsorption (Parsons and Jefferson, 2006a). This makes activated carbon useful for the removal of uncharged organic material (Uyak *et al.*, 2007; Zhang *et al.*, 2008). The humic and fulvic acid fractions of the NOM (containing negatively charged $COOH^-$ groups) have been identified as main DBP precursors (Goslan et al., 2002). Zr-OCl increased the removal of humic and fulvic acids which can account for the superior ability to reduce THM-FP in relation to activated carbon.

A major advantage with chosing Zr-OCl for enhanced NOM removal compared to several other treatment options is that there is no need for capital investment in the treatment plant facility. The use of MIEX® pre-treatment for example, requires the installation of a separate treatment system consisting of a mixing reactor, settler and a regeneration unit (Mergen *et al.*, 2008). When using GAC, adsorber contactors need to be put in place in a treatment plant and for oxidation systems a variety of different additional systems need to be installed to enable the use of an oxidation process (Parsons and Jefferson, 2006a). Ozone also has to be produced on site by passing a silent corona discharge through air or oxygen (Parsons and Jefferson, 2006a). PAC also needs to be prepared on site making it difficult to handle at a WTP. No additional systems need to be put in place for the implementation of Zr-OCl.

One of the key disadvantages of Zr-OCl in relation to MIEX®, activated carbon and polymers is the cost. Oxidation using ozone also has an advantage over Zr-OCl in terms of cost but the most efficient AOPs are still not currently not economical to be used at full scale (Murray and Parsons, 2004a; Murray and Parsons, 2004b). A complete cost benefit analysis is outside the scope of this study; however as in indicator, at present the cost of Zr-OCl is at least five times the cost of Fe-Coag.

Coagulation performance increased with increased amount of Zr-OCl in a blend of Zr-OCl and Fe-Coag (Section 5.2). This implies that addition of Zr-OCl to the standard coagulation process during periods of elevated NOM could be considered an option for when conventional treatment cannot remove enough NOM. The benefit of being able to apply additional treatment during periods of high NOM concentrations is shared by PAC and polymers.

In addition, Before Zr-OCl can be used as a coagulant at full scale there are still some questions which need to be answered. One of them regards the potential risks associated with residual Zr-OCl in distribution systems after treatment. One of the initial aims of this study was to measure the residual Zr in the treated water. The method described in Section 4.4.8 was applied. However, no reliable data on residual Zr could be produced. This showed the need for a reliable method for measuring zirconium in coagulated water. If the levels of Zr in treated water are higher than in natural water, then a toxicity assessment needs to be carried out before it can get approved by drinking water regulators, such as the DWI in the UK. Zr is generally thought to be nontoxic as an element or in its compounds and exists mostly in a physiologically inert dioxide form at pH levels associated with biological activity (Blumenthal, 1976; Kroschwitz and Howe-Grant, 1999). Zr has hence not shown any potential to be harmful to humans, but this still needs to be verified. Since Zr-OCl is an acidic solution it could also cause corrosion damage to mixing and flocculation tanks at a WTP. Another issue is the amount of sludge formed during treatment with Zr, which was not measured in this study.

Zr is less abundant and more expensive than Fe. The world mining production of Zr in 2008 was 1 360 000 tons with Australia being the largest producer followed by South Africa (U.S. Geological Survey, 2009). The price in 2008 was 32 US dollars/ kg (U.S. Geological Survey, 2009). The world mining production of Fe ore was 2, 200 million tonnes with a price of 66 US dollars / tonne (U.S. Geological Survey, 2009). This limits the possibility of using Zr as a coagulant with regards to availabily and cost.

Table 5.8: Summary of results from testing of Zr-OCl as a treatment option for enhanced NOM removal.

Treatment option	**Raw water characteristics**	**Increased removal compared with conventional coagulation**	**Advantage over conventional coagulation**	**Disadvantage compared with conventional coagulation**	**Reference**
		Water with SUVA 3.0 > mg $m^{-1}L^{-1}$			
Zr coagulation	*SUVA: 5.2mg $m^{-1}L^{-1}$ DOC: 8.7mgL^{-1} UV_{254}: 45.1m^{-1} Turbidity: 1.3NTU*	*7% increased DOC removal 7% increased UV_{254} removal 62% increased turbidity 38% lower THM-FP*	*Less floc breakage during DAF*		*This study Pilot scale 14 July*
	SUVA: 4.7mg $m^{-1}L^{-1}$ DOC: 8.4mgL^{-1} UV_{254}: 39.6m^{-1} Turbidity: 2.4NTU	*10% increased DOC removal 6% increased UV_{254} removal No increased turbidity removal*			*This study Bench scale 25 March*
	SUVA: 4.5mg $m^{-1}L^{-1}$ DOC: 8.6mgL^{-1} UV_{254}: 38.9m^{-1} Turbidity: 3.5NTU	*NO increased DOC removal 2% increased UV_{254} removal 46% increased turbidity removal Increasing performance with increasing amount of Zr in a blend*	*Bigger, stronger and faster growing flocs*		*This study Bench scale 16 May*
	SUVA: 3.4mg $m^{-1}L^{-1}$ DOC: 13.1mgL^{-1} UV_{254}: 44.7m^{-1} Turbidity: 3.9NTU	*No increased DOC removal 10% increased UV_{254} removal 31% increased turbidity removal 23% lower THM-FP*	*Less floc breakage during DAF*		*This study Pilot scale 26 November*

6. Conclusions

This study has investigated the performance of Zr as a coagulant and bench marked with the results found with Fe. Treatment with Zr and Fe and blends of both coagulants at bench and pilot scale were carried out. Information from the literature on the coagulation process and other treatment options for enhanced coagulation performance were reviewed. The performance of Zr was discussed and compared with other treatment options and this resulted in the following conclusions regarding the use of Zr as a coagulant for enhanced NOM removal:

- Zr was more effective at removing DOC, UV_{254} and turbidity than Fe for the same dose at both bench scale and pilot scale.
- The THM-FP potential of water treated with Zr was lower than water treated with Fe in continuous operation at pilot-scale. This was linked to a more efficient removal of DBP precursors.
- The flocs formed during bench scale treatment with Zr displayed a larger steady state size for a given shear rate as well as better resistance to increased shear rates than flocs formed during treatment with Fe. This implied that the Zr flocs were stronger then the Fe flocs.
- The turbidity after DAF was lower during continuous pilot-scale treatment using Zr compared with Fe. This implied less breakage of Zr flocs in the DAF system.
- The zeta potential in water treated with Zr was higher than with Fe. This implied that Zr added more charge to the coagulation system than Fe.
- The operational zeta window was wider for Zr than for Fe. This implied that more charge could be added to the coagulation system without re-stabilising the NOM.
- Increased removal of uncharged NOM and a wider zeta potential window indicated the occurrence of complexation and adsorption mechanisms following strong bonds between Zr and functional groups of the NOM.

- When blends of Fe and Zr were used there was an incremental increase in NOM removal, zeta potential and floc size as a result of increased amount of Zr in the blend for a given total coagulant dose.
- Zr as a treatment option offers advantages in terms of capital investment and handling, and disadvantages in terms of operational costs due to the current high cost of the coagulant compared with Fe coagulants.

7. Future work

Before Zr can be used as a coagulant at full-scale more work needs to be done. Suggested work is listed below:

- If the Zr concentrations in the treated water exceed that of natural waters, an evaluation of the toxicity of Zr must be conducted before Zr-OCl can be approved as a coagulant by drinking water regulators.
- Full scale testing needs to be carried out. This will provide more information such as the amount of sludge that is formed and if Zr-OCl causes any corrosive damage to mixing and flocculation tanks.
- Costs benefit analysis of the use of blends needs to be performed. This would be useful to evaluate the application of Zr-OCl in a blend with conventional coagulants during periods of elevated NOM levels.
- To increase the understanding of the ability of Zr-OCl to remove different fractions of the NOM, resin fractionation of water before and after treatment with Zr-OCl is suggested.
- A reliable method for measuring Zr in coagulated water would be beneficial in order to determine the concentrations of Zr in the treated water.
- A cost benefit analysis of the use of Zr-OCl compared to other coagulants is needed to evaluate the possibility of using the coagulant at full scale.

8. References

Amal, R., Raper, J.A., Waite, T.D. 1991 Effect of fulvic acid adsorption on the aggregation kinetics and structure of hermatite particles. J. Colloid Interface Sci. **151**(1) 244-257.

Amal, R., Raper, J.A., Waite, T.D. 1990 Fractal structure of hermatite aggregates. J. Colloid Interface Sci. **140**(1) 158-168.

Amirtharajah, A. and O'Melia, C.R. 1990 Coagulation Processes: Destabilisation, Mixing and Flocculation. In Pontius, F.W. (Ed.) 1990 American Water Works Association Water Quality and Treatment A Handbook of Community Water Supplies 4th edition, McGraw – Hill, USA 269-365.

Bache, D.H., Johnson, C., McGilligan, J.F., Rasool, E. 1997 A conceptual view of floc structure in the sweep floc domain. Wat. Sci. Technol. **36**(4) 49-56.

Baouhua, G., Schmitt, J., Chen, Z., Liang, L., McCarthy, J.F. 1994 Adsorption and desorption of natural organic matter on iron oxide: mechanisms and models. Environ. Sci. Technol. **28**(1) 38-56.

Becker, W.C. and O'Melia, C.R. 2001 Ozone: Its effect on coagulation and filtration. Wat. Sci. Technol. Water Supply **1**(4) 81-88.

Belfort, G. 1979 Selective adsorption of organic homologues onto activated carbon from dilute aqueous solutions. Solvophobic interaction approach and correlation of molar adsorptivity with physicochemical parameters. Environ. Sci. Technol. **13**(8) 939-94.

Bell-Ajy, K., Abbaszadegan, M., Ibrahim, E., Verges, D., LeChevallier, M. 2000 Conventional and optimised coagulation for NOM removal. J. Am. Water Works Assn. **92**(10) 44-58.

Berg, J.M., Claesson, P.M., Neuman, R.D. 1993 Interactions between mica surfaces in sodium polyacrylate solutions containing calcium ions. J. Colloid Interface Sci. **161**(1) 182-189.

Bertelli, M., and Selli, E. 2006 Reaction paths and efficiency of photocatalysis on TiO_2 and H_2O_2 photolysis in the degradation of 2-chlorophenol. J. Hazard. Mater. **138**(1) 46-52.

Biggs, C.A. and Lant, P.A. 2000 Activated sludge flocculation: On-line determination of floc size and the effect of shear. Wat. Res. **34**(9) 2542- 2550.

Black, A.P., Singley, J.E., Whittle, G.P., Maulding, J.S. 1963 Stoichiometry of the coagulation of colour-causing organic compounds with ferric sulphate. J. Am. Water Works Assn. **55**(10) 1347-1366.

Black, A.P. and Willems, D.G. 1961 Electrophoretic studies of coagulation for removal of organic colour. J. Am. Water Works Assn. **53**(5) 589-604.

Blumenthal, W.B. 1963 Zirconium in organic chemistry. Ind. Eng. Chem. **55**(4) 50-57.

Boller, M, Blaser, S. 1998 Particles under stress. Wat. Sci. Technol. **37**(10) 9-29.

Bolto, B., Abbt-Braun, G., Dixon, D., Eldrigde, R., Frimmel, F., Hesse, S., King, S., Toifl, M. 1999 Experimental evaluation of cationic polyelectrolytes for removing natural organic matter from water. Wat. Sci. Technol. **40**(9) 71-79.

Bolto, B., Dixon, D., Eldridge, R., King, S. 2001 Cationic polymer and clay or metal oxide combinations for natural organic matter removal. Wat. Res. **35**(11) 2669-2676.

Bolto, B. and Gregory, J. 2007 Organic polyelectrolytes in water treatment. Wat. Res. **41**(11) 2301-2324.

Bose, P. and Reckhow, D.A. 2007 The effect of ozonation on natural organic matter removal by alum coagulation. Wat. Res. **41**(7) 1516-1524.

Boyer, T.H., Singer, P.C. 2006 A pilot-scale evaluation of magnetic ion exchange treatment for removal of natural organic material and inorganic anions. Wat. Res. **40**(15) 2865-2876.

Boyer, T.H., and Singer, P.C. 2005 Bench-scale testing of a magnetic ion exchange resin for removal of disinfection by-product precursors. Wat. Res. **39**(7) 1265-1276.

Budd, G.V., Hess, A.F., Shortney-Darby, H., Neeman, J.J., Spencer, C.M., Bellamy, J.D., Hargette, P.H. 2004 Coagulation applications for new treatment goals. J. Am. Water Works Assn. **96**(2) 103-113.

Bratby, J. 2006 Flocculation. In Bratby, J. (Ed.) 2006 Coagulation and flocculation in water and wastewater treatment, IWA Publishing, UK, 240-279.

Chen, C., Zhang, X., He, W., Lu, W., Han, H. 2007 Comparison of seven kinds of drinking water treatment processes to enhance organic material removal: A pilot test. Sci. Total Environ. **382**(1) 93-102.

Cho, H-R., Walter, C., Rothe, J., Neck, V., Denecke, M.A., Dardenne, K., Fanghanel, T. 2005. Combined LIBD and XAFS investigation of the formation and structure of Zr(IV) colloids. Anal. Bioanal. Chem. **383**(1) 28-40.

Chon, H.K., Vigneswaran, S., Ngo, H.H., Kim, J.H. 2005 Chemical coupling of photocatalysis with flocculation and adsorption in the removal of organic matter. Wat. Res. **39**(12) 2549-2558.

Coughlin, R.W. and Ezira, F. 1968 Role of surface acidity in adsorption of organic pollutants on the surface of carbon. Environ. Sci. Technol. **2**(4) 291 - 297.

Cotton, F.A., Wilkinson, G., Murillo, C.A., Bochmann, M. 1999a Part 3, The chemistry of the transition elements, 17 E, Iron. In: Cotton, F.A. (Ed.) Advanced inorganic chemistry, sixth edition. John Wiley & Sons, Inc, USA, 775-813.

Cotton, F.A., Wilkinson, G., Murillo, C.A., Bochmann, M. 1999b Part 3, The chemistry of the transition elements, 18 A, Zirconium and Hafnium. In: Cotton, F.A. (Ed.) Advanced inorganic chemistry, sixth edition. John Wiley & Sons, Inc, USA, 878-894.

Crozes, G., White, P., Marshall, M. 1995 Enhanced coagulation; it's effect on NOM removal and chemical costs. J. Am. Water Works Assn. **87**(1) 78-89.

Dempsey, B.A. 1984 Removal of naturally occurring compounds by coagulation and sedimentation. Crit. Rev. Environ. Contr. **14**(4) 311-331.

Dempsey, B.A., Sheu, H., Ahmed, T.M.T., Mentink, J. 1985 Polyaluminium chloride and alum coagulation of clay-fulvic acid suspensions. J. Am. Water Works Assn. **77**(3) 74-80.

Deng, Y. 1997 Formation of iron(III) hydroxides from homogenous solutions. Wat. Res. **31**(6) 1347-1354.

Dentel, S.K. 1991 Coagulant control in water treatment. Crit. Rev. Environ. Control **21**(1) 41-135.

Dirksen, J. 1992 The precipitation of basic zirconium sulphate in a continuous stirred tank reactor as a precursor for zirconia ceramics. PhD thesis, Ecole Polytechnique Federale de Lausanne

Drikas, M., Chow, C.W.K., Cook, D. 2003 The impact of recalcitrant organic character on disinfection stability, trihalomethane formation and bacterial regrowth: An evaluation of magnetic ion exchange resin (MIEX®) and alum coagulation. J. Wat. Supply: Res. Technol. AQUA **52**(7) 475-487.

Drinking Water Inspectorate, UK. New drinking water regulations in the UK, 1998.

Duan, J. and Gregory, J. 2003 Coagulation by hydrolysing metal salts. Adv. Colloid Interface Sci. **100-102** 475-502.

Duan, J., Wang, J., Graham, N., Wilson, J. 2002 Coagulation of humic acid by aluminium sulphate in saline water conditions. Desalination **150**(1) 1-14.

Dudeney, A.W.L., Abdei-Ghani, M., Kelsall, G.H., Monhemius, A.J., Zhang, L. 1991 An aqueous precipitation-phase extraction route to hydrous zirconia particles. Powder Technol. **65**(1-3) 207-217.

Edzwald, J.K. 1993 Coagulation in drinking water treatment: Particles organics and coagulants. Wat. Sci. Technol. **27**(11) 21-35.

Edzwald, J.K. 1995. Principles and applications of dissolved air flotation. Wat. Sci. Technol. **31**(3-4) 1-23.

Edzwald, J.K. and Tobiasson, J.E. 1999 Enhanced coagulation: US requirements and a broader view. Wat. Sci. Technol. **40**(9) 63-70.

Ekberg, C., Kallvenius, G., Albinsson, Y., Brown, P.L. 2003 Studies on the hydrolytic behaviour of zirconium(IV). J. Sol. Chem. **33**(1) 47-79.

Faust, S.D. and Aly, O.M. 1987 Adsorption of organic compounds. In: Faust, S.D. and Aly, O.M. (Ed.) 1987 Adsorption processes for water treatment, Butterworth, UK, 193-287

Faust, S.D. and Aly, O.M. 1998 Removal of organics and inorganics by activated carbon. In Faust, S.D and Aly, O.M. (Ed.) 1998 Chemistry of water treatment (second edition), Ann Arbor Press, USA.

Faust, S.D. and Aly, O.M. 1998 Removal of particulate matter by coagulation. In Faust, S.D and Aly, O.M. (Ed.) 1998 Chemistry of water treatment (second edition), Ann Arbor Press, USA.

Fearing, D.A., Banks, J., Guyetand, S., Monfort Eroles, C., Jefferson, B., Wilson, D., Hillis, P., Campbell, A.T., Parsons, S.A. 2004 Combination of ferric and MIEX® for the treatment of a humic rich water. Wat. Res. **38**(10) 2551-2558.

Francois, R.J., 1987 Strength of aluminium hydroxide flocs. Wat. Res. **21**(9) 1023-1030.

Fryer, J.R., Hutchingson, J.L., Paterson, R. 1970 An electron microscopic study of the hydrolysis products of zirconyl chloride. J. Colloid. Interface. Sci. **34**(2) 238-248.

Fukushi, K., Tambo, N., Matsui, Y. 1995 A kinetic model for dissolved air flotation in water and wastewater treatment. Wat. Sci. Technol. **31**(3–4) 37-47.

Goslan, E.H., Fearing, D.A., Banks, J., Wilson, D., Hills, P., Campbell, A.T., Parsons, S.A. 2002 Seasonal variations in the disinfection by-product precursor profile of a reservoir water. J. Wat. Supply: Res. Technol. – AQUA **51**(8) 475-482.

Goslan, E.H. 2003 Natural organic matter character and reactivity: Assessing seasonal variation in a moorland water PhD thesis, Cranfield University, UK.

Goslan, E.H., Wilson, D., Banks, J., Hillis, P., Campbell, A., Parsons, S.A. 2004 Natural organic matter fractionation: XAD resins versus UF membranes. An investigation into THM formation. Wat. Sci. Technol: Water Supply **4**(5-6) 113-119.

Giusti, D.M., Conway, R.A., Lawson, C.T. 1974 Activated carbon adsorption of petrochemicals. Journal of the Water Pollution Control Federation **46**(5) 947 – 965.

Greenwood, N.N. and Earnshaw, A. 1998 Titanium, Zirconium and Hafnium. In: Greenwood, N.N. and Earnshaw, A. (Ed.) Chemistry of the elements, second edition. Butterworth-Heinemann, UK, 954-972.

Gregor, J.E., Nokes, C.J., Fenton, E. 1997 Optimising natural organic matter removal from low turbidity water by controlled pH adjustment of aluminium coagulation. Wat. Res. **31**(12) 2949-2958.

Gregory, J. and O'Melia, C.R. 1989 Fundamentals of flocculation. Crit. Rev. Env. Sci. Technol. **19**(3) 185-230.

Gregory, J. 1993 The role of colloid interactions in solid-liquid separation. Wat. Sci. Technol. **27**(10) 1-17.

Hall, E.S., Packham, R.F. 1965 Coagulation of organic colour with hydrolyzing salts. J. Am. Water Works Assn. **57**(9) 1149-1166.

Hong-Xiao, T. and Stumm, W. 1987 The coagulation behaviours of Fe(III) polymeric species – I Preformed polymers by base addition. Wat. Res. **21**(1) 115-121.

Hooper, S.M., Summers, R.S., Solarik, G., Owen, D.M. 1996 Improving GAC performance by optimised coagulation. J. Am. Water Works Assn. **88**(8) 107-120.

Huang, C., Pan, J.R., Huang, S. 1999 Collision efficiencies of algae and kaolin in depth filter: The effect of surface properties of particles. Wat. Res. **33**(5) 1278-1286.

Huang, X., Leal, M., Li, Q. 2008 Degradation of natural organic matter by TiO2 photocatalytic oxidation and its effect on fouling of low-pressure membranes. Wat. Res. **42**(4-5) 1142-1150.

Jarvis., P., Jefferson, B., Gregory, J., Parsons, S.A. 2005a A review on floc strength and breakage. Wat. Res. **39**(14) 3121-3137.

Jarvis, P., Jefferson, B., Parsons, S.A. 2006b Floc structural characteristics using conventional coagulation for a high DOC, low alkalinity surface water source. Wat. Res. **40**(14) 2727-2737.

Jarvis, P., Jefferson, B., Parsons, S.A. 2005c Breakage, regrowth and fractal nature of natural organic matter flocs. Environ. Sci. Technol. **39**(7) 2307-2314.

Jarvis, P., Jefferson, B., Parsons, S.A. 2005d How the natural organic matter to coagulant ratio impacts on floc structural properties. Environ. Sci. Technol. **39**(22) 8919-8924.

Jarvis, P., Banks, J., Molinder, R., Stephenson, T., Parsons, S.A., Jefferson, B. 2008 Processes for enhanced NOM removal: beyond Fe and Al coagulation. Water Science and Technology: Water Supply 8(6) 709-716.

Jefferson, B., Jarvis, P., Parsons, S.A. 2004 The effect of coagulant type on natural organic matter floc structure and strength. 11th International Gothenburg Symposium on Chemical Treatment of Water and Wastewater, Sweden.

Johnson, P.N. and Amirtharajah, A. 1983 Ferric chloride and alum as single and dual coagulants. J. Am. Water Works Assn. **75**(5) 232-239.

Jonhson, C.J. and Singer, P.C. 2004 Impact of a magnetic ion exchange resin on ozone demand and bromate formation during drinking water treatment. Wat. Res. **38**(17) 3803-3811.

Kam, S.K., Gregory, J. 2001 The interaction of humic substances with cationic polyelectrolytes. Wat. Res. **35**(15) 3557-3566.

Kastl, G., Sathasivian, A., Fisher, I., van Leeuwen, J. 2004 Modelling DOC removal by enhanced coagulation. J. Am. Water Works Assn. **96**(2) 79-89.

Kavanaugh, M.C. 1978 Modified coagulation for improved removal of trihalomethane precursors. J. Am. Water Works Assn. **70**(11) 613-620.

Kobayashi, T., Sasaki, T., Takagi, I., Moriyama, H. 2007 Solubility of Zriconium(IV) hydrous oxides. J. Nucl. Sci. Technol. **44**(1) 90-94.

Kleimann, J., Gehin-Delval, Auweter, H., Borkovec, M. 2005 Super-stoichiometric charge neutralisation in particle-polyeletrolyte systems. Langmuir **21**(8) 3688-3698

Krasner, S.W. and Amy, G. 1995 Jar-test evaluations of enhanced coagulation. J. Am. Water Works Assn. **87**(10) 93-107.

Kroschwitz, J. I., Howe-Grant, M. Zirconium and zirconium compounds. In Kroschwitz, J. I., Howe-Grant, M. (Ed.) Encyclopedia of chemical technology, 4th edition, Vol 25, John Wiley and Sons, New York 853-896.

Kim, S.H., Moon, B.H., Lee, H.I. 2001 Effects of pH and dosage on pollutant removal and floc structure during coagulation. Microchem. J. **68**(2-3) 197-203.

Kitis, M., Ilker Harman, B., Yigit, N.O., Beyhan, M., Nguyen, H., Adams, B. The removal of natural organic matter from selected Turkish source waters using magnetic ion exchange resin (MIEX®). React. Funct. Polym. **67**(12 spec. iss.) 1495-1504.

Kvinnesland, T. and Oedegaard, H. 2004 The effects of polymer characteristics on nano particle separation in humic substances removal by cationic polymer coagulation. Wat. Sci. Technol. **50**(12) p. 185-191.

LaMer, V.K. and Healy, T.W. 1963 Adsorption-flocculation reactions of macromolecules at the solid liquid interface. Rev. Pure Appl. Chem. **13** 112-132.

Lee, M.C., Snoeyink, V.L., Crittenden, J.C. 1981 Activated carbon adsorption of humic substances. J. Am. Water Works Assn. **73**(8) 440-446.

Li, M. 2003 Making spherical zirconia particles from inorganic zirconium aqueous sols. Powder Technol. **137**(1-2) 95-98.

Liu, S., Lim, M., Fabris, R., Chow, C., Chiang, K., Drikas, M., Amal, R. 2008 Removal of humic acid using TiO_2 photocatalytic process – Fractionation and molecular weight characterisation studies. Chemosphere **72**(2) 263-271.

Lowalekar, V., Raghavan, S., Pandit, V., Parks, H.G., Jeon, J. 2006 Contamination of silicon dioxide films by aqueous zirconium and hafnium species. J. Appl. Phys. **99**(2) 024503.

Matijevic, G.E, Janauer, G.E., Kerker, M. 1963 Reversal of charge of lyophobic colloids by hydrolysed metal ions I. Aluminium nitrate[1,2]. J. Colloid Sci. **19**(4) 333-346.

McCurdy, K., Carlson, K., Gregory, D. 2004 Floc morphology and cyclic shearing recovery: comparison of alum and polyaluminium chloride coagulants. Wat. Res. **38**(2) 486-494.

McCreary, J.J. and Snoeyink, V.L. 1980 Characterisation and activated carbon adsorption of several humic substances. Wat. Res. 14(2) 151-160.

Mergen, M.R.D. 2008 Impact of magnetic resin on DOC removal and downstream water treatment processes. PhD thesis, Cranfield University, UK.

Mergen, M.R.D, Jefferson, B., Parsons, S.A., Jarvis, P. 2008 Magnetic ion-exchange resin treatment: impact of water type and resin use. Wat. Res. **42**(8-9) 1977-1988.

Murray, C.A. and Parsons, S.A. 2004b Advanced oxidation processes: flowsheet options for bulk natural organic removal. Water Science and Technology: Water supply **4**(4) 113-119.

Murray, C.A. and Parsons, S.A. 2004a Comparison of AOPs for the removal of natural organic matter: performance and economic aspects. Wat. Sci. Technol. **49**(4) 267-272.

Najm, I., Tate, C., Selby, D. 1998 Optimising enhanced coagulation with PAC: a case study. J. Am. Water Works Assn. **90**(10) 88-95.

Nowack, K.O., Cannon, F.S., Arora, H. 1999 Ferric chloride plus GAC for removing TOC. J. Am. Water Works Assn. **91**(2) 65-78.

Owen, D.M., Amy, G.L., Chowdhury, Z.K., Paode, R., McCoy, G. Viscosil, K. 1995 NOM-characterization and treatability J. Am. Water Works Assn. **87**(1) 46-63.

Packham, R.F. 1965 Some studies of the coagulation of dispersed clays with hydrolysing salts. J. Colloid Interface Sci. **20**(1) 81-92.

Parsons, S.A. and Williams, M. 2004 Introduction In: Parsons, S.A. (Ed.) Advanced Oxidation Processes for Water and Waste Water Treatment, IWA Publishing, UK, 1-7.

Parsons, S.A. and Byrne, A. 2006 Water Treatment Applications. In. Parsons, S.A. (Ed.) 2006 Advanced Oxidation Processes for Water and Wastewater Treatment, IWA Publishing, UK 329-347.

Parsons, S.A. and Jefferson, B. 2006a Adsorption Processes. In: Parsons, S.A. (Ed.) Introduction to potable water treatment. Blackwell Publishing, UK, 113-128.

Parsons, S.A. and Jefferson, B. 2006b Organics Removal. In: Parsons, S.A. (Ed.) Introduction to potable water treatment. Blackwell Publishing, UK, 140-153.

Parsons, S.A. and Jefferson, B. 2006c Dissolved air flotation. In: Parsons, S.A. (Ed.) Introduction to potable water treatment, Blackwell Publishing, UK 58-72.

Puri, R.P. 1980. In Suffet, I.H. and McGuire, M.J. (Ed.) Activated carbon adsorption of organics from the aqueous phase 1, Ann Arbor Science Publishers inc, 353-411.

Purvis, K.L., Lu, G., Schwarthz, J., Bernasek, S.L. 1998 Ligand metathesis in surface-bound alkoxyzirconium complexes. 2. Preparation of alkanecarboxylate complexes in ultrahigh vacuum. Langmuir **14**(13) 3720-3722.

Randtke, S.J. 1988 organic contaminant removal by coagulation and related process combinations. J. Am. Water Works Assn. **80**(5) 40-56.

Ratnaweera, H., Hiller, N., Bunse, U. 1999 Comparison of the coagulation behaviour of different Norwegian aquatic NOM sources. Environ. Int. **25**(2-3) 347-355.

Reckhow, D.A., Singer, P.C., Malcolm, R.L. 1990 Chlorination of humic materials: byproduct formation and chemical interpretations. Environ. Sci. Technol. **24**(11) 1655- 1664.

Regli, S., Cromwell, J.E., Zhang, X., Gelderloos, A.B., Grubbs, W.D., Letkiewicz, F., Machler, B.A. 1992 Framework for decision-making: an EPA perspective. Report No. EPA 811-R-92-005, US Environmental Protection Agency (EPA), Washington, DC, USA.

Richens, D.T. 1997 Group 4 elements: Titanium, Zirconium and Hafnium In Richends, D.T. (Ed.) 1997 The chemistry of aqua ions, John Wiley & Sons, UK 207-222.

Rose, J., Vilge, A., Olivie-Lauquet, Masion, A., Frechou, C., Bottero, J.Y. 1998. Iron speciation in natural organic matter colloids. Colloids Surf., A **136**(1-3) 11-19.

Sani, A., Rossi, L., Lubello, C., Zacchei, S. Effects of ion exchange resin pre-treatment on GAC adsorption. Wat. Sci. Technol: Water supply **8**(2) 181-187.

Semmens, M.J. and Field, T.K. 1980 Coagulation: experiences in organic removal. J. Am. Water Works Assn . **72**(8) 476-483.

Sharp, E.L., Banks, J., Billica, J.A., Gertig, K.R., Henderson, R., Parsons, S.A., Wilson, D., Jefferson, B. 2005. Application of zeta potential measurements for coagulation control: pilot plant experiences from UK and US waters with elevated organics. Wat. Sci. Technol. Water Supply **5**(5) 49-56.

Sharp, E.L. 2005 Natural organic matter coagulation. PhD thesis, Cranfield University, UK.

Sharp, E.L., Jarvis, P., Parsons, S.A., Jefferson, B. 2006a Impact of fractional character on the coagulation of NOM. Colloids Surf., A **286**(1-3) 104-111.

Sharp, E. L., Parsons, S.A., Jefferson, B. 2006b The impact of seasonal variations in DOC arising from a moorland peat catchment on coagulation with iron and aluminium salts. Environ. pollut. **140**(3) 436-443.

Sharp, E.L., Jarvis, P., Parsons, S.A., Jefferson, B. 2006c The impact of zeta potential on the physical properties of Ferric-NOM flocs. Environ. Sci.Technol. **40**(12) 3934-3940.

Sharp, E.L., Parsons, S.A., Jefferson, B. 2006d Coagulation of NOM: linking character to treatment. Wat. Sci. Technol. **53**(7) 67-76.

Shon, H.K., Vigneswaran, S., Ngo, H.H., Kim, J.-H. 2005 Chemical coupling of photocatalysis with flocculation and adsorption in the removal of organic matter. Wat. Res. **39**(12) 2549-2558.

Singer, PC., Bylik, K. 2002 Enhanced coagulation using a magnetic ion exchange resin. Wat. Res. **36**(16) 4009-4022.

Singer, P.C., Scheider, M., Edwards – Brandt, Budd, G.C. 2007 MIEX® for removal of DBP precursors: Pilot plant findings. J. Am. Water Works Assn. **99**(4) 128-139.

Snoeyink, V.L. 1990 Adsorption of Organic Compounds. In Pontius, F.W. (Ed.) 1990 American Water Works Association Water Quality and Treatment A Handbook of Community Water Supplies 4th edition, McGraw – Hill, USA 269-365.

Sun, L., Carr, P.W. 1995 Mixed-mode retention of peptides on phosphate-modified polybutadiene-coated zirconia. Anal. Chem. **67**(15) 2517-2523.

Tamamushi, B, and Tamaki, K. 1959 The action of long chain cations on negative silver iodide sols. Colloid. Polym. Sci. **163**(2) 122-126.

Thomas, D.N., Judd, S.J., Fawcett, N. 1999 Flocculation modelling: a review. Wat. Res. **33**(7) 1579-1592.

Tomaszewska, M., Mozia, S., Morawski, A.W. 2004 Removal of organic matter by coagulation enhanced with adsorption on PAC. Desalination **161**(1) 79-87.

US Environmental protection agency. National drinking water regulations: Disinfections and disinfection by-products; final rule. Federal register 1998;63(241):69390-476.

U.S. Geological Survey. 2009. Mineral Commodity Summaries 2009. ISBN 978-1-4113-295-0.

Uyak, V., Yavuz, S., Toroz, I., Ozaydin, S., Ates Genceli, E. 2007 Disinfection by-products precurors removal by enhanced coagulation and PAC adsorption. Desalination **216**(1-3), 334-344.

Vanderkam, S.K., Bocarsly, A.B., Schwartz, J. 1998 Enhanced bonding of poly(ethylene-co-acrylic acid) to oxides through surface-bound alkoxyzirconium complex interfaces. Chem. Mater. **10**(3) 685-687.

Vilge-Ritter, A., Rose, J., Masion, A., Bottero, J.Y., Laine, J.M. 1999 Chemistry and structure of aggregates formed with Fe-salts and natural organic matter. Colloids Surf. A **147**(3) 297-308.

Von Gunten, U. 2003 Ozonation of drinking water: Part I. Oxidation kinetics and product formation. Wat. Res. **37**(7) 1443-1467.

Von Smoluchowski 1917 Versuch einer mathematischen theorie der koagulationskinetik kolloider losungen. Z. Phys. Chem. **92** 129-168.

Wadley, S. and Waite, T.D. 2004 Fenton processes. In: Parsons, S.A. (Ed.) Advanced Oxidation Processes for Water and Waster Water Treatment, IWA Publishing, 111-137.

Weber, W.J. and Morris, J.C. 1964 Equilibria and capacities for adsorption on carbon. Journal of Sanitation and Engineering **90** 79-107

White, M.C., Thompson, J.D., Harrington, G.W., Singer, P.C. 1997 Evaluating criteria for enhanced coagulation compliance. J. Am. Water Works Assn. **89**(5) 64-77.

William, G.H. 1999 Chemical oxidation. In Pontius, F.W. (Ed.) 1990 American Water Works Association Water Quality and Treatment A Handbook of Community Water Supplies 4th edition, McGraw – Hill, USA 269-365.

Worrall, F. and Burt, T. Time series analysis of long-term river dissolved organic carbon records. Hydrol. Processes **18**(5) 893-911.

Yan, M., Wang, D., Shi, B., Wang, M., Yan, Y. 2007. Effect of pre-ozonation on optimized coagulation of a typical north China source water. Chemosphere **69**(11) 1695-1702.

Yukselen, M.A. and Gregory, J. 2004 The effect of rapid mixing on the break-up and re-formation of flocs. J. Chem. Technol. Biotechnol. **79**(7) 782-788.

Yukselen, M.A. and Gregory, J. 2004 The reversibility of floc strength. Int. J. Miner. Process. **73**(2-4) 251-259.

Zhang, L.L., Yang, D., Zhong, Z.J., Gu, P. 2008 Application of hybrid coagulation-microfiltration process for treatment of membrane backwash water from waterworks. Sep. Purif. Technol. **62**(2) 415-422.

APPENDIX A

This appendix provides details on the statistical analysis performed on the data collected during pilot scale treatment with Fe, Zr and blends of both coagulants on water sampled on the 14th of July and on the 26th of November.

1: Zr vs. Fe 14th of July

1:1 Flocculator tank

1:1:1 UV_{254}

Mann-Whitney Test Zr vs. Fe
Zr: N = 36, Median = 1.5750
Fe: N = 32, Median = 3.0750
Point estimate for ETA1-ETA2 is -1.5250
95.1 Percent CI for ETA1-ETA2 is (-1.5750,-1.4500)
W = 666.0
Test of ETA1 = ETA2 vs. ETA1 < ETA2 is significant at 0.0000
The test is significant at 0.0000 (adjusted for ties)

1:1:2 Zeta potential

Two-sample T-test for Zr vs. Fe
Zr: N = 42, Mean = 2.671, StDev = 0.641, SE Mean = 0.099
Fe: N = 51, Mean = -6.38, StDev = 4.50, SE Mean = 0.63
Difference = mu (Zr) - mu (Fe)
Estimate for difference: 9.048
95% lower bound for difference: 7.980
T-Test of difference = 0 (vs. >): T-Value = 14.19 P-Value = 0.000 DF = 52

1:2 DAF

1:2:1 UV_{254}

Mann-Whitney Test Zr vs. Fe
Zr: N = 30, Median = 1.9500
Fe: N = 27, Median = 3.4000
Point estimate for ETA1-ETA2 is -1.4375
95.2 Percent CI for ETA1-ETA2 is (-1.6751,-1.3000)
W = 465.0
Test of ETA1 = ETA2 vs. ETA1 < ETA2 is significant at 0.0000
The test is significant at 0.0000 (adjusted for ties)

1:2:2 DOC

Mann-Whitney Test Zr vs. Fe
Zr: N = 9, Median = 1.1410
Fe: N = 11, Median = 1.7310
Point estimate for ETA1-ETA2 is -0.5900
95.2 Percent CI for ETA1-ETA2 is (-0.7831,-0.2650)
W = 45.0
Test of ETA1 = ETA2 vs. ETA1 < ETA2 is significant at 0.0001
The test is significant at 0.0001 (adjusted for ties)

1:2:3 Turbidity

Mann-Whitney Test Zr vs. Fe
Zr: N = 26, Median = 2.277
Fe: N = 36, Median = 3.885
Point estimate for ETA1-ETA2 is -1.587
95.0 Percent CI for ETA1-ETA2 is (-6.741,-0.560)
W = 587.0
Test of ETA1 = ETA2 vs. ETA1 < ETA2 is significant at 0.0005
The test is significant at 0.0005 (adjusted for ties)

1:2:4 Zeta potential

Mann-Whitney Test Zr vs. Fe
Zr: N = 39, Median = 0.200
Fe: N = 36, Median = -14.500
Point estimate for ETA1-ETA2 is 14.200
95.1 Percent CI for ETA1-ETA2 is (12.900, 15.301)
W = 2184.0
Test of ETA1 = ETA2 vs. ETA1 > ETA2 is significant at 0.0000
The test is significant at 0.0000 (adjusted for ties)

1:3 Filter

1:3:1 UV_{254}

Mann-Whitney Test Zr vs. Fe
Zr: N = 36, Median = 3.362
Fe: N = 36, Median = 5.862
Point estimate for ETA1-ETA2 is -2.425
95.1 Percent CI for ETA1-ETA2 is (-3.675,-1.925)
W = 666.0
Test of ETA1 = ETA2 vs. ETA1 < ETA2 is significant at 0.0000

The test is significant at 0.0000 (adjusted for ties)

1:3:2 DOC

Two-sample T-test Zr vs. Fe
Zr: N = 24, Mean = 1.539, StDev = 0.120, SE Mean = 0.024
Fe: N = 20, Mean = 2.135, StDev = 0.346, SE Mean = 0.077
Difference = mu (D Filter Zr) - mu (D Filter Fe)
Estimate for difference: -0.5959
95% upper bound for difference: -0.4567
T-Test of difference = 0 (vs. <): T-Value = -7.35 P-Value = 0.000 DF = 22

1:3:3 Turbidity

Mann-Whitney Test Zr vs. Fe
Zr: N = 32, Median = 0.4210
Fe: N = 28, Median = 1.0900
Point estimate for ETA1-ETA2 is -0.6765
95.0 Percent CI for ETA1-ETA2 is (-0.8199,-0.5301)
W = 528.0
Test of ETA1 = ETA2 vs.ETA1 < ETA2 is significant at 0.0000
The test is significant at 0.0000 (adjusted for ties)

1:3:4 Zeta potential

Two-Sample T-Test and Zr vs. Fe
Zr: N = 39, Mean = -15.48, StDev = 1.05, SE Mean = 0.17
Fe: N = 39, Mean = -18.28, StDev = 2.01, SE Mean = 0.32
Difference = mu (Z Fil Zr) - mu (Z Fil Fe)
Estimate for difference: 2.803
95% lower bound for difference: 2.197
T-Test of difference = 0 (vs. >): T-Value = 7.74 P-Value = 0.000 DF = 57

1:3:5 THM-FP

Mann-Whitney Test Zr vs. Fe
Zr: N = 11, Median = 99.38
Fe: N = 12, Median = 145.06
Point estimate for ETA1-ETA2 is -51.65
95.5 Percent CI for ETA1-ETA2 is (-96.60,-32.22)
W = 67.0
Test of ETA1 = ETA2 vs. ETA1 < ETA2 is significant at 0.0000

1:3:6 THM-FP / DOC

Two-sample T-test Zr vs. Fe
Zr: N = 11, Mean = 68.26, StDev = 8.20, SE Mean = 2.5
Fe: N = 12, Mean = 75.61, StDev = 5.51, SE Mean = 1.6
Difference = mu (THM/DOC Zr) - mu (THM/DOC Fe)
Estimate for difference: -7.34
95% upper bound for difference: -2.37
T-Test of difference = 0 (vs. <): T-Value = -2.54 P-Value = 0.009 DF = 21
Both use Pooled StDev = 6.9217

2: Zr vs. Fe 26th of November

2:1 Flocculator tank

2:1:1 UV_{254}

Mann-Whitney Test Zr vs. Fe
U Flo Zr: N = 72, Median = 2.5000
U Flo Fe: N = 36, Median = 5.3875
Point estimate for ETA1-ETA2 is -2.9750
95.1 Percent CI for ETA1-ETA2 is (-3.0750,-2.8501)
W = 2628.0
Test of ETA1 = ETA2 vs. ETA1 < ETA2 is significant at 0.0000
The test is significant at 0.0000 (adjusted for ties)

2:1:2 Zeta potential

Two-Sample T-Test Zr vs. Fe
Zr: N = 71, Mean = 3.41, StDev = 1.10, SE Mean = 0.13
Fe: N = 35, Mean = 3.909, StDev = 0.400, SE Mean = 0.068
Difference = mu (Z Flo Zr) - mu (Z Flo Fe)
Estimate for difference: -0.494
95% upper bound for difference: -0.175
T-Test of difference = 0 (vs. <): T-Value = -2.57 P-Value = 0.006 DF = 104
Both use Pooled StDev = 0.9329

2:2 DAF

2:2:1 UV_{254}

Mann-Whitney Test Zr vs. Fe
Zr: N = 60, Median = 2.7125
Fe: N = 36, Median = 4.1000

Point estimate for ETA1-ETA2 is -1.4000
95.0 Percent CI for ETA1-ETA2 is (-1.5499,-1.2250)
W = 1830.0
Test of ETA1 = ETA2 vs. ETA1 < ETA2 is significant at 0.0000
The test is significant at 0.0000 (adjusted for ties)

2:2:2 DOC

Two-Sample T-Test Zr vs. Fe
Zr: = 19, Mean = 1.512, StDev = 0.284 SE Mean = 0.065
Fe: = 12, Mean = 1.675, StDev = 0.129, SE Mean = 0.037
Difference = mu (D DAF Zr) - mu (D DAF Fe)
Estimate for difference: -0.1632
95% upper bound for difference: -0.0353
T-Test of difference = 0 (vs. <): T-Value = -2.18 P-Value = 0.019 DF = 26

2:2:3 Turbidity

Mann-Whitney Test Zr vs. Fe
Zr: N = 96, Median = 5.175
Fe: N = 48, Median = 11.450
Point estimate for ETA1-ETA2 is -6.120
95.0 Percent CI for ETA1-ETA2 is (-7.040,-5.240)
W = 4678.0
Test of ETA1 = ETA2 vs. ETA1 < ETA2 is significant at 0.0000
The test is significant at 0.0000 (adjusted for ties)

2:2:4 Zeta potential

Mann-Whitney Test Zr vs. Fe
Zr: N = 66, Median = 0.450
Fe: N = 31, Median = -1.000
Point estimate for ETA1-ETA2 is 1.500
95.0 Percent CI for ETA1-ETA2 is (0.101, 2.600)
W = 3513.5
Test of ETA1 = ETA2 vs. ETA1 > ETA2 is significant at 0.0154
The test is significant at 0.0154 (adjusted for ties)

2:3 Filter

2:3:1 UV_{254}

Mann-Whitney Test Zr vs. Fe
Zr: N = 69, Median = 7.875
Fe: N = 36, Median = 14.088
Point estimate for ETA1-ETA2 is -5.175
95.0 Percent CI for ETA1-ETA2 is (-6.000,-4.050)
W = 2668.0
Test of ETA1 = ETA2 vs. ETA1 < ETA2 is significant at 0.0000

The test is significant at 0.0000 (adjusted for ties)

2:3:2 DOC

Mann-Whitney Test Zr vs. Fe
Zr: N = 33, Median = 2.5080
Fe: N = 18, Median = 2.8470
Point estimate for ETA1-ETA2 is -0.2780
95.0 Percent CI for ETA1-ETA2 is (-0.4979, 0.1142)
W = 779.0
Test of ETA1 = ETA2 vs. ETA1 < ETA2 is significant at 0.0609
The test is significant at 0.0609 (adjusted for ties)

2:3:4 Turbidity

Mann-Whitney Test Zr vs. Fe
Zr: N = 96, Median = 1.8200
Fe: N = 48, Median = 3.2250
Point estimate for ETA1-ETA2 is -1.2700
95.0 Percent CI for ETA1-ETA2 is (-1.4600,-1.0200)
W = 5138.5
Test of ETA1 = ETA2 vs. ETA1 < ETA2 is significant at 0.0000
The test is significant at 0.0000 (adjusted for ties)

2:3:5 Zeta potential

Two-Sample T-Test Zr vs. Fe
Zr: N = 71, Mean = -17.20, StDev = 1.63, SE Mean = 0.19
Fe: N = 36, Mean = -16.28, StDev = 1.35, SE Mean = 0.22
Difference = mu (Z Fil Zr) - mu (Z Fil Fe)
Estimate for difference: -0.914
95% lower bound for difference: -1.436
T-Test of difference = 0 (vs. >): T-Value = -2.90 P-Value = 0.998 DF = 105
Both use Pooled StDev = 1.5379

2:3:6 THM-FP

Two-Sample T-Test Zr vs. Fe
Zr: N = 11, Mean = 150.5, StDev = 30.1, SE Mean = 9.1
Fe: N = 6, Mean = 194.6, StDev = 24.1, SE Mean = 9.8
Difference = mu (THM Zr) - mu (THM Fe)
Estimate for difference: -44.1
95% upper bound for difference: -19.0
T-Test of difference = 0 (vs. <): T-Value = -3.07 P-Value = 0.004 DF = 15
Both use Pooled StDev = 28.2573

2:3:7 THM / DOC

Two-Sample T-Test Zr vs. Fe
Zr: N = 11, Mean = 59.91, StDev = 8.06, SE Mean = 2.4
Fe: N = 6, Mean = 67.00, StDev = 2.03, SE Mean = 0.83
Difference = mu (THM/DOC Zr) - mu (THM/DOC Fe)
Estimate for difference: -7.09
95% upper bound for difference: -2.51
T-Test of difference = 0 (vs. <): T-Value = -2.76 P-Value = 0.009 DF = 12

3: Blending 14th of July

3:1 Flocculator tank

3:1:1 UV_{254}

Two-sample T-Test 0% vs. 20%
0%: N = 32, Mean = 3.082, StDev = 0.126, SE Mean = 0.022
20%: N = 18, Mean = 4.331, StDev = 0.822, SE Mean = 0.19
Difference = mu (U Flo Fe) - mu (U Flo 20%)
Estimate for difference: -1.249
95% upper bound for difference: -0.909
T-Test of difference = 0 (vs. <): T-Value = -6.40 P-Value = 0.000 DF = 17

Mann-Whitney Test 20% vs. 80%
20%: N = 18, Median = 4.4500
80%: N = 18, Median = 1.7625
Point estimate for ETA1-ETA2 is 2.6750
95.2 Percent CI for ETA1-ETA2 is (2.0749, 3.1748)
W = 495.0
Test of ETA1 = ETA2 vs. ETA1 > ETA2 is significant at 0.0000
The test is significant at 0.0000 (adjusted for ties)

Mann-Whitney Test 80% vs. 100%
80%: N = 18, Median = 1.7625
100%: N = 36, Median = 1.5750
Point estimate for ETA1-ETA2 is 0.2000
95.1 Percent CI for ETA1-ETA2 is (0.1500, 0.2750)
W = 789.0
Test of ETA1 = ETA2 vs. ETA1 > ETA2 is significant at 0.0000
The test is significant at 0.0000 (adjusted for ties)

3:1:2 Zeta potential

Two-Sample T-Test 0% vs. 20%
0%: N = 51, Mean = -6.38, StDev = 4.50, SE Mean = 0.63
20%: N = 19, Mean = -13.32, StDev = 1.27, SE Mean = 0.29
Difference = mu (Z Flo Fe) - mu (Z Flo 20%)
Estimate for difference: 6.939
95% lower bound for difference: 5.781
T-Test of difference = 0 (vs. >): T-Value = 9.99 P-Value = 0.000 DF = 65

Mann-Whitney Test 20% vs. 80%
80%: N = 18, Median = 1.550
20%: N = 19, Median = -13.700
Point estimate for ETA1-ETA2 is 14.900
95.3 Percent CI for ETA1-ETA2 is (13.701, 15.700)
W = 513.0
Test of ETA1 = ETA2 vs. ETA1 > ETA2 is significant at 0.0000
The test is significant at 0.0000 (adjusted for ties)

Mann-Whitney Test 80% vs. 100%
100%: N = 42, Median = 2.700
80%: N = 18, Median = 1.550
Point estimate for ETA1-ETA2 is 1.100
95.2 Percent CI for ETA1-ETA2 is (0.700, 1.700)
W = 1537.5
Test of ETA1 = ETA2 vs. ETA1 > ETA2 is significant at 0.0000
The test is significant at 0.0000 (adjusted for ties)

3:2 DAF

3:2:1 UV_{254}

Two-Sample T-Test 0% vs. 20%
0%: N = 27, Mean = 3.489, StDev = 0.431, SE Mean = 0.083
20%: N = 18, Mean = 4.815, StDev = 0.939, SE Mean = 0.22
Difference = mu (U DAF Fe) - mu (U DAF 20%)
Estimate for difference: -1.326
95% upper bound for difference: -0.920
T-Test of difference = 0 (vs. <): T-Value = -5.61 P-Value = 0.000 DF = 21

Mann-Whitney Test 20% vs. 80%
20%: N = 18, Median = 4.8500
80%: N = 15, Median = 2.5500
Point estimate for ETA1-ETA2 is 2.1000

95.1 Percent CI for ETA1-ETA2 is (1.6003, 2.7998)
W = 441.0
Test of ETA1 = ETA2 vs. ETA1 > ETA2 is significant at 0.0000
The test is significant at 0.0000 (adjusted for ties)

Mann-Whitney Test 80% vs. 100%
80%: N = 15, Median = 2.5500
100%: N = 30, Median = 1.9500
Point estimate for ETA1-ETA2 is 0.6000
95.0 Percent CI for ETA1-ETA2 is (0.4750, 0.9249)
W = 570.0
Test of ETA1 = ETA2 vs. ETA1 > ETA2 is significant at 0.0000
The test is significant at 0.0000 (adjusted for ties)

3:2:2 DOC

Two-Sample T-Test 0% vs. 20%
0%: N = 11, Mean = 1.699, StDev = 0.294, SE Mean = 0.089
20%: N = 6, Mean = 2.089, StDev = 0.107, SE Mean = 0.044
Difference = mu (D DAF Fe) - mu (D DAF 20%)
Estimate for difference: -0.3901
95% upper bound for difference: -0.2150
T-Test of difference = 0 (vs. <): T-Value = -3.94 P-Value = 0.001 DF = 13

Two-Sample T-Test 20% vs. 80%
20%: N = 6, Mean = 2.089, StDev = 0.107, SE Mean = 0.044
80%: N = 6, Mean = 1.555, StDev = 0.137, SE Mean = 0.056
Difference = mu (D DAF 20%) - mu (D DAF 80%)
Estimate for difference: 0.5340
95% lower bound for difference: 0.4053
T-Test of difference = 0 (vs >): T-Value = 7.52 P-Value = 0.000 DF = 10
Both use Pooled StDev = 0.1229

Two-Sample T-Test 80% vs. 100%
100%: N = 9, Mean = 1.1520, StDev = 0.0663, SE Mean = 0.022
80%: N = 6, Mean = 1.555, StDev = 0.137, SE Mean = 0.056
Difference = mu (D DAF Zr) - mu (D DAF 80%)
Estimate for difference: -0.4032
95% upper bound for difference: -0.3102
T-Test of difference = 0 (vs <): T-Value = -7.68 P-Value = 0.000 DF = 13
Both use Pooled StDev = 0.0996

3:2:3 Turbidity

Mann-Whitney Test 0% vs. 20%
20%: N = 18, Median = 4.804
0%: N = 36, Median = 3.885
Point estimate for ETA1-ETA2 is -0.538
95.1 Percent CI for ETA1-ETA2 is (-2.180, 0.776)

W = 431.0
Test of ETA1 = ETA2 vs. ETA1 < ETA2 is significant at 0.1220
The test is significant at 0.1219 (adjusted for ties)

Mann-Whitney Test 20% vs. 80%
80%: N = 18, Median = 2.604
20%: N = 18, Median = 4.804
Point estimate for ETA1-ETA2 is -1.587
95.2 Percent CI for ETA1-ETA2 is (-6.746,-0.605)
W = 252.0
Test of ETA1 = ETA2 vs. ETA1 < ETA2 is significant at 0.0054

Mann-Whitney Test 80% vs. 100%
100%: N = 26, Median = 2.277
80%: N = 18, Median = 2.604
Point estimate for ETA1-ETA2 is -0.269
95.1 Percent CI for ETA1-ETA2 is (-2.651, 1.542)
W = 585.0
Test of ETA1 = ETA2 vs. ETA1 < ETA2 is significant at 0.5000
The test is significant at 0.5000 (adjusted for ties)

3:2:4 Zeta potential

Two-Sample T-Test 0% vs. 20%
0%: N = 36, Mean = -14.39, StDev = 1.83, SE Mean = 0.30
20%: N = 14, Mean = -15.450, StDev = 0.661, SE Mean = 0.18
Difference = mu (Z DAF Fe) - mu (Z DAF 20%)
Estimate for difference: 1.064
95% lower bound for difference: 0.473
T-Test of difference = 0 (vs. >): T-Value = 3.02 P-Value = 0.002 DF = 47

Mann-Whitney Test 20% vs. 80%
20%: N = 14, Median = -15.450
80%: N = 21, Median = -9.600
Point estimate for ETA1-ETA2 is -5.550
95.1 Percent CI for ETA1-ETA2 is (-11.400,-2.899)
W = 107.0
Test of ETA1 = ETA2 vs. ETA1 < ETA2 is significant at 0.0000
The test is significant at 0.0000 (adjusted for ties)

Mann-Whitney Test 80% vs. 100%
80%: N = 21, Median = -9.600
100%: N = 39, Median = 0.200
Point estimate for ETA1-ETA2 is -8.300
95.1 Percent CI for ETA1-ETA2 is (-11.199,-4.700)
W = 332.5
Test of ETA1 = ETA2 vs. ETA1 < ETA2 is significant at 0.0000
The test is significant at 0.0000 (adjusted for ties)

3:3 Filter

3:3:1 UV_{254}

Mann-Whitney Test 0% vs. 20%
0%: N = 36, Median = 5.862
20%: N = 15, Median = 6.775
Point estimate for ETA1-ETA2 is -0.675
95.2 Percent CI for ETA1-ETA2 is (-1.300, 0.800)
W = 900.0
Test of ETA1 = ETA2 vs. ETA1 > ETA2
Cannot reject since W is < 936.0

Mann-Whitney Test 20% vs. 80%
80%: N = 18, Median = 4.6125
20%: N = 15, Median = 6.7750
Point estimate for ETA1-ETA2 is -2.1375
95.1 Percent CI for ETA1-ETA2 is (-2.4000,-1.7251)
W = 171.0
Test of ETA1 = ETA2 vs. ETA1 < ETA2 is significant at 0.0000
The test is significant at 0.0000 (adjusted for ties)

Mann-Whitney Test 80% vs. 100%
100%: N = 36, Median = 3.3625
80%: N = 18, Median = 4.6125
Point estimate for ETA1-ETA2 is -1.0625
95.1 Percent CI for ETA1-ETA2 is (-1.3499,-0.6000)
W = 754.0
Test of ETA1 = ETA2 vs. ETA1 < ETA2 is significant at 0.0000
The test is significant at 0.0000 (adjusted for ties)

3:3:2 DOC

Mann-Whitney Test 0% vs. 20%
0%: N = 20, Median = 2.0050
20%: N = 12, Median = 2.0495
Point estimate for ETA1-ETA2 is -0.0330
95.1 Percent CI for ETA1-ETA2 is (-0.1940, 0.3029)
W = 317.5
Test of ETA1 = ETA2 vs. ETA1 > ETA2
Cannot reject since W is < 330.0

Mann-Whitney Test 20% vs. 80%
80%: N = 12, Median = 1.6360

20%: N = 12, Median = 2.0495
Point estimate for ETA1-ETA2 is -0.4475
95.4 Percent CI for ETA1-ETA2 is (-0.6109,-0.2819)
W = 79.0
Test of ETA1 = ETA2 vs. ETA1 < ETA2 is significant at 0.0000

Mann-Whitney Test 80% vs. 100%
100%: N = 24, Median = 1.5280
80%: N = 12, Median = 1.6360
Point estimate for ETA1-ETA2 is -0.0985
95.0 Percent CI for ETA1-ETA2 is (-0.2459, 0.0270)
W = 397.0
Test of ETA1 = ETA2 vs. ETA1 < ETA2 is significant at 0.0593
The test is significant at 0.0593 (adjusted for ties)

3:3:3 Turbidity

Mann-Whitney Test 0% vs. 20%
20%: N = 15, Median = 1.3000
0%: N = 28, Median = 1.0900
Point estimate for ETA1-ETA2 is 0.2500
95.2 Percent CI for ETA1-ETA2 is (-0.0828, 0.5000)
W = 379.5
Test of ETA1 = ETA2 vs. ETA1 < ETA2
Cannot reject since W is > 330.0

Mann-Whitney Test 20% vs. 80%
80%: N = 15, Median = 0.3910
20%: N = 15, Median = 1.3000
Point estimate for ETA1-ETA2 is -0.9000
95.4 Percent CI for ETA1-ETA2 is (-1.2039,-0.6670)
W = 120.0
Test of ETA1 = ETA2 vs. ETA1 < ETA2 is significant at 0.0000
The test is significant at 0.0000 (adjusted for ties)

Mann-Whitney Test 80% vs. 100%
100%: N = 32, Median = 0.42100
80%: N = 15, Median = 0.39100
Point estimate for ETA1-ETA2 is 0.03350
95.2 Percent CI for ETA1-ETA2 is (-0.00699, 0.07599)
W = 833.5
Test of ETA1 = ETA2 vs. ETA1 < ETA2
Cannot reject since W is > 768.0

3:3:4 Zeta potential

Two-Sample T-Test 0% vs. 20%
0%: N = 39, Mean = -18.28, StDev = 2.01, SE Mean = 0.32
20%: N = 21, Mean = -17.962, StDev = 0.979, SE Mean = 0.21
Difference = mu (Z Fil Fe) - mu (Z Filter 20%)

Estimate for difference: -0.318
95% upper bound for difference: 0.327
T-Test of difference = 0 (vs. <): T-Value = -0.82 P-Value = 0.207 DF = 57

Two-Sample T-Test 20% vs. 80%
80%: N = 20, Mean = -15.55, StDev = 1.62, SE Mean = 0.36
20%: N = 21, Mean = -17.962, StDev = 0.979, SE Mean = 0.21
Difference = mu (Z Filter 80%) - mu (Z Filter 20%)
Estimate for difference: 2.412
95% lower bound for difference: 1.698
T-Test of difference = 0 (vs. >): T-Value = 5.73 P-Value = 0.000 DF = 30

Two-Sample T-Test 80% vs. 100%
80%: N = 20, Mean = -15.55, StDev = 1.62, SE Mean = 0.36
100%: N = 39, Mean = -15.48, StDev = 1.05, SE Mean = 0.17
Difference = mu (Z Filter 80%) - mu (Z Fil Zr)
Estimate for difference: -0.073
95% upper bound for difference: 0.607
T-Test of difference = 0 (vs. <): T-Value = -0.18 P-Value = 0.428 DF = 27

3:3:5 THM-FP

Mann-Whitney Test 0% vs. 20%
20%: N = 5, Median = 176.24
0%: N = 12, Median = 145.06
Point estimate for ETA1-ETA2 is 29.27
96.0 Percent CI for ETA1-ETA2 is (-29.88, 50.92)
W = 54.0
Test of ETA1 = ETA2 vs. ETA1 > ETA2 is significant at 0.1851

Mann-Whitney Test 20% vs. 80%
20%: N = 5, Median = 176.24
80%: N = 5, Median = 150.36
Point estimate for ETA1-ETA2 is 34.51
96.3 Percent CI for ETA1-ETA2 is (-2.80, 76.32)
W = 37.0
Test of ETA1 = ETA2 vs. ETA1 > ETA2 is significant at 0.0301

Two-Sample T-Test 80% vs. 100%
80%: N = 5, Mean = 143.4, StDev = 27.7, SE Mean = 12
100%: N = 11, Mean = 100.7, StDev = 15.0, SE Mean = 4.5
Difference = mu (THM 80%) - mu (THM Zr)
Estimate for difference: 42.7
95% lower bound for difference: 24.2
T-Test of difference = 0 (vs. >): T-Value = 4.06 P-Value = 0.001 DF = 14
Both use Pooled StDev = 19.4934

3:3:6 THM / DOC

Two-Sample T-Test 0% vs. 20%
20%: N = 5, Mean = 86.39, StDev = 4.10, SE Mean = 1.8
0%: N = 12, Mean = 75.61, StDev = 5.51, SE Mean = 1.6
Difference = mu (THM/DOC 20%) - mu (THM/DOC Fe)
Estimate for difference: 10.78
95% upper bound for difference: 15.61
T-Test of difference = 0 (vs. <): T-Value = 3.91 P-Value = 0.999 DF = 15
Both use Pooled StDev = 5.1762

Two-Sample T-Test 20% vs. 80%
80%: N = 5, Mean = 85.81, StDev = 9.06, SE Mean = 4.1
20%: N = 5, Mean = 86.39, StDev = 4.10, SE Mean = 1.8
Difference = mu (THM/DOC 80%) - mu (THM/DOC 20%)
Estimate for difference: -0.57
95% upper bound for difference: 7.69
T-Test of difference = 0 (vs. <): T-Value = -0.13 P-Value = 0.450 DF = 8
Both use Pooled StDev = 7.0307

Two-Sample T-Test 80% vs. 100%
100%: N = 11, Mean = 68.26, StDev = 8.20, SE Mean = 2.5
80%: N = 5, Mean = 85.81, StDev = 9.06, SE Mean = 4.1
Difference = mu (THM/DOC Zr) - mu (THM/DOC 80%)
Estimate for difference: -17.55
95% upper bound for difference: -9.52
T-Test of difference = 0 (vs. <): T-Value = -3.85 P-Value = 0.001 DF = 14
Both use Pooled StDev = 8.4501

4: Blending 26th of November

4:1 Flocculator tank

4:1:1 UV_{254}

Mann-Whitney Test 0% vs. 20%
20%: N = 36, Median = 5.0875
0%: N = 36, Median = 5.3875
Point estimate for ETA1-ETA2 is -0.3500
95.1 Percent CI for ETA1-ETA2 is (-0.4500,-0.2251)
W = 952.0
Test of ETA1 = ETA2 vs. ETA1 < ETA2 is significant at 0.0000
The test is significant at 0.0000 (adjusted for ties)

Two-Sample T-Test 20% vs. 80%
20%: N = 36, Mean = 5.147, StDev = 0.229, SE Mean = 0.038
80%: N = 26, Mean = 3.5048, StDev = 0.0600, SE Mean = 0.012
Difference = mu (U Flo 20%) - mu (U Flo 80%)
Estimate for difference: 1.6417
95% lower bound for difference: 1.5745
T-Test of difference = 0 (vs. >): T-Value = 41.12 P-Value = 0.000 DF = 41

Mann-Whitney Test 80% vs. 100%
100%: N = 72, Median = 2.5000
80%: N = 26, Median = 3.5000
Point estimate for ETA1-ETA2 is -1.0000
95.1 Percent CI for ETA1-ETA2 is (-1.1000,-0.9500)
W = 2628.0
Test of ETA1 = ETA2 vs. ETA1 < ETA2 is significant at 0.0000
The test is significant at 0.0000 (adjusted for ties)

4:1:2 Zeta potential

Two-Sample T-Test 0% vs. 20%
20%: N = 36, Mean = 3.783, StDev = 0.292, SE Mean = 0.049
0%: N = 35, Mean = 3.909, StDev = 0.400, SE Mean = 0.068
Difference = mu (Z Flo 20%) - mu (Z Flo Fe)
Estimate for difference: -0.1252
95% lower bound for difference: -0.2636
T-Test of difference = 0 (vs. >): T-Value = -1.51 P-Value = 0.932 DF = 69
Both use Pooled StDev = 0.3497

Two-Sample T-Test 20% vs. 80%
80%: N = 36, Mean = 4.636, StDev = 0.387, SE Mean = 0.065
20%: N = 36, Mean = 3.783, StDev = 0.292, SE Mean = 0.049
Difference = mu (Z Flo 80%) - mu (Z Flo 20%)
Estimate for difference: 0.8528
95% lower bound for difference: 0.7180
T-Test of difference = 0 (vs. >): T-Value = 10.55 P-Value = 0.000 DF = 70
Both use Pooled StDev = 0.3430

Two-Sample T-Test 80% vs. 100%
100%: N = 71, Mean = 3.41, StDev = 1.10, SE Mean = 0.13
80%: N = 36, Mean = 4.636, StDev = 0.387, SE Mean = 0.065
Difference = mu (Z Flo Zr) - mu (Z Flo 80%)
Estimate for difference: -1.222
95% lower bound for difference: -1.464
T-Test of difference = 0 (vs.>): T-Value = -8.38 P-Value = 1.000 DF = 96

4:2 DAF

4:2:1 UV_{254}

Mann-Whitney Test 0% vs. 20%
0%: N = 36, Median = 4.1000
20%: N = 36, Median = 4.2750
Point estimate for ETA1-ETA2 is -0.2500
95.1 Percent CI for ETA1-ETA2 is (-0.4499,-0.0250)
W = 1116.0
Test of ETA1 = ETA2 vs. ETA1 not = ETA2 is significant at 0.0261
The test is significant at 0.0260 (adjusted for ties)

Mann-Whitney Test 20% vs. 80%
20%: N = 36, Median = 4.2750
80%: N = 33, Median = 3.0000
Point estimate for ETA1-ETA2 is 1.2250
95.0 Percent CI for ETA1-ETA2 is (1.0751, 1.3501)
W = 1793.5
Test of ETA1 = ETA2 vs. ETA1 > ETA2 is significant at 0.0000
The test is significant at 0.0000 (adjusted for ties)

Mann-Whitney Test 80% vs. 100%
100%: N = 60, Median = 2.7125
80%: N = 33, Median = 3.0000
Point estimate for ETA1-ETA2 is -0.4000
95.0 Percent CI for ETA1-ETA2 is (-0.4999,-0.3000)
W = 2004.0
Test of ETA1 = ETA2 vs. ETA1 < ETA2 is significant at 0.0000
The test is significant at 0.0000 (adjusted for ties)

4:2:2 DOC

Two-Sample T-Test 0% vs. 20%
20%: N = 12, Mean = 1.6625, StDev = 0.0902, SE Mean = 0.026
0%: N = 12, Mean = 1.675, StDev = 0.129, SE Mean = 0.037
Difference = mu (D DAF 20%) - mu (D DAF Fe)
Estimate for difference: -0.0127
95% upper bound for difference: 0.0654
T-Test of difference = 0 (vs. <): T-Value = -0.28 P-Value = 0.392 DF = 22
Both use Pooled StDev = 0.1114

Two-Sample T-Test 20% vs. 80%
80%: N = 12, Mean = 1.5842, StDev = 0.0906, SE Mean = 0.026

20%: N = 12, Mean = 1.6625, StDev = 0.0902, SE Mean = 0.026
Difference = mu (D DAF 80%) - mu (D DAF 20%)
Estimate for difference: -0.0783
95% upper bound for difference: -0.0149
T-Test of difference = 0 (vs. <): T-Value = -2.12 P-Value = 0.023 DF = 22
Both use Pooled StDev = 0.0904
Two-Sample T-Test 80% vs. 100%
100%: N = 19, Mean = 1.512, StDev = 0.284, SE Mean = 0.065
80%: N = 12, Mean = 1.5842, StDev = 0.0906, SE Mean = 0.026
Difference = mu (D DAF Zr) - mu (D DAF 80%)
Estimate for difference: -0.0723
95% upper bound for difference: 0.0479
T-Test of difference = 0 (vs. <): T-Value = -1.03 P-Value = 0.157 DF = 23

4:2:3 Turbidity

Mann-Whitney Test 0% vs. 20%
20%: N = 48, Median = 7.760
0%: N = 48, Median = 11.450
Point estimate for ETA1-ETA2 is -3.690
95.0 Percent CI for ETA1-ETA2 is (-4.920,-2.730)
W = 1508.5
Test of ETA1 = ETA2 vs. ETA1 < ETA2 is significant at 0.0000
The test is significant at 0.0000 (adjusted for ties)

Mann-Whitney Test 20% vs. 80%
80%: N = 48, Median = 6.635
20%: N = 48, Median = 7.760
Point estimate for ETA1-ETA2 is -1.150
95.0 Percent CI for ETA1-ETA2 is (-2.080,-0.260)
W = 1955.5
Test of ETA1 = ETA2 vs. ETA1 < ETA2 is significant at 0.0033
The test is significant at 0.0033 (adjusted for ties)

Mann-Whitney Test 80% vs. 100%
100%: N = 96, Median = 5.175
80%: N = 48, Median = 6.635
Point estimate for ETA1-ETA2 is -1.245
95.0 Percent CI for ETA1-ETA2 is (-1.900,-0.710)
W = 5941.0
Test of ETA1 = ETA2 vs. ETA1 < ETA2 is significant at 0.0000
The test is significant at 0.0000 (adjusted for ties)

4:2:4 Zeta potential

Mann-Whitney Test 0% vs. 20%
20%: N = 36, Median = -0.250
0%: N = 31, Median = -1.000
Point estimate for ETA1-ETA2 is 0.900
95.1 Percent CI for ETA1-ETA2 is (0.100, 1.400)

W = 1393.0
Test of ETA1 = ETA2 vs. ETA1 > ETA2 is significant at 0.0171
The test is significant at 0.0170 (adjusted for ties)

Mann-Whitney Test 20% vs. 80%
80%: N = 23, Median = 3.600
20%: N = 36, Median = -0.250
Point estimate for ETA1-ETA2 is 3.600
95.1 Percent CI for ETA1-ETA2 is (3.100, 4.299)
W = 1104.0
Test of ETA1 = ETA2 vs. ETA1 > ETA2 is significant at 0.0000
The test is significant at 0.0000 (adjusted for ties)

Two-Sample T-Test 80% vs. 100%
100%: N = 66, Mean = -0.38, StDev = 3.35, SE Mean = 0.41
80%: N = 23, Mean = 3.183, StDev = 0.875, SE Mean = 0.18
Difference = mu (Z DAF Zr) - mu (Z DAF 80%)
Estimate for difference: -3.561
95% upper bound for difference: -2.811
T-Test of difference = 0 (vs. <): T-Value = -7.89 P-Value = 0.000 DF = 83

4:3 Filter

4:3:1 UV_{254}

Mann-Whitney Test 0% vs. 20%
0%: N = 36, Median = 14.088
20%: N = 36, Median = 11.225
Point estimate for ETA1-ETA2 is 2.125
95.1 Percent CI for ETA1-ETA2 is (0.974, 3.299)
W = 1647.5
Test of ETA1 = ETA2 vs. ETA1 > ETA2 is significant at 0.0001
The test is significant at 0.0001 (adjusted for ties)

Mann-Whitney Test 20% vs. 80%
20%: N = 36, Median = 11.225
80%: N = 36, Median = 6.775
Point estimate for ETA1-ETA2 is 4.350
95.1 Percent CI for ETA1-ETA2 is (1.799, 5.400)
W = 1795.5
Test of ETA1 = ETA2 vs. ETA1 > ETA2 is significant at 0.0000
The test is significant at 0.0000 (adjusted for ties)

Two-Sample T-Test 80% vs. 100%
100%: N = 69, Mean = 8.33, StDev = 1.49, SE Mean = 0.18
80%: N = 36, Mean = 6.94, StDev = 1.02, SE Mean = 0.17
Difference = mu (U Filter Zr) - mu (U Fil 80%)
Estimate for difference: 1.393

95% CI for difference: (0.903, 1.883)
T-Test of difference = 0 (vs. not =): T-Value = 5.64 P-Value = 0.000 DF = 95

4:3:2 DOC

Mann-Whitney Test 0% vs. 20%
20%: N = 18, Median = 2.4535
0%: N = 18, Median = 2.8470
Point estimate for ETA1-ETA2 is -0.3800
95.2 Percent CI for ETA1-ETA2 is (-0.5669,-0.1349)
W = 254.0
Test of ETA1 = ETA2 vs. ETA1 < ETA2 is significant at 0.0065

Two-Sample T-Test 20% vs. 80%
20%: N = 18, Mean = 2.437, StDev = 0.295, SE Mean = 0.070
80%: N = 18, Mean = 2.252, StDev = 0.300, SE Mean = 0.071
Difference = mu (D Fil 20%) - mu (D Fil 80%)
Estimate for difference: 0.1843
95% lower bound for difference: 0.0165
T-Test of difference = 0 (vs. >): T-Value = 1.86 P-Value = 0.036 DF = 34
Both use Pooled StDev = 0.2977

Mann-Whitney Test 80% vs. 100%
80%: N = 18, Median = 2.2400
100% N = 33, Median = 2.5080
Point estimate for ETA1-ETA2 is -0.2735
95.0 Percent CI for ETA1-ETA2 is (-0.5239,-0.0550)
W = 349.0
Test of ETA1 = ETA2 vs. ETA1 < ETA2 is significant at 0.0098
The test is significant at 0.0098 (adjusted for ties)

4:3:3 Turbidity

Mann-Whitney Test 0% vs. 20%
20%: N = 48, Median = 3.1800
0%: N = 48, Median = 3.2250
Point estimate for ETA1-ETA2 is -0.0300
95.0 Percent CI for ETA1-ETA2 is (-0.3801, 0.2601)
W = 2309.0
Test of ETA1 = ETA2 vs. ETA1 < ETA2 is significant at 0.4475
The test is significant at 0.4475 (adjusted for ties)

Mann-Whitney Test 20% vs. 80%
80%: N = 48, Median = 1.8300
20%: N = 48, Median = 3.1800
Point estimate for ETA1-ETA2 is -1.1400
95.0 Percent CI for ETA1-ETA2 is (-1.5400, -0.8499)

W = 1420.0
Test of ETA1 = ETA2 vs. ETA1 < ETA2 is significant at 0.0000
The test is significant at 0.0000 (adjusted for ties)

Mann-Whitney Test 80% vs. 100%
100%: N = 96, Median = 1.8200
80%: N = 48, Median = 1.8300
Point estimate for ETA1-ETA2 is -0.0200
95.0 Percent CI for ETA1-ETA2 is (-0.1701, 0.1601)
W = 6895.0
Test of ETA1 = ETA2 vs. ETA1 < ETA2 is significant at 0.3923
The test is significant at 0.3923 (adjusted for ties)

4:3:4 Zeta potential

Mann-Whitney Test 0% vs. 20%
0%: N = 36, Median = -16.300
20%: N = 36, Median = -15.350
Point estimate for ETA1-ETA2 is -0.700
95.1 Percent CI for ETA1-ETA2 is (-1.400, -0.100)
W = 1125.0
Test of ETA1 = ETA2 vs. ETA1 < ETA2 is significant at 0.0169
The test is significant at 0.0168 (adjusted for ties)

Mann-Whitney Test 20% vs. 80%
20%: N = 36, Median = -15.350
80%: N = 36, Median = -15.250
Point estimate for ETA1-ETA2 is -0.100
95.1 Percent CI for ETA1-ETA2 is (-0.600, 0.500)
W = 1285.5
Test of ETA1 = ETA2 vs. ETA1 < ETA2 is significant at 0.3763
The test is significant at 0.3761 (adjusted for ties)

Two-Sample T-Test 80% vs. 100%
80%: N = 36, Mean = -15.431, StDev = 0.991, SE Mean = 0.17
100%: N = 71, Mean = -17.20, StDev = 1.63, SE Mean = 0.19
Difference = mu (Z Filter 80%) - mu (Z Fil Zr)
Estimate for difference: 1.767
95% upper bound for difference: 2.188
T-Test of difference = 0 (vs. <): T-Value = 6.96 P-Value = 1.000 DF = 101

4:3:5 THM-FP

Two-Sample T-Test 0% vs. 20%
20%: N = 6, Mean = 149.4, StDev = 28.2, SE Mean = 12
0%: N = 6, Mean = 194.6, StDev = 24.1, SE Mean = 9.8
Difference = mu (THM 20%) - mu (THM Fe)
Estimate for difference: -45.2

95% upper bound for difference: -17.4
T-Test of difference = 0 (vs. <): T-Value = -2.98 P-Value = 0.008 DF = 9

Two-Sample T-Test 20% vs. 80%
80%: N = 6, Mean = 131.6, StDev = 22.5, SE Mean = 9.2
20%: N = 6, Mean = 149.4, StDev = 28.2, SE Mean = 12
Difference = mu (THM 80%) - mu (THM 20%)
Estimate for difference: -17.9
95% upper bound for difference: 9.2
T-Test of difference = 0 (vs. <): T-Value = -1.21 P-Value = 0.128 DF = 9

Two-Sample T-Test 80% vs. 100%
100%: N = 11, Mean = 150.5, StDev = 30.1, SE Mean = 9.1
80%: N = 6, Mean = 131.6, StDev = 22.5, SE Mean = 9.2
Difference = mu (THM Zr) - mu (THM 80%)
Estimate for difference: 19.0
95% upper bound for difference: 41.8
T-Test of difference = 0 (vs. <): T-Value = 1.47 P-Value = 0.917 DF = 13

4:3:6 THM / DOC

Two-Sample T-Test 0% vs. 20%
20%: N = 6, Mean = 58.27, StDev = 7.32, SE Mean = 3.0
0%: N = 6, Mean = 67.00, StDev = 2.03, SE Mean = 0.83
Difference = mu (THM/DOC 20%) - mu (THM/DOC Fe)
Estimate for difference: -8.73
95% upper bound for difference: -2.48
T-Test of difference = 0 (vs. <): T-Value = -2.82 P-Value = 0.019 DF = 5

Two-Sample T-Test 20% vs. 80%
80%: N = 6, Mean = 53.66, StDev = 3.94, SE Mean = 1.6
20%: N = 6, Mean = 58.27, StDev = 7.32, SE Mean = 3.0
Difference = mu (THM/DOC 80%) - mu (THM/DOC 20%)
Estimate for difference: -4.62
95% upper bound for difference: 1.81
T-Test of difference = 0 (vs. <): T-Value = -1.36 P-Value = 0.108 DF = 7

Two-Sample T-Test 80% vs. 100%
100%: N = 11, Mean = 59.91, StDev = 8.06, SE Mean = 2.4
80%: N = 6, Mean = 53.66, StDev = 3.94, SE Mean = 1.6
Difference = mu (THM/DOC Zr) - mu (THM/DOC 80%)
Estimate for difference: 6.25
95% upper bound for difference: 12.45
T-Test of difference = 0 (vs. <): T-Value = 1.77 P-Value = 0.951 DF = 15
Both use Pooled StDev = 6.9641

APPENDIX B

This appendix provides details on the statistical analysis performed on the data collected during floc size measurements with Fe, Zr and blends of both coagulants on water sampled on the 16th of May

1: Zr vs. Fe

Two-Sample T-Test Zr vs. Fe
Fe: N = 167, Mean = 667.6, StDev = 64.1, SE Mean = 5.0
Zr: N = 153, Mean = 958.6, StDev = 49.0, SE Mean = 4.0
Difference = mu (Fe Floc size) - mu (Zr Floc size)
Estimate for difference: -291.02
95% upper bound for difference: -280.54
T-Test of difference = 0 (vs. <): T-Value = -45.84 P-Value = 0.000 DF = 308

Two-Sample T-Test Fe 50 rpm after breakage vs. Fe 50 rpm before breakage
Fe 50 rpm after breakage: N = 9, Mean = 479.5, StDev = 14.6, SE Mean = 4.9
Fe 50 rpm before breakage: N = 28, Mean = 693.7, StDev = 43.9, SE Mean = 8.3
Difference = mu (Fe 50 rpm after breakage) - mu (Fe 50 rpm before breakage)
Estimate for difference: -214.23
95% upper bound for difference: -197.96
T-Test of difference = 0 (vs. <): T-Value = -22.26 P-Value = 0.000 DF = 34

2: Blending

Mann-Whitney Test 0% vs. 20%
20%: N = 166, Median = 708.51
0%: N = 167, Median = 660.34
Point estimate for ETA1-ETA2 is 43.10
95.0 Percent CI for ETA1-ETA2 is (31.25, 55.06)
W = 33583.5
Test of ETA1 = ETA2 vs. ETA1 > ETA2 is significant at 0.0000
The test is significant at 0.0000 (adjusted for ties)

Two-Sample T-Test 20% vs. 80%
80%: N = 165, Mean = 929.7, StDev = 44.8, SE Mean = 3.5
20%: N = 166, Mean = 707.1, StDev = 42.2, SE Mean = 3.3
Difference = mu (80% Blend Floc size) - mu (20% Blend Floc size)
Estimate for difference: 222.62
95% lower bound for difference: 214.74
T-Test of difference = 0 (vs. >): T-Value = 46.56 P-Value = 0.000 DF = 329

Both use Pooled StDev = 43.4937

Two-Sample T-Test 80% vs. 100%
100%: N = 153, Mean = 958.6, StDev = 49.0, SE Mean = 4.0
80%: N = 165, Mean = 929.7, StDev = 44.8, SE Mean = 3.5
Difference = mu (Zr Floc size) - mu (80% Blend Floc size)
Estimate for difference: 28.90
95% lower bound for difference: 20.23
T-Test of difference = 0 (vs. >): T-Value = 5.50 P-Value = 0.000 DF = 316
Both use Pooled StDev = 46.8496